Technical Report Documentation Page

1. REPORT No.
TE 71-8

2. GOVERNMENT ACCESSION No.

3. RECIPIENT'S CATALOG No.

4. TITLE AND SUBTITLE
Design Considerations For Asphalt Pavements

5. REPORT DATE
December 1971

6. PERFORMING ORGANIZATION

7. AUTHOR(S)
C.L. Monismith and D. B. McLean

8. PERFORMING ORGANIZATION REPORT No.
TE 71-8

9. PERFORMING ORGANIZATION NAME AND ADDRESS
State of California
Division of Highways
Materials and Research Department

10. WORK UNIT No.

11. CONTRACT OR GRANT No.

12. SPONSORING AGENCY NAME AND ADDRESS

13. TYPE OF REPORT & PERIOD COVERED

14. SPONSORING AGENCY CODE

15. SUPPLEMENTARY NOTES

16. ABSTRACT

Introduction: This report describes research completed during the 1970-71 period on the project concerned with design considerations for asphalt pavements. Investigations have been conducted in both the fatigue and permanent deformation areas. Figs. 1 and 2 illustrate schematic representations of subsystems of the pavement design system to permit consideration of these modes of distress in the design process.

In the fatigue area, a laboratory study of the influence of specimen width on mixture behavior in repeated flexure is reported. The purpose of this study has been to define the influence of a biaxial stress state (more closely approximating that existing in actual pavements) on fatigue response. Also reported are recent studies of the Ygnacio Valley Road pavement, the design of which was reported in TE 70-5 (1). The studies associated with this project are intended to provide "feedback" to the design process of Fig. 1 since the pavement has now been in service for approximately 2-1/2 years.

Because of a developing interest in the testing of soils in repeated loading, to measure their dynamic stiffnesses (resilient moduli) - also a part of the design process of Fig. 1- a detailed testing procedure for such determination is included as Appendix A to this report.

Research efforts in the permanent deformation area have been concerned primarily with defining limiting criteria for vertical compressive strains in the surface of the subgrade for pavements designed according to the California (R value) procedure. To establish these criteria, representative pavements have been analyzed utilizing elastic procedures described in Report TE 70-5 to determine the vertical compressive strains at the subgrade surface.

17. KEYWORDS
TE 71-8

18. No. OF PAGES:
108

19. DRI WEBSITE LINK
http://www.dot.ca.gov/hq/research/researchreports/1971/TE71-8.pdf

20. FILE NAME
TE71-8.pdf

SOIL MECHANICS AND BITUMINOUS MATERIALS
RESEARCH LABORATORY

DESIGN CONSIDERATIONS FOR ASPHALT PAVEMENTS

by
C. L. MONISMITH
and
D. B. McLEAN

REPORT NO. TE 71-8
to
THE MATERIALS AND RESEARCH DEPARTMENT
DIVISION OF HIGHWAYS
STATE OF CALIFORNIA

PREPARED IN COOPERATION WITH
THE UNITED STATES DEPARTMENT OF TRANSPORTATION
FEDERAL HIGHWAY ADMINISTRATION

DEPARTMENT OF CIVIL ENGINEERING
INSTITUTE OF TRANSPORTATION AND TRAFFIC ENGINEERING

University of California · Berkeley

Soil Mechanics and Bituminous Materials
Research Laboratory

DESIGN CONSIDERATIONS FOR ASPHALT PAVEMENTS

A report on an investigation

by

C. L. Monismith
Professor of Civil Engineering and
Research Engineer
and
D. B. McLean
Research Assistant

to

The Materials and Research Department
Division of Highways
State of California

under

Research Technical Agreement 13945-191202 UCB
HPR-PR-1(8) D0601

Prepared in cooperation with
The United States Department of Transportation
Federal Highway Administration

Report No. TE 71-8, Office of Research Services
University of California, Berkeley, California
December 1971

INTRODUCTION

This report describes research completed during the 1970-71 period on the project concerned with design considerations for asphalt pavements. Investigations have been conducted in both the fatigue and permanent deformation areas. Figs. 1 and 2 illustrate schematic representations of subsystems of the pavement design system to permit consideration of these modes of distress in the design process.

In the fatigue area, a laboratory study of the influence of specimen width on mixture behavior in repeated flexure is reported. The purpose of this study has been to define the influence of a biaxial stress state (more closely approximating that existing in actual pavements) on fatigue response. Also reported are recent studies of the Ygnacio Valley Road pavement, the design of which was reported in TE 70-5 (1). The studies associated with this project are intended to provide "feedback" to the design process of Fig. 1 since the pavement has now been in service for approximately 2-1/2 years.

Because of a developing interest in the testing of soils in repeated loading, to measure their dynamic stiffnesses (resilient moduli) - also a part of the design process of Fig. 1 - a detailed testing procedure for such determination is included as Appendix A to this report.

Research efforts in the permanent deformation area have been concerned primarily with defining limiting criteria for vertical compressive strains in the surface of the subgrade for pavements designed according to the California (R value) procedure. To establish these criteria, representative pavements have been analyzed utilizing elastic procedures described in Report TE 70-5 to determine the vertical compressive strains at the subgrade surface.

The report also contains a brief summary of recent efforts by a number of investigators directed to various aspects of the distortion subsystem of Fig. 2.

INFLUENCE OF SPECIMEN SIZE (WIDTH) ON LABORATORY DETERMINED FLEXURAL FATIGUE PROPERTIES OF ASPHALT CONCRETE

This study, initiated to determine the influence of a biaxial state of stress on laboratory-determined flexural fatigue characteristics, involved fatigue testing of beam specimens 1.5 in. deep and with widths varying in 0.5 in. increments from 1.5 to 3.0 in. Tests were performed at 68°F in only the controlled-stress mode of loading; ten specimens at each of three stress levels were used to define the fatigue characteristics.

Materials

The aggregate, a crushed granite from Watsonville, California, having been separated into individual size fractions by sieving was blended to meet the 1/2 in. maximum median gradation of the State of California (2). As seen in Fig. 3 the resultant grading closely followed the center of the specification band.

An 85-100 penetration asphalt cement, supplied by the Chevron Asphalt Company, was used and an asphalt content of 6.0 percent (by weight of aggregate) was selected as being representative of a value that might be used with this material in practice. Properties of the asphalt prior to mixing, together with properties of the asphalt recovered from the mix after testing, are shown in Table 1.

Beam specimens, prepared by kneading compaction (3) were cut to the required dimensions using a diamond-tipped saw. A summary of the characteristics of the mixes tested in this series is included in Table 2.

Test Procedures

The test equipment, Fig. 4, is similar to that used in the earlier investigations (1); however, it has the capability to test specimens up to

3 in. by 3 in. in cross sectional area. In addition, hydraulic cylinders are used to clamp the beams in place by means of one-direction flow values. A close-up view of the clamping system is shown in Fig. 5. This system results in a uniform clamping force during the course of a test and thus has an advantage over the earlier mechanical system which required periodic adjustments in the clamping forces.

Pulse-type loading was applied at frequency of 100 repetitions per minute and with a duration of 0.1 sec. Stiffness moduli and initial bending strains reported correspond to those determined at 200 repetitions of the applied load. Fatigue lives reported are those associated with complete rupture in each specimen.

Test Results

Mixture stiffnesses, computed by the Shell procedure based on recovered asphalt properties as well as the other required mix characteristics, are shown in Table 3. Comparison of the computed values with those measured during fatigue testing (Table 2) indicate excellent agreement.

Results of the fatigue tests are summarized in Table 4* and have been plotted in Figs. 6 through 13. Stress vs. fatigue life (N_f) are included in Figs. 6 through 9 for the 1.5, 2.0, 2.5 and 3.0 in. wide specimens respectively. Similarly, Figs. 10 through 13 contain the initial strain vs. fatigue life data for the four test series. Figs. 14 and 15 illustrate

*Appendix B contains a listing of the individual fatigue test results for all test series.

comparison of the mean fatigue curves (based on least squares regressions) for the various test series.

Statistical comparisons of the data have also been made to ascertain the influence of specimen size. Table 5 contains regression coefficients together with standard errors for both the stress vs. fatigue life and strain vs. fatigue life relationships for all of the test series. To test for the significance of differences in the spread of the data about the regression lines as measured by the standard error of the estimate, the F-test was utilized. Results of this analysis are shown in Table 6. A significant difference is observed in the results obtained for the 1.5 in. wide specimens as compared to those for the other series, while the results of the tests on the 2.0, 2.5 and 3.0 in. specimens are statistically the same.

The t-test was applied to the test results for the 2.0, 2.5 and 3.0 in. specimens since these data were not shown to be significantly different. As seen in Table 7 there is no significant difference in the slopes of the regression lines for these three series. Accordingly, all of the data were treated together and the slopes of the resulting regression lines are also shown in Table 7.

These data have also been compared in Fig. 16 to results developed earlies and summarized in a "generalized" fatigue diagram in report TE 70-5 (1). For a mixture with a stiffness of about 300,000 psi and an air void content of 5 percent, the slope, n, of the strain vs. fatigue life relationship would be about 3.5 as obtained from the diagram. Results of the t-test applied to the hypothesis that the slopes of the strain vs. cycles to failure relationships for the data reported herein are shown in Table 8. From the information presented in this table, it can be concluded that slope of the

line for the results from tests on the 1.5 in. wide specimens is not signficantly different from the value of 3.5 but that the results for tests on the wider specimens are significantly different.

The data in Table 8 indicate that the standard error of the estimate decreases with increasing specimen width and corresponds to results reported by Kallas and Puzinauskas (4). In addition, the data suggest that specimen size may be an important factor in establishing the influence of air void content on fatigue life.

TABLE 1 - PHYSICAL PROPERTIES OF 85-100 PENETRATION GRADE ASPHALT CEMENT

(a) Before Mixing*

Test	
Specific Gravity	1.01
Penetration at 77°F (100 gms, 5 sec) - dmm	92
Penetration at 39.2°F (200 gms, 60 sec) - dmm	33
Viscosity at 140°F - 10^3 poises	1.33
Viscosity at 275°F - centistokes	276
Rolling thin film oven test, 75 min, 325°F	
weight loss - percent	0.19
retained penetration - percent	57.6
viscosity at 140°F - 10^3 poises	3.34
viscosity at 275°F - centistokes	427

(b) Recovered from Mix**

Test	
Penetration at 77°F (100 gms, 5 sec) - dmm	42
Softening point (ring and ball) - °F.	131

* Tests performed by Chevron Research Company, Richmond, California

** Tests performed at Materials and Research Department Laboratories, Sacramento, California.

TABLE 2 - MIXTURE PROPERTIES - LABORATORY PREPARED SPECIMENS, SPECIMEN WIDTH STUDY; TEMPERATURE OF TEST - 68°F

Identification of Mixture	Bending Stress psi	No. of Specimens Tested	Stiffness - 10^3 psi 0.1 sec Load Duration			Air Void Content Percent		
			Mean	Standard Deviation	C_v	Mean	Standard Deviation	C_v
1.5 in. wide specimens	75	10	320.3	39.6	12.3	4.5	0.4	8.4
	100	10	307.0	56.7	18.5	4.6	0.5	10.1
	150	10	274.3	23.8	8.6	4.4	0.3	7.1
	All	30	302.3	45.0	14.9	4.5	0.4	8.8
2.0 in. wide specimens	75	10	320.9	29.2	9.0	4.4	0.4	9.3
	100	10	325.8	52.1	15.9	4.5	0.6	12.9
	150	10	326.6	18.4	5.6	4.4	0.3	7.5
	All	30	324.4	34.9	10.7	4.4	0.4	9.9
2.5 in. wide specimens	75	10	293.5	54.8	18.6	4.9	0.5	9.2
	100	10	280.4	23.7	8.4	4.8	0.5	11.2
	150	10	267.8	8.9	3.3	4.8	0.6	11.4
	All	30	280.5	35.2	12.5	4.9	0.5	10.3
3.0 in. wide specimens	75	10	314.1	40.3	12.8	4.6	0.9	19.1
	100	10	286.9	38.0	13.2	4.6	0.8	17.9
	150	10	267.6	38.7	14.5	4.5	0.7	16.1
	All	30	289.5	42.4	14.6	4.6	0.8	17.2

TABLE 3 - COMPARISON OF COMPUTED AND MEASURED MIXTURE STIFFNESS: TEMPERATURE OF TEST - 68°F; VOLUME CONCENTRATION OF AGGREGATE - 0.855

Identification of Mixture	Bending Stress psi	No. of Specimens Tested	Mean Air Void Content Percent	Stiffness - 10^3 psi		
				Measured		
				Mean	Standard Deviation	Calculated
1.5 in. specimens	75	10	4.5	320.3	39.6	308.7
	100	10	4.6	307.0	56.7	297.5
	150	10	4.4	274.3	23.8	315.2
	All	30	4.6	302.3	45.0	307.4
2.0 in specimens	75	10	4.4	320.8	29.2	315.2
	100	10	4.5	325.8	52.1	310.3
	150	10	4.4	326.6	18.4	315.2
	All	30	4.4	324.4	34.9	312.3
2.5 in. specimens	75	10	4.9	293.5	54.8	290.8
	100	10	4.8	280.4	23.7	295.5
	150	10	4.8	267.8	8.9	295.5
	All	30	4.9	280.6	35.2	292.8
3.0 in. specimens	75	10	4.6	314.1	40.3	303.8
	100	10	4.6	286.9	38.0	306.7
	150	10	4.5	267.6	38.7	311.0
	All	30	4.6	298.5	42.4	307.4

TABLE 4 - FATIGUE DATA - SPECIMEN WIDTH STUDY;
TEMPERATURE OF TESTS - 68°F

Identification of Mixture	Bending Stress psi	No. of Specimens Tested	Fatigue Life - N_f		
			Mean	Standard Deviation	C_v
1.5 in. wide specimens	75	10	318,357	137,749	43.2
	100	10	42,615	38,127	89.5
	150	10	9,459	3,460	36.5
2.0 in. wide specimens	75	10	415,638	206,257	49.6
	100	10	83,532	31,403	37.5
	150	10	10,373	4,467	43.0
2.5 in. wide specimens	75	10	297,195	76,942	25.8
	100	10	78,653	22,211	28.2
	150	10	8,852	1,568	17.7
3.0 in. wide specimens	75	10	406,666	173,779	42.7
	100	10	114,809	65,985	57.5
	150	10	12,965	6,288	48.5

TABLE 5 - RESULTS OF REGRESSION ANALYSIS ON FATIGUE DATA, SPECIMEN WIDTH STUDY; TEMPERATURE OF TESTS - 68°F

Mixture Identification	No. of Specimens	$N_f = k_1(1/\varepsilon_{mix})^{n_1}$					$N_f = k_2(1/\sigma_{mix})^{n_2}$			
		k_1	n_1	Corr. Coef.	Standard Error of Estimate	Standard Error of Coef. n_1	k_2	n_2	Standard Error of Estimate	Standard Error of Coef. n_2
1.5 in. width	29	3.2×10^{-9}	3.80	0.91	0.287	0.327	8.0×10^{14}	5.08	0.92	0.274	0.414
2.0 in. width	30	5.5×10^{-13}	4.89	0.93	0.257	0.366	2.7×10^{15}	5.26	0.96	0.187	0.277
2.5 in. width	30	2.4×10^{-10}	4.19	0.96	0.174	.218	9.0×10^{14}	5.06	0.98	0.116	0.172
3.0 in. width	30	9.7×10^{-10}	4.00	0.97	0.154	0.173	9.3×10^{14}	5.01	0.92	0.269	0.398
All 2.0, 2.5 and 3.0 in. widths	90	2.6×10^{-10}	4.17	0.94	0.233	0.166	1.3×10^{15}	5.11	0.95	0.201	0.172

TABLE 6 - F-TEST - TEST OF THE EQUALITY OF THE POPULATIONS
STANDARD ERROR OF ESTIMATE

Comparison of:	With:		S_1^2	S_2^2	F	n_1	n_2	$F_{\alpha/2}(n_1-1,n_2-1)$	Reject	Accept or Reserve Judgement
1.5 in. wide	2.0 in. wide	σ-N_f	.0750	.0349	2.15	29	30	2.11*		✓
		ε-N_f	.0821	.0660	1.24	29	30	2.11*		✓
1.5 in. wide	2.5 in. wide	σ-N_f	.0750	.0134	5.59	29	30	2.11*	✓	
		ε-N_f	.0821	.0302	2.72	29	30	2.11*	✓	
1.5 in. wide	3.0 in. wide	σ-N_f	.0750	.0723	1.04	29	30	2.11*		✓
		ε-N_f	.0821	.0237	3.47	29	30	2.11*	✓	
2.0 in. wide	2.5 in. wide	σ-N_f	.0349	.0134	2.60	30	30	2.67**		✓
		ε-N_f	.0660	.0302	2.18	30	30	2.10*		✓
2.5 in. wide	3.0 in. wide	σ-N_f	.0349	.0723	2.07	30	30	2.10*	✓	✓
		ε-N_f	.0660	.0237	2.78	30	30	2.67**	✓	

* α = .05
**α = .01

TABLE 7 - t - TEST - SIGNIFICANCE OF THE DIFFERENCE BETWEEN THE SLOPE COEFFICIENTS "b" OR TWO DIFFERENT EQUATIONS

Comparison of:	With:		b_1	b_2	n_1	n_2	t	$t_{\alpha/2,(n_1-2,n_2-2)}$	Reject	Accept or Reserve Judgment
2.0 in. wide	2.5 in. wide	σ-N_f	5.26	5.05	30	30	0.62	2.0*		✓
		ε-N_f	4.89	4.19	30	30	1.68	2.0*		✓
2.0 in. wide	3.0 in. wide	σ-N_f	5.26	5.01	30	30	0.52	2.0*		✓
		ε-N_f	4.89	4.03	30	30	2.23	2.39**		✓
2.5 in. wide	3.0 in. wide	σ-N_f	5.05	5.01	30	30	0.09	2.0*		✓
		ε-N_f	4.19	4.03	30	30	0.50	2.0*		✓

* $\alpha = 0.05$
** $\alpha = 0.02$

TABLE 8 - t - TEST - TEST FOR HYPOTHESIS THAT SLOPE OF POPULATION, $\varepsilon - N_f$, REGRESSION LINE HAS A VALUE OF 3.5

Mixture	S_b	b	n	t	$t_{\alpha/2}$, n - 2*	Reject	Accept or Reserve Judgment
1.5 in. beams	0.327	3.80	29	0.92	2.05		✓
2.0 in. beams	0.366	4.89	30	3.79	2.05	✓	
2.5 in. beams	0.218	4.19	30	3.16	2.05	✓	
3.0 in. beams	0.173	4.03	30	3.06	2.05	✓	
2.0, 2.5, 3.0 in. beams	0.166	4.17	90	4.04	2.05	✓	

* $\alpha = 0.05$

ADDITIONAL STUDIES - YGNACIO VALLEY ROAD PAVEMENT

Use of the fatigue subsystem for the design of the Ygnacio Valley Road (designation: 04-cc-800-WC) has been reported in a number of earlier publications (e.g. Ref. 1). Since this pavement has now been in service for approximately 2-1/2 years, measurements and observation of performance have the potential to provide important "feedback" to the design process as illustrated in Fig. 1.

This section presents the results of field measurements by staffs of both the Materials Testing Division of the County of Contra Costa and the Materials and Research Department of the California Division of Highways and analyses of these results using procedures developed as a part of this continuing investigation of pavement response to loading.

Field Testing and Sampling

Traveling Deflectometer deflection data were obtained by staff of the Division of Highways on May 19 and 20, 1970, on sections of the highway. Results of this deflection survey (under 15,000 lb axle load and 70 psi tire inflation pressure) are summarized in Table 9.

In October 1970, three 12-in. diameter asphalt concrete cores were obtained from the pavement (also by staff of the Division of Highways) for laboratory testing. Each core, approximately 13-in. thick, was cut into beam specimens as shown in Fig. 17. In addition, as seen in this figure, portions of the cores were used for asphalt recovery by the Materials and Research Department.

At the time of coring it was also planned to extract undisturbed samples of the subgrade using thin-walled tubes. Because of the excessively stiff nature of the subgrade (much stiffer than anticipated) it was not possible to obtain undisturbed samples. Accordingly, as will be seen subsequently,

TABLE 9 - DEFLECTION SURVEY RESULTS* YGNACIO VALLEY ROAD (04-CC-800-WC)

Location	Mean Deflection - in.		80 Percentile - in.	
	IWT	OWT	IWT	OWT
Sta 115+50 - 120+50 SOL**	0.007	0.011	0.000	0.013
120+50 - 125+50 SOL	0.011	0.011	0.014	0.014
150+00 - 145+00 NOL	0.010	0.012	0.011	0.014
135+00 - 130+00 NOL	0.011	0.012	0.014	0.015
125+25 - 120+50 NOL	0.015	0.014	0.017	0.017
104+00 - 99+00 NOL	0.010	0.014	0.011	0.020
121+50 - 126+50 SML	0.015	0.012	0.020	0.016
133+00 - 138+00 SML	0.011	0.008	0.012	-
152+00 - 147+00 NML	0.009	-	0.011	-
120+00 - 115+00 NML	0.008	-	0.010	-
113+50 - 108+50 NML	0.010	-	0.011	-
134+00 - 139+00 SIL	0.013	-	0.014	-

* May 19 and 20, 1970

** SOL - South Outer Lane
NOL - North Outer Lane
SML - South Middle Lane
NML - North Middle Lane
SIL - South Inner Lane
NIL - North Inner Lane

the stiffness could only be assessed from the deflection measurements using elastic-layered analyses.

At the time the pavement was constructed, thermocouples were installed to record pavement temperatures throughout the depth of the section. The staff of Materials Testing Division of Contra Costa County periodically have recorded such temperatures and a portion of the data which they obtained are shown in Fig. 24. Such measurements provide a check on the efficacy of the temperature simulation program to reasonably predict temperature profiles in thicklift type pavement structures using available weather data.

Laboratory Test Results

Results of tests on recovered asphalt samples performed by staff of the Materials and Research Department are shown in Table 10. To assess the influence of void content on asphalt hardening, recovered penetration have been plotted as a function of an approximate air void content in Fig. 18; the void contents have been termed approximate since they were obtained from beam specimens corresponding to the appropriate depths. With these void data a relationship between depth and air void content for this pavement can also be plotted as shown in Fig. 19.

Stiffness moduli of the beam specimens were determined at three stress levels in repeated flexure at each of three temperatures, 38°, 66°, and 82°F. In these tests a frequency of 100 repetitions per minute and a load duration of 0.1 sec were utilized. Results* are shown in Fig. 20, 21, and 22.

* Detailed results are summarized in Appendix C.

TABLE 10 - PROPERTIES* FROM YGNACIO VALLEY ROAD CORE SPECIMENS

Identification	Penetration at 77°F dmm	Ring and Ball Soft Pt. - °F	Penetration Index
YV-1-B	20	153	+0.4
YV-1-C	43	137.5	+0.4
YV-1-D	47	136	+0.5
YV-1-E	51	132	+0.2
YV-2-A	20	146	-0.3
YV-2-B	23	143	-0.3
YV-2-C	45	124	-1.1
YV-2-D	55	124	-0.8
YV-2-E	34	143	+0.5
YV-3-B	33	141.5	+0.2
YV-3-C	38	140-5	+0.5
YV-3-D**	72	124	0.0
YV-3-E	27	151	+0.8

* Tests performed at Materials and Research Department, State of California Division of Highways, Sacramento, on samples removed from roadway, October 6, 1970.

** Result appears to be out of order for 60-70 penetration grade of the original asphalt.

Moduli were also determined at 66°F using a load duration of 0.05 sec and a frequency of 109 repetitions per minute -- this increased frequency resulting from the maintenance of the same time period between load application as for the 0.1 sec duration tests. Results of these tests are shown in Fig. 23.

It will be noted in Figs. 20 through 23 that stiffness moduli tend to increase with increases in air void content rather than decrease as normally might be expected.

To examine this behavior in more detail, the Shell procedure was used to estimate the range in stiffnesses which might be expected, based on the stiffness characteristics of the recovered asphalts. Data in Table 10 indicate that specimen YV-2-A contained the stiffest (hardest) asphalt while specimen YV-1-D the least stiff material these specimens were designated "hard" and "soft" respectively. With the recovered asphalt properties and the measured properties of the mixtures, stiffnesses were determined for a range in air void contents. The computed stiffnesses have been superimposed on the data of Figs. 20 through 23. These computations indicate that asphalt stiffness has a more significant influence on mixture stiffness than does air void content and accounts for trends in the data shown in these figures.

For the analyses of the response of the pavement structure to load, the mixture was assumed to contain an asphalt with the following characteristics: penetration - 36 dmm; softening point - 136°F. Computed mixture stiffnesses for these conditions are also shown in Figs. 20 through 22. As noted in these figures, the values which have been used define a reasonable range in mean stiffness response.

Pavement Analyses

To simulate pavement temperatures during the period when the deflection measurements were made, weather data for May 19, 1970, were obtained from the weather station at Buchanan Field, Concord, and used in the pavement temperature simulation program developed earlier (5). Computed and measured temperatures are compared in Fig. 24a with reasonable correspondence indicated.

Using the computed temperature profiles, stiffness profiles were determined with stiffness corresponding to a time of loading of 0.1 sec -- a time which should represent reasonably well that associated with the slow speed of the Traveling Deflectometer (used to obtain the deflection measurements). The resulting stiffness profiles are shown in Fig. 24b. It should be noted that in developing these profiles consideration was given to the air void content variation with depth (Fig. 19) -- and hence variation in asphalt stiffness. For this condition, the effect of asphalt stiffness offsets the influence of temperature with the result that mixture stiffness varies only slightly with depth. Accordingly, for the deflection computations, the asphalt layer was assumed to have a uniform stiffness modulus throughout its depth.

Surface deflections were computed for a range in stiffnesses of both the asphalt concrete layer and the subgrade soil using the multilayer elastic analysis (CHEV 5L). Results of these computations are shown in Fig. 25. Also shown in this figure is the range in the mean deflections measured with the Traveling Deflectometer together with the range in stiffnesses of the asphalt concrete. The intersection of the lines defining the limits in stiffness and deflection delineate an area which defines the probable range in subgrade sitffnesses. From Fig. 25 it will be noted that the

subgrade modulus estimated from the computations is somewhat larger than the value of 5,000 psi used in the original analysis* (1). Accordingly, the pavement may exhibit a longer time to first cracking (associated with load) than originally anticipated.

* Difficulties experienced in attempting to sample this material at the time of the deflection measurements, noted earlier, would tend to substantiate this analysis.

DISTORTION SUBSYSTEM

A format for the distortion (permament deformation) subsystem has already been shown in Fig. 2. An alternative way of describing this subsystem is illustrated in Fig. 26.

Distortion can result from a variety of causes. These have been summarized in Table 11* (6) and, as seen in the table, can be grouped into traffic and non-traffic associated causes.

A number of the existing methods of pavement design have as their goal selection of thickness to minimize excessive permanent deformation in any of the components of the pavement structure (e.g., 7 and 8) for the repeated load applications to which the pavement will be subjected. For untreated materials these methods generally involve the measurement of a strength index for each of the components (e.g., "R" values (7) or CBR values (8)); thickness selection is in turn based on data obtained from studies of test roads and in-service pavements which have been correlated to the strength indices. This type of approach, required because of the complex nature of the pavement design, has generally provided adequately performing pavements within the realm of conditions from which the correlations were developed -- viz. the success of the State of California procedure (7).

As a part of the design procedure, the paving mixture must also be designed with adequate resistance to excessive permanent deformation under repetitive traffic loading or standing loads (Table 11). Such design is usually accomplished by selecting the materials to be consistent with

---

* Not necessarily a complete listing of all causes of distortion.

TABLE 11 - EXAMPLES OF THE DISTORTION MODE OF DISTRESS FOR ASPHALT PAVEMENTS

General Cause	Specific Causative Factor	Example of Distress
Traffic-load Associated	Single or comparatively few excessive loads	Plastic flow (shear distortion)
	Long term (or static) load	Creep (time-dependent deformation
	Repetitive traffic loading (generally large numbers of repetitions)	Rutting (resulting from accumulation of small permanent deformations associated with passage of wheel loads)
Non-traffic Associated	Expansive subgrade soil*	Swell or shrinkage
	Compressible material underlying pavement structure	Consolidation settlement
	Frost-susceptible material	Heave (particularly differential amounts)

---

* Soils in this cateogry generally exhibit high shrinkage as well as swell characteristics.

the traffic loading and environmental conditions as well as construction capabilities (e.g., Ref. (9).

Traffic Load Associated Considerations

Uniformly Moving and Standing Traffic. Considering first the design of asphalt mixtures to minimize rutting under uniformly moving taffic, two of the present methods in widespread use (9, 8) have the capability to produce reasonably performing mixtures so long as the actual service conditions correspond to those for which the basic design criteria were developed.

To broaden the range of mixture design, a number of investigators have suggested the use of triaxial compression tests on paving mixtures together with analysis of systems considered to be representative of pavement structures.

Nijboer (10) has used the bearing capacity relationship developed by Prandtl for a material whose strength characteristics are expressed by the equation:

$$\tau = c + \sigma \tan \phi \qquad (1)$$

where:

τ = shear strength, psi or kg per sq cm

c = cohesion, psi or kg per sq cm

σ = normal stress, psi or kg per sq cm

ϕ = angle of internal friction

He suggested a form of triaxial compression testing of the asphalt mix to estimate c and ϕ at the expected maximum temperature to be encountered in the field and at a rate of loading to simulate slow-moving vehicles.

With these parameters, the ultimate bearing capacity of a continuous strip can be estimated from:

$$q_{ult} = c \cdot F(\phi) \qquad (2)$$

where:

q_{ult} = bearing capacity, psi or kg per sq cm

$F(\phi)$ = function dependent on ϕ; e.g., for

$\phi = 25°$, $F(\phi) = 20.7$.

When q_{ult} is made equal to a specific contact pressure, c and ϕ are related as shown in Fig. 27. In this figure, a mixture with a value of c and ϕ lying on or to the right of the curve would be adequate for vehicles equipped with 100 psi tires.

Saal (11) has suggested modification of this relationship recognizing that the bearing capacity for a circular area is larger than that for a continuous strip. The corresponding values for c and ϕ according to this relationship are also shown in Fig. 27.

Smith (12) has presented a relationship between c and ϕ and bearing capacity for a circular area based on a yield criterion rather than a plastic flow condition as in the above formulations. For the same contact pressure, larger values of c and ϕ are required than in the previous case, as seen in Fig. 27. Smith also suggests a minimum angle of friction of 25° to minimize the development of instability from repeated loading.

The relationships suggested by Saal would appear reasonable for standing load conditions with c and ϕ determined from triaxial compression tests at a very slow rate of loading and a temperature corresponding to an average high value expected in service. For moving traffic, Smith's

relationship would appear most suitable; in this case, however, the values for c and ϕ should be developed under conditions representative of moving traffic and an average high temperature expected in service.

Data suggest that ϕ is relative unaffected by rate of loading and the investigations both of Nijboer (10) and Smith (12) indicate a desirable minimum value for ϕ of 25°. To develop ϕ values equal to or greater than this, the aggregate should be rough textured, angular, and well graded. To obtain specific values of c necessary for the conditions of loading, the investigations of Nijboer (10) can be of assistance. He has demonstrated that c increases with an increase in asphalt viscosity; is dependent on the type and fineness of mineral filler (minus 0.074 mm fraction) and increases with an increase in the amount of filler; increases up to a point with an increase in the amount of asphalt; increases with an increase in rate of loading; and increases as the density of the compacted mix increases. Viscosity effects have also been well documented by Speer, et al (13) in tests on a miniature test track; they showed that an increase in asphalt viscosity resulted in a reduction in rutting after 1×10^6 load repetitions over the range in temperature investigated.

The above procedures are limited, however, in that they do not give an indication of the actual maount of rutting which may occur under repetitive traffic loading. Unfortunately no methods presently exist whereby such estimates can be made. Promising procedures include the use of linear viscoelastic theory (14) and an "ad hoc" adaptation of linear elastic theory suggested by Heukeolm and Klomp (15) for asphalt-bound layers and examined more recently by Romain (16).

In the Heukeolm and Klomp procedure, the vertical strain distribution along a vertical axis can be estimated within the asphalt bound layers as

shown in Fig. 28 and permanent deformation determined by means of the equation:

$$\delta_p = \int_n^o f(\varepsilon_v)\, dz \qquad (3)$$

where:

δ_p = permanent deformation

$f(\varepsilon_v)$ = function relating permanent strain, ε_p^*, to total strain, ε_v; $\varepsilon_p = f(\varepsilon_v)$

Such a technique appears useful at this time to assess, at least, the effects of changes in tire pressure and/or gear configuration (and load) on asphalt-bound layers, e.g., Fig. 29. In addition, it may be possible to establish limiting values for ε_p (as required by equation (1)) by comparing computed strains for particular field sections for which well-documented field measurements are avaiable. Like fatigue characteristics, however, it is highly probable that any such criteria established for permanent deformation will be dependent on mixture stiffness (and thus temperature).

While the above techniques have been concerned primarily with the asphalt-bound layer(s), one should also consider procedures and criteria to estimate and/or minimize permanent deformation in other components of the pavement structure.

Dormon and Metcalf (17) have suggested criteria for limiting vertical strain in subgrade soils to minimze excessive permanent deformation at the

---

* In the example shown in Fig. 28, ε_p has been set at 5×10^{-4} in. per in. for illustrative purposes.

pavement surface contributed by the subgrade. These strains, dependent on load repetitions, are shown in Table 12 and were developed from examination of stresses and deformations (using elastic theory) in pavements tested at the AASHO Road Test as well as in pavements designed according to the CBR procedure. From a design standpoint a pavement thickness could thus be established to insure that the strain at the subgrade surface does not exceed the value shown in Table 12 depending on the load repetitions; this procedure is embodied in the Shell Method (18) of asphalt concrete pavement design.

Other investigations have suggested that the subgrade stress may be a reasonable criteria (Vesic and Damaschuk (19) and Kirk (20) -- both based on the elastic analyses of pavements in the AASHO Road Test). No definitive values, however, have been suggested as yet.

Accelerating and Decelerating Traffic. The above analyses have been developed for uniformly moving or standing loads; some additional considerations may be necessary for decelerating or accelerating loads. Results of one such analysis by McLeod (21) for a load with a contact (or tire) pressure of 100 psi are presented in Fig. 30. The terms P and Q are measures of friction between tire and pavement and pavement and base respectively. The curves A and B in this figure indicate the importance of pavement thickness in minimizing this form of instability when a frictionless contact between asphalt concrete surfacing and base is assumed ($P - Q = 1$). As the asphalt concrete thickness increases, the ratio ℓ/t (ratio of length of tire tread to asphalt concrete thickness) decreases, resulting in lower values of c at a given ϕ to prevent instability.

TABLE 12 - SUBGRADE COMPRESSIVE STRAIN VALUES CORRESPONDING TO DIFFERENT LOAD APPLICATIONS*

Weighted Load Applications	Compressive Strain At Surface of Subgrade (in. per in. x 10^{-4})
10^5	10.5
10^6	6.5
10^7	4.2
10^8	2.6

* After Dorman and Metcalf (17).

When P - Q = 0 (full friction between pavement and base -- a more practical situation in well designed and constructed pavements) and the thickness of the asphalt concrete is in the range of 4 to 6 in. (curve C), the more critical conditions are defined by the curve suggested by Smith as shown in Fig. 30.

Nijboer (22) and Saal (11) have considered shoving by decelerating traffic to be the accumulation of permanent parts of successive vicso-elastic deformations and these permanent deformations to occur above a shear strain of one percent for time and temperature conditions critical for shoving (0.33 sec and 122°F for their experience).

Using the relationship:

$$S_{min} = 3\tau \cdot \frac{1}{\gamma} \qquad (4)$$

where:

γ = shear strain (e.g., one percent)

τ = shear (braking) stress at surface

and considering a coefficient of friction between tire and pavement of about 0.5, a minimum stiffness at this time and temperature of about 15,000 psi is indicated for a contact pressure of 100 psi.

Non-traffic Associated Considerations

As seen in Table 12, permanent deformation may result from a number of non-traffic causes. Well-developed procedures are available to estimate settlements resulting from underlying compressible materials. Techniques are also available to estimate depths of frost penetration and pavement thicknesses to minimize the detrimental effects of frost (8). Accordingly, these will not be discussed herein.

For climatic conditions representative of much of California it is possible to estimate the surface distortion of a pavement structure due to volume change in the subgrades using a technique developed by Richards (23) for Australian conditions. Heave (or settlement) can be computed using the suction profile developed at the time of construction, the equilibrium suction profile, and some measure of the moisture content (or void ratio) vs. suction relationship for the subgrade soil. If an expansive soil was expected, such an analysis performed ahead of time would be used to guide the engineer in selecting compaction conditions to guide the engineer in selecting compaction conditions to minimize heave. This procedure may be thought of as a modification (second iteration) to the present California procedure wherein the expansion pressure for thickness selection of portland cement concrete pavement structures is influenced by considerations of field placement conditions (24).

Distress Criteria

As a part of the distortion subsystem, some level of permanent deformation must be established beyond which the pavement is considered unserviceable. For the fatigue mode of distress, initial cracking has been utilized as the measure in the fatigue subsystem described in Report No. TE70-5 (1). While this may provide somewhat conservative estimates of performance since the service life is based on the controlled-stress mode of loading and since results of this type of test include comparatively few repetitions associated with crack propagation, it nevertheless provides a reasonably well defined distress criteria. Such is not the case with distortion, at least at this stage in time.

Some attempts have been made to establish performance criteria for distorion at the AASHO Road Test where slope variance and rut depth were

measured and incorporated in the equation for present servability (25). Other agencies have used visual observations to declare a pavement unserviceable (26).

Generally the level of permanent deformation beyond which the pavement is considered not serviceable should be dependent upon its influence on safety in vehicle operation. Such a point is illustrated in Fig. 31 (27) which shows the ponding of water in the distorted portion of the pavement and which has the potential to lead to "hydroplaning*", as seen in Fig. 32 (28). For such a potential the limiting value for rutting might therefore reflect, in a particular area, the influence of design standards,** surface texture, rainfall intensity and duration together with some measure of traffic intensity.

The subsequent section details some efforts which have been completed to date to establish distress criteria from existing information.

Subgrade Strain Criteria

To minimize load associated distortion (or rutting) at the pavement surface resulting from permanent deformation within the subgrade, one might use the criteria developed by Shell for strain at the surface of the subgrade. These criteria, as noted earlier, were developed using elastic analyses for pavement structures representative of those at the

---

* Water depth of 0.2 in. considered minimum depth for hydroplaning (29).

** For a pavement with a rut approximately 2 ft wide in a wheel path and with a crown slope of 1.5 percent, the allowable rut depth is approximately 3/8 in. at the center of the wheel path for a water depth of 0.2 in. and considering a comparatively smooth surface texture on the pavement surface.

AASHO Road Test as well as those designed according to the CBR procedure. Considering the performance results for the AASHO Road Test in terms of rut-depth, the criteria in Table 12 may be thought to be associated with ultimate rut depths of the order of 3/4 in. If one is not willing to accept these criteria, it is possible to analyze representative pavement structures designed according to some other procedure to establish a different set of strain criteria.

This section contains an analysis of pavements designed according to the State of California procedure to illustrate the establishment of a different set of criteria. Prior to carrying out such an analysis, however, some consideration will be given to the influence of material variables, namely stiffness and Poisson's ratio (since an elastic analysis will be used and, in determining subgrade strain values.

Material Variables. To illustrate the influence of material characteristics, in this case stiffness (or modulus) and Poisson's ratio, on the subgrade strain, values were computed in a two-layer system for a range in subgrade stiffnesses, two different values for Poisson's ratio of the subgrade -- ν_2 = 0.5 and 0.35, and two values of stiffness of the overlying layer. These results are shown in Fig. 33; it will be noted that Poisson's ratio of the subgrade exerts a significant influence on the computed strain values. It should also be noted that this range in Poisson's ratio is that obtained in laboratory tests on subgrade materials for the densities and water contents normally obtained in practice in this area.

In developing the subgrade strain data of Table 12, Dormon and Metcalf (17) used stiffness values for the asphalt bound layer dependent on layer

depth and which ranged from approximately 140,000 psi for a thickness of 2 in. to about 240,000 psi for a depth of 20 in., Fig. 34. These stiffnesses resulted from the use of an assumed value for air temperature of 95°F; the modulus values so determined would correspond to warmest conditions for a moderate climate. For a climate with more severe (hotter) summer conditions, a higher air temperature and therefore a lower modulus should be used, e.g., Fig. 35.

The influence of layer stiffness is also shown in Fig. 34 where subgrade strains have been estimated for stiffnesses of both 100,000 and 200,000 psi. (Note: the 200,000 psi value would correspond to that used by Dormon and Metcalf for a 12 in. thick asphalt bound layer).

Subgrade Strain -- California Designed Pavements. Subgrade strains were estimated in pavements designed according to the State of California procedure assuming each pavement structure to be represented by a multi-layer elastic solid. Variables included (Fig. 36):

(1) Three depths of asphalt concrete, 5, 6, and 7 in.

(2) Three stiffness moduli for the asphalt concrete, 100,000, 400,000 and 900,000 psi.

(3) Three subgrade moduli, 4,500, 10,000, and 20,000 psi

(4) Depths of granular material determined for traffic indices of 8, 10, 12 and 14.

The applied load, Fig. 36, corresponds to an 18,000 lb single-axle load applied to dual tires at a contact pressure of 80 psi.

To reduce the number of sections considered in the analysis, the base course thickness was set at 6 inches and the material was assumed to exhibit a stress vs. modulus relationship corresponding to that for the Class 2 base course aggregate used in the Folsom project (1). Similarly

the relationship for the subbase material was representative of that for the subbase material from the Folsom project.

To develop a correspondence between subgrade stiffness (or modulus) and R value the relationship in Fig. 37 was utilized and is based on an approximate relationship between CBR and R value and the CBR vs. stiffness relationship used by the Shell investigators (E = 1,500 CBR (psi).

Results of the computations (using the CHEV 5L program with stress-modulus iteration) - 108 solutions - are summarized in Table 13 and in Figs. 38 through 40. The Shell criteria from Table 12 are also shown in these figures for purposes of comparison. Generally it will be noted that the strain values are less than those suggested by Shell. It is probable, however, the smaller limiting values of permanent deformation are considered in pavements designed by the California procedure.

In Figs. 38 through 40 some scatter in the computed vertical compressive strains is noted, particularly at lower Traffic Indices. Because of this scatter, additional analyses were performed. These analyses made use of the stiffness vs. depth of asphalt layer relationship used by Shell, Fig. 34. The resulting values are plotted in Fig. 41; rather than using Traffic Index as the abscissa, however, traffic has been expressed in terms of the average daily equivalent 18,000 lb axle load application for some subsequent comparisons. It will be noted that the scatter has been reduced somewhat (data in upper portion of figure).

Earlier it had been indicated that Poisson's ratio exerts a significant influence on the computed vertical strains. In the laboratory it has been observed that Poisson's ratio for subgrade soils may be related to their stiffness moduli, generally decreasing with increase in stiffness. Accordingly some additional computations were performed for the section with the

TABLE 13 - TABLES OF VERTICAL STRAIN IN SUBGRADE *

Subgrade Modulus, psi	For 18K Axle Load on Dual Tires, 80 psi Tire Pressure											
	Traffic Index, TI											
	TI = 8			TI = 10			TI = 12			TI = 14		
	Asphalt Concrete Stiffness, psi											
	1×10^5	4×10^5	9×10^5	1×10^5	4×10^5	9×10^5	1×10^5	4×10^5	9×10^5	1×10^5	4×10^5	9×10^5
	5 in. thick asphalt concrete layer											
4,500	818	617	474	477	402	335	233	217	200	211	199	184
10,000	678	498	372	433	368	295	235	211	187	227	205	181
20,000	500	388	269	410	318	243	228	198	169	235	203	171
	6 in. thick asphalt concrete layer											
4,500	826	508	371	497	384	302	241	214	189	218	197	176
10,000	710	444	307	445	343	260	243	206	174	234	200	169
20,000	546	331	222	434	294	204	235	189	153	237	193	155
	7 in. thick asphalt concrete layer											
4,500	844	497	326	505	357	262	247	207	174	266	191	163
10,000	684	384	248	464	312	222	248	196	156	250	190	153
20,000	489	276	178	422	258	174	236	176	135	242	178	136

* 10^{-6} in/in.

subgrade where stiffness was 20,000 psi. For this condition, Poisson's ratio was assumed equal to 0.35, a not unreasonable value based on available laboratory data. As noted in the lower portion of Fig. 41 this change reduces considerably the scatter in the computed values.

On Fig. 41 a line has been drawn through the data to establish some perliminary criteria that might be utilized for California conditions.

In addition to vertical strains, other criteria are possible, e.g., vertical stress was noted earlier. In examining the data obtained from the computations, a number of different stresses and deformations were examined. A promising factor appears to be the difference between the maximum vertical stress and the minimum horizontal stress occurring at the subgrade surface. The values have been summarized in Table 14 and plotted in Fig. 42 for the condition where the asphalt concrete modulus was 100,000 psi.

Applicability of Subgrade Strain Criteria to Pavement Design Procedures

To compare the subgrade strain criteria established in the preceding section (Fig. 41) with values obtained by different pavement design procedures, thick lift asphalt concrete sections for a specific environmental condition have been designed by the Asphalt Institute (30), Shell (18), State of California (7) and with the fatigue sybsystem described in TE TE 70-5 (1). The environmental and traffic conditions represent those for the Ygnacio Valley Road in Contra Costa County, California. These as well as other necessary data, for the use of the fatigue sybsystem have already been reported in TE 70-5. The resulting designs are plotted in Fig. 43 as a function of average daily equivalent 18,000 lb axle load applications.

Fig. 44 summarizes the subgrade strains determined for three of the four designs of Fig. 43 (California design not included). In this figure

TABLE 14 - STRESS DIFFERENCE ($\sigma_v - \sigma_r$) IN SUBGRADE SURFACE*

Subgrade Modulus, psi	Stress Difference, ($\sigma_v - \sigma_r$) in Subgrade Surface											
	Traffic Index, TI											
	TI = 8			TI = 10			TI = 12			TI = 14		
	Asphalt Concrete Stiffness, psi											
	1×10^5	4×10^5	9×10^5	1×10^5	4×10^5	9×10^5	1×10^5	4×10^5	9×10^5	1×10^5	4×10^5	9×10^5
	5 in. thick asphalt concrete layer											
4,500	3.8	2.8	2.2	2.2	1.8	1.5	1.1	1.0	0.9	1.0	0.9	0.8
10,000	7.2	5.2	3.8	4.5	3.8	3.0	2.4	2.1	1.9	2.3	2.1	1.8
20,000	12.2	8.3	5.7	8.7	6.6	5.0	4.7	4.0	3.4	4.8	4.1	3.5
	6 in. thick asphalt concrete layer											
4,500	3.4	3.3	1.7	2.3	1.8	1.4	1.1	1.0	0.9	1.0	0.9	0.8
10,000	7.4	4.6	3.2	4.6	3.5	2.6	2.5	2.1	1.8	2.4	2.0	1.7
20,000	12.1	7.2	4.7	9.3	6.1	4.2	4.8	3.8	3.1	4.9	3.9	3.1
	7 in. thick asphalt concrete layer											
4,500	3.9	7.3	1.5	2.3	1.6	1.2	1.2	0.9	0.8	1.2	0.9	0.7
10,000	7.3	4.0	2.6	4.8	3.2	2.3	2.5	2.0	1.6	2.5	1.9	1.5
20,000	10.7	5.9	3.8	9.0	5.4	3.6	4.8	3.5	2.7	5.0	3.6	2.8

* psi

it will be noted that sections designed both by the Asphalt Institute and fatigue subsystem procedures exhibit vertical compressive strains less than the Shell criteria and less than or about the same as the California values.

SUMMARY AND DISCUSSION

In this report a number of facets of the pavement design process have been examined.

Results of the beam width study suggest that it may be worthwhile to use larger size fatigue test specimens than used in earlier investigations in order to obtain more uniform test results. Such testing will require equipment (e.g., that illustrated in Fig. 4) with capabilities of testing up to 3 in. by 3 in. beams for aggregates up to 3/4 in. maximum size. In addition, results of this study indicate that the fatigue data obtained from the generalized fatigue diagram reported in TE 70-5 may be somewhat conservative in the lower strain (larger repetitions) area. As a consequence, a somewhat conservative estimate of pavement thickness will be obtained using the generalized diagram. In the analysis of existing pavements shorter lives in fatigue will also probably be obtained. Thus, as emphasized earlier, the generalized diagram should be considered a conservative representation of the fatigue response of California type mixes. Interestingly, however, in the case of thick-lift asphalt pavements, use of this diagram results in thicknesses when compared to those developed by the Asphalt Institute thickness design procedure, which are about the same at a Traffic Index of 7 and approximately 20 percent larger at a Traffic Index of 14.

The investigations associated with the Ygnacio Valley pavement further substantiate that theory together with laboratory measurements can be used to predict the response of the pavement to load and to the effects of temperature.

Analysis of the deflectometer data indicate that the subgrade, at the time the deflection measurements were obtained (May 1970), was stiffer than had been assumed for the initial design. Accordingly, the pavement may

exhibit a longer time to first cracking from repeated loading than originally anticipated.

While techniques for characterizing materials and for analyzing systems representative of pavement structures to predict the accumulation of permanent deformation resulting from traffic loading are not yet available, it is possible to use presently available techniques to make comparative estimates of such response. For example, one could assess the effect of change in tire pressure or gear configuration on rutting in asphalt-bound layers utilizing elastic layered-system theory together with stiffness characteristics of asphalt concrete.

The vertical compressive strain criteria developed from elastic analyase of pavements designed according to the State of California procedure provide criteria which can be used at this time with some confidence. The values so developed tend to be more conservative than the Shell values which may be due to differences in the limiting values of permanent deformation considered in the California design procedure as compared to the Shell procedure -- it has been estimated 3/8 in. vs 3/4 in.

Some aspects of non-load associated permanent deformation can also be examined at this stage in time. For example, it is possible to estimate the surface distortion of a pavement structure due to volume change in the subgrade. Heave or settlement can be estimated utilizing the suction profile developed at the time of construction, the equilibrium suction profile, and some measure of the moisture content (or void ratio) vs suction relationship for the subgrade soil. If an expansive soil was expected, such an analysis performed ahead of construction could also be used to guide the engineer in selecting compaction conditions to minimize heave.

It can thus be seen that while the distortion subsystem of Fig. 2 is not generally as well defined as the fatigue subsystem, specific facets can be readily examined at this stage in time to assist in the making of reasonable engineering decisions regarding either traffic associated or non-traffic aspects of permanent deformation.

ACKNOWLEDGMENTS

The authors wish to acknowledge the support provided this project by the Institute of Transportation and Traffic Engineering of the University of California, Berkeley, in the form of shop and office and research facilities.

The contributions of Mr. Rustu Yuce, on leave from the Department of Civil Engineering of the Middle Eastern Technical University, Ankara, Turkey, and Mr. C. G. Wilmot, Research Assistant, are also gratefully acknowledged.

REFERENCES

1. Monismith, C. L., J. A. Epps, D. A. Kasianchuk, and D. B. McLean, Asphalt Mixture Behavior in Repeated Flexure, Report No. TE 70-5, University of California, Berkeley, 1971.

2. State of California, Division of Highways, Standard Specifications, January, 1969.

3. Monismith, C. L., Asphalt Mixture Behavior in Repeated Flexure, Report No. TE 66-6, University of California, Berkeley, 1967.

4. Kallas, B. F. and V. P. Puzinauskas, "Flexural Fatigue of Bituminous Mixtures" in Fatigue of Compacted Bituminous Aggregate Mixtures - STP 508, American Society for Testing and Materials, 1972.

5. Kasianchuk, D. A., Fatigue Considerations in the Design of Asphalt Concrete Pavements. Ph.D. Dissertation, University of California, Berkeley.

6. Materials Research and Development, Translating AASHO Road Test Findings, Basic Properties of Pavement Components. Wash., D.C.: Dec. 1970. (Highway Research Board NCHRP. Final report project nos. 1-10 and 1-10/1).

7. State of California, Division of Highways, Materials Manual, Vol. I, "Test Method No. California 301-F," September, 1964.

8. U. S. Corps of Engineers. Flexible Airfield Pavements. Wash., D. C.: U. S. Govt. Printing Office, 1958. (EM1110-45-302, pt. 12)

9. California Division of Highways, "Test Method No. 304," in Materials Manual, I, 1963.

10. Nijboer, L. W., Plasticity as a Factor in the Design of Dense Bituminous Carpets. N. Y., Elsevier Publishing Co., 1948.

11. Saal, R. N. J., "Mechanics of Technical Applications of Asphalt," Preprint of Proceedings, Symposium of Fundamental Nature of Asphalt, 1960.

12. Smith, V. R., "Triaxial Stability Methods for Flexible Pavement Design," Proceedings, Association of Asphalt Paving Technologists, 1949, pp. 63-94.

13. Speer, T. L., L. C. Brunstrum, A. W. Sisko, L. E. Ott, and J. V. Evans, "Asphalt Viscosity as related to Pavement Performance," Proceedings, Association of Asphalt Paving Technologists, 1963, pp. 236-247.

14. Moavenzadeh, F. "Damage and Distress in Highway Pavements," In Structural Design of Asphalt Concrete Pavement Systems. Highway Research Board, Special Report No. 126, Wash., D. C.: 1971.

15. Heukelom, W. and A. J. G. Klomp, "Consideration of Calculated Strains at Various Depths in Connection with the Stability of Asphalt Pavements," Proceedings, 2nd International Conference on the Structural Design of Asphalt Pavements, 1967, pp. 155-168.

16. Romain, J. E. Rut Depth Prediction in Asphalt Pavements. Centre de Recherches Routieres: Bruzelles, December 1969. (Research Report No. 150/JER/1969).

17. Dorman, G. M. and C. T. Metcalf, "Design Curves for Flexible Pavements Based on Layered System Theory," In Flexible Pavement Design 1963 and 1964, Highway Research Record 71, Highway Research Board, 1965.

18. Shell Oil Company, Shell 1963 Design Charts for Flexible Pavements, New York: 1963.

19. Vesic, A. S. and L. Dunaschuk, Theoretical Analysis of the Structural Behavior of Road Test Flexible Pavements, NCHRP Report No. 10, 1964.

20. Kirk, J. M., "Analysis of Deflection Data from the AASHO Road Test" Proceedings, Second International Conference on the Structural Design of Asphalt Pavements, 1967.

21. McLeod, N. W., "A Rational Approach to the Design of Bituminous Paving Mixtures," Proceedings, Association of Asphalt Paving Technologists, 1950, pp. 82-224.

22. Nijboer, L. W., "Mechanical Properties of Asphalt Materials and Structural Design of Asphalt Roads," Proceedings, Highway Research Board, 1954, pp. 185-200.

23. Richards, B. G., "Moisture Flow and Equilibria in Unsaturated Soils for Shallow Foundations," In American Society for Testing and Materials, Permeability and Capillarity of Soils, STP 417, Phila; 1967.

24. State of California, Division of Highways, Materials Manual, Vol. I, "Test Method No. Calif. 354-B" April, 1965.

25. Carey, W. N. and Irick, P. E., "The Present Serviceability-Performance Concept," Highway Research Board Bulletin 250, 1960.

26. LeClerc, R. V. and T. R. Marshall, 'A Pavement Condition Rating System and Its Use," Proceedings, The Association of Asphalt Paving Technologists, 1969.

27. Highway Research Board, The AASHO Road Test; Part 5: Pavement Research, Special Report No. 61E. Wash., D. C.: 1962.

28. Horne, W. B., "Tire Hydroplaning and its Effect on Tire Traction," Highway Research Record, No. 214, HRB, 1968.

29. U. S. National Aeronautics and Space Administration, Pavement Grooving and Traction Studies, NASA, SP-5073, Washington, D. C. 1969.

30. Asphalt Institute, Thickness Design - Asphalt Pavement Structures for Highways and Streets, 7th ed. College Park: Maryland, 1963. (Manual Series No. 1).

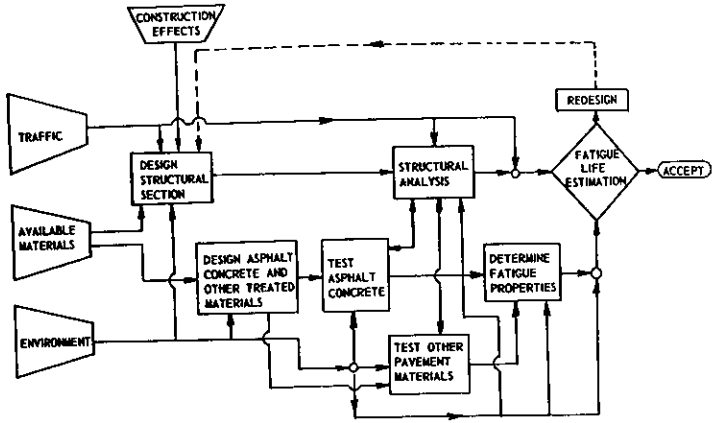

Fig. 1 — Block diagram of a fatigue subsystem.

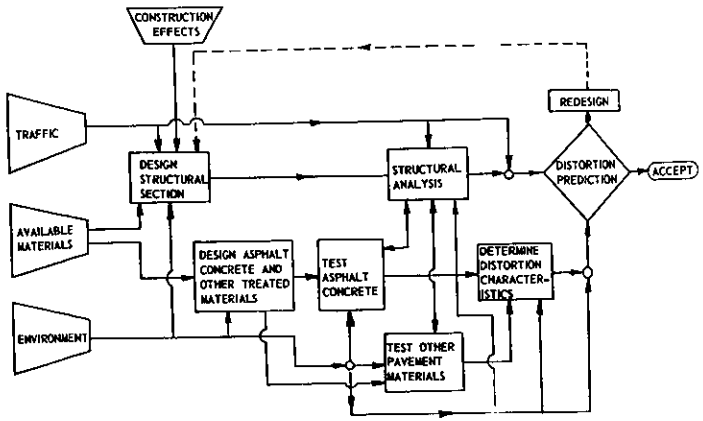

Fig. 2 — Block diagram of a distortion subsystem.

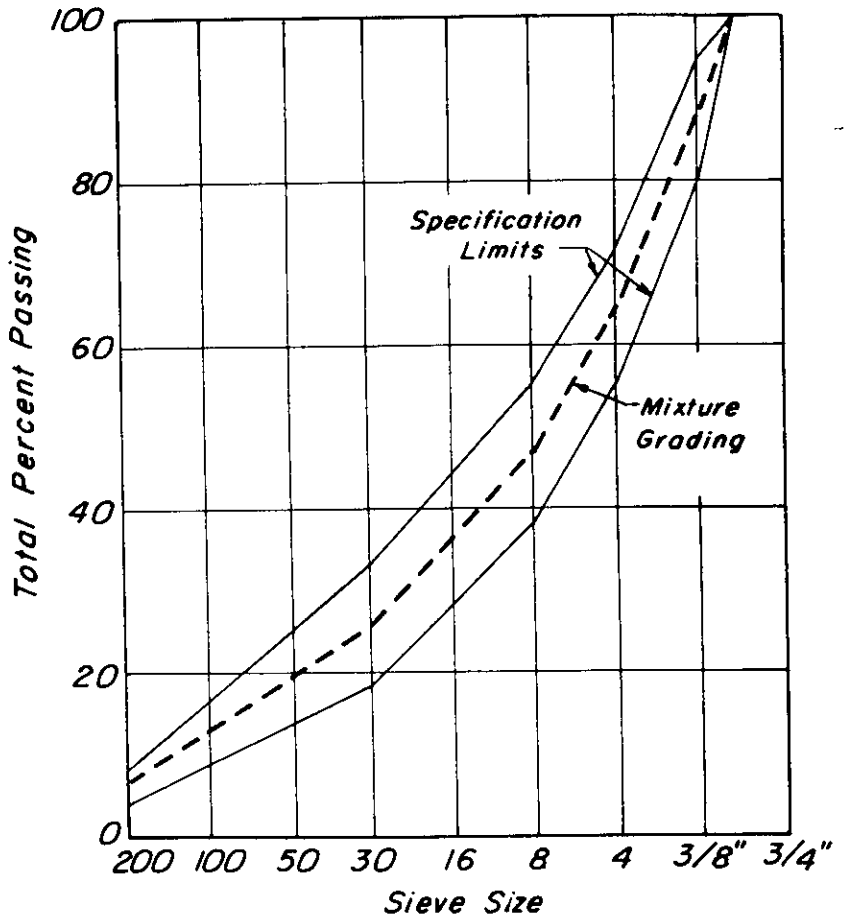

Fig. 3 — Aggregate gradation.

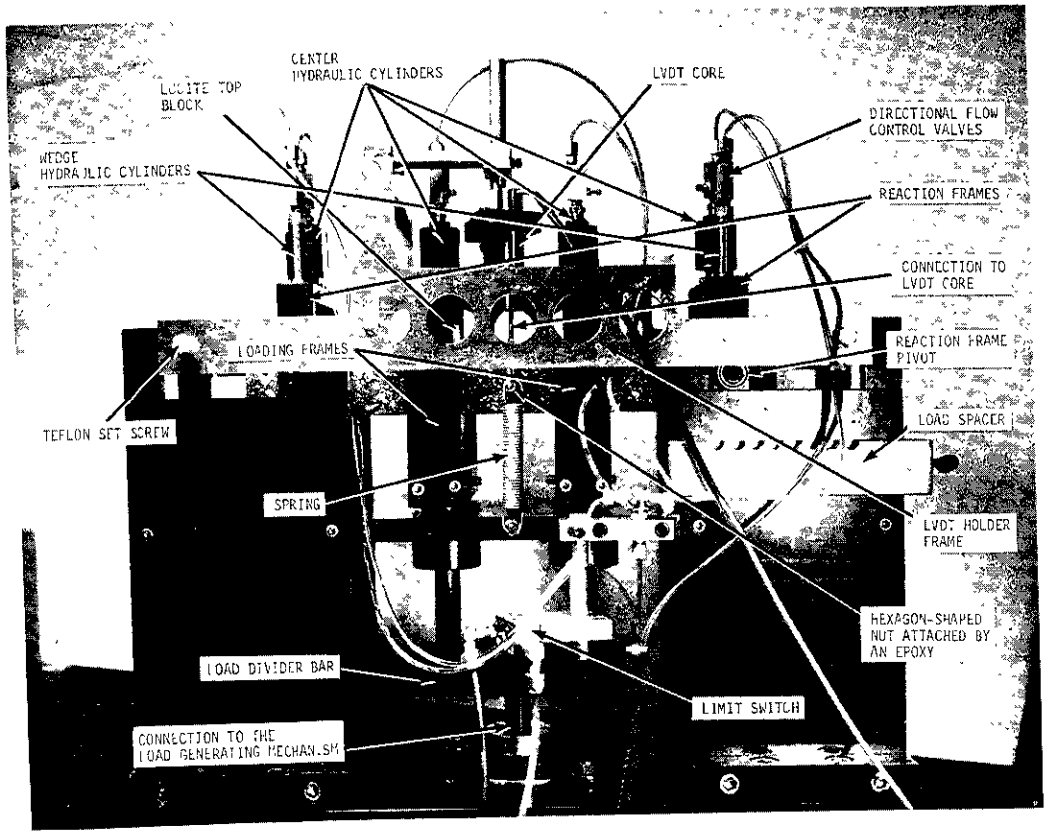

Fig. 4 — Repeated flexure device.

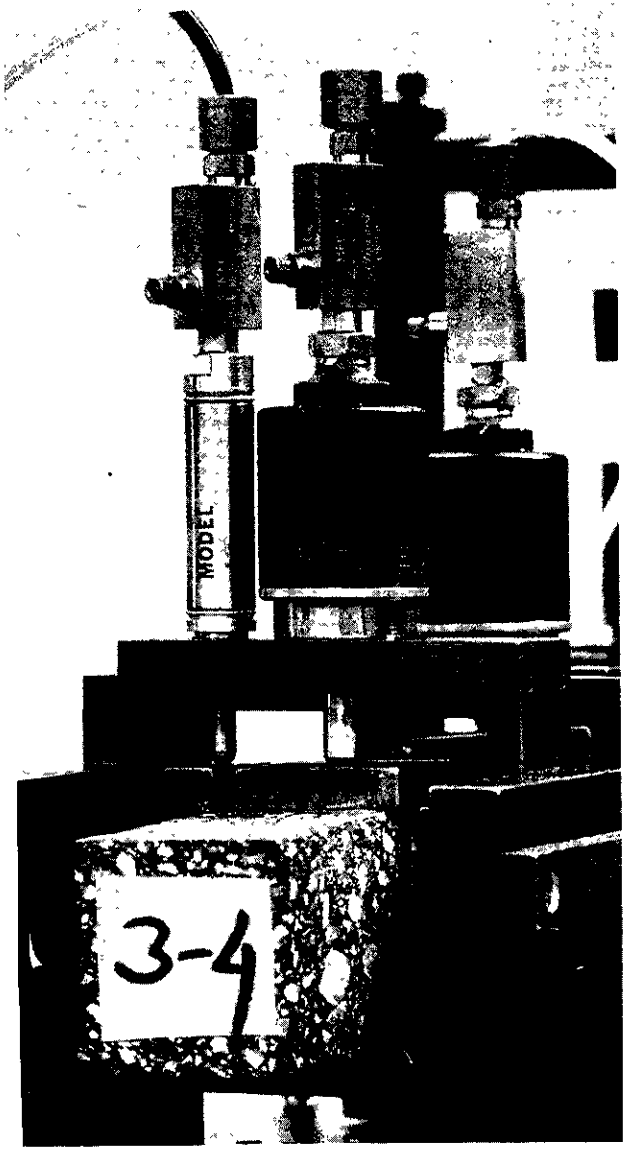

Fig. 5 — Beam clamping system — repeated flexure device.

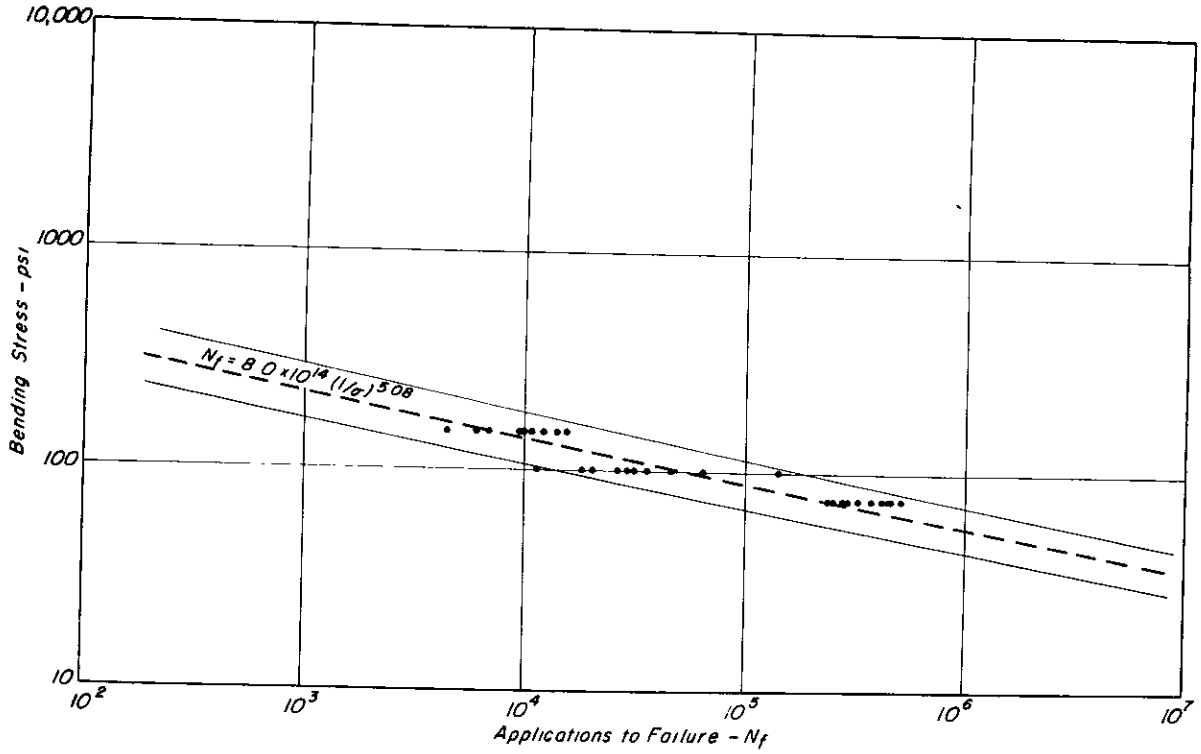

Fig. 6 — Mixture bending stress vs applications to failure controlled stress tests, laboratory prepared specimens, specimen width - 1.5 in., temperature of test - 68°F.

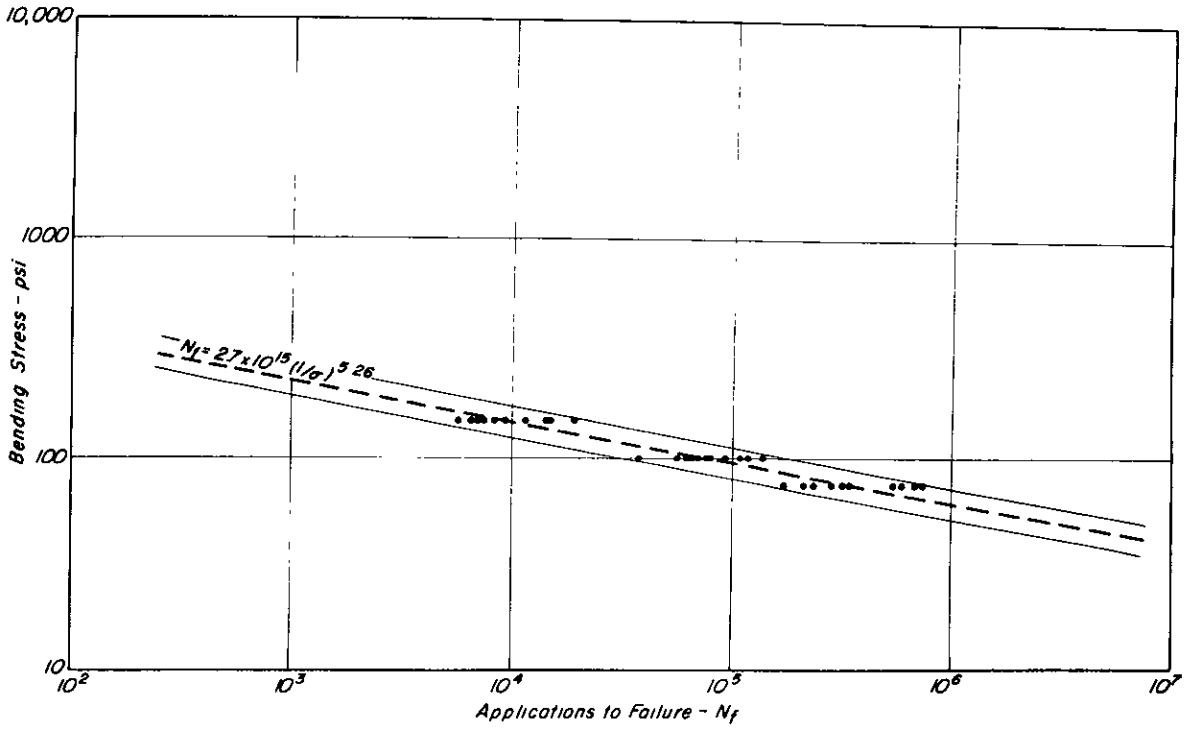

Fig. 7 — Mixture bending stress vs applications to failure, controlled stress tests, laboratory prepared specimens, specimen width - 2.0 in., temperature of test - 68°F.

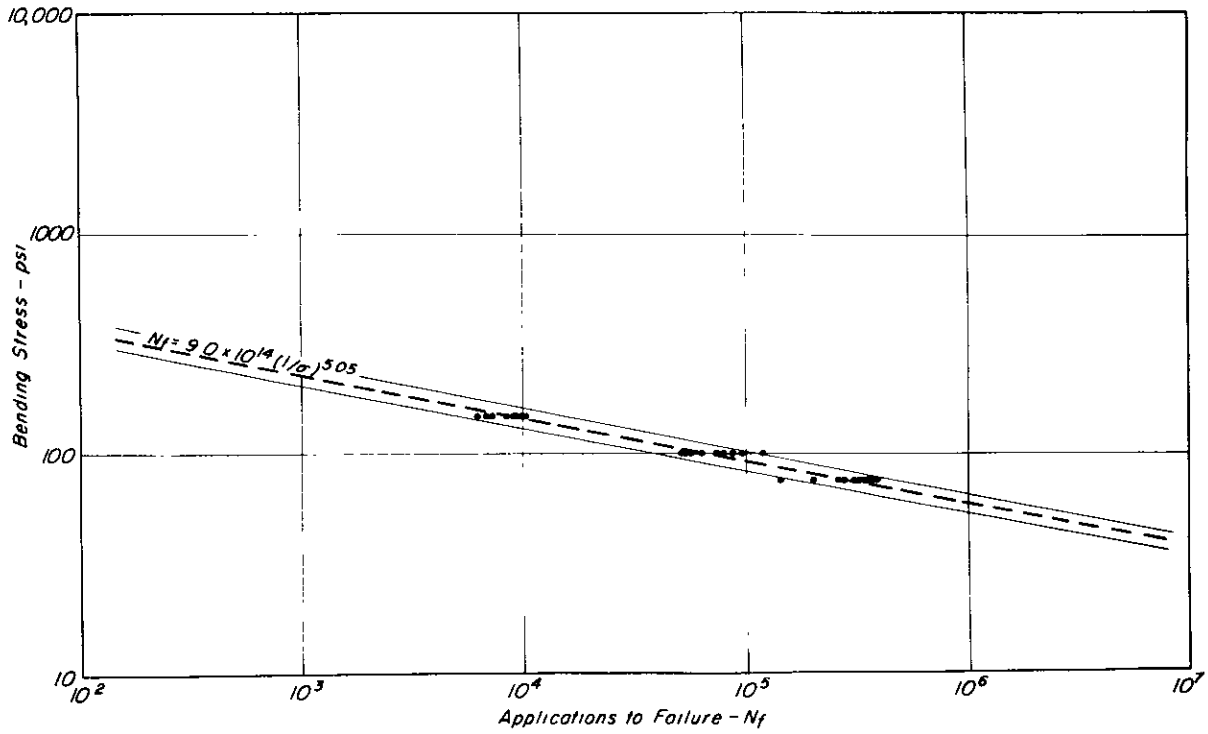

Fig. 8 – Mixture bending stress vs applications to failure, controlled stress tests, laboratory prepared specimens, specimen width – 2.5 in., temperature of test – 68°F.

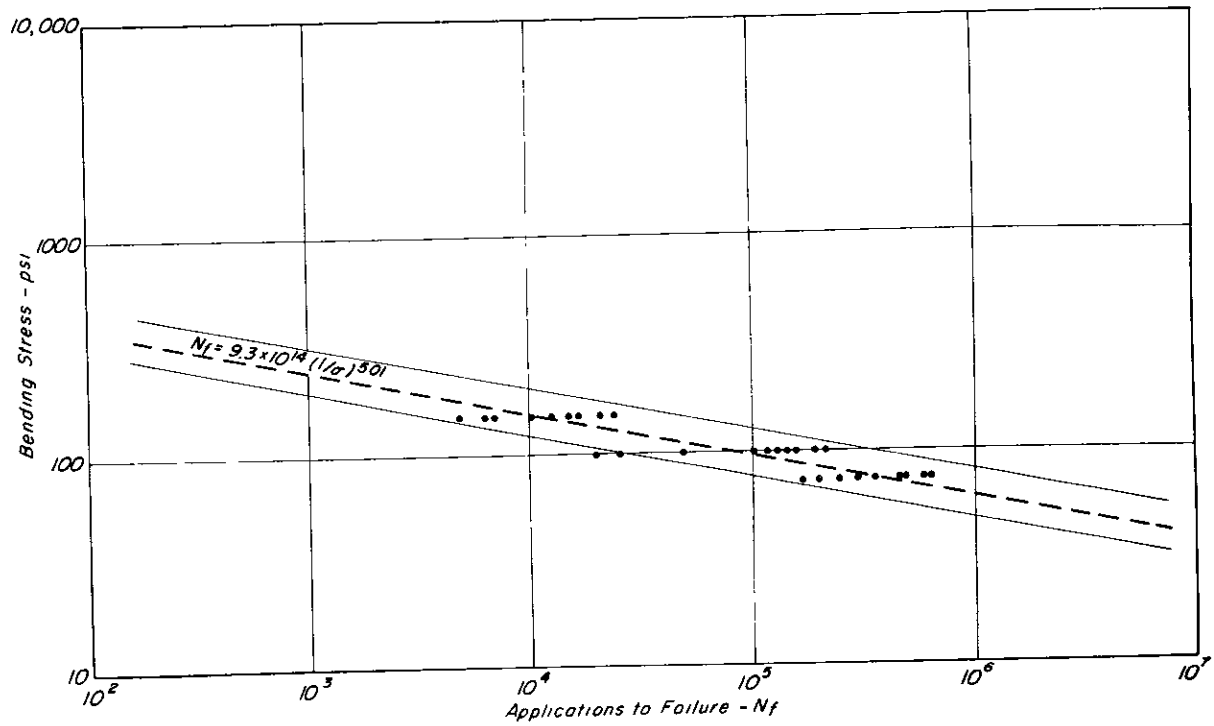

Fig. 9 – Mixture bending stress vs applications to failure, controlled stress tests, laboratory prepared specimens, specimen width – 3.0 in., temperature of test – 68°F.

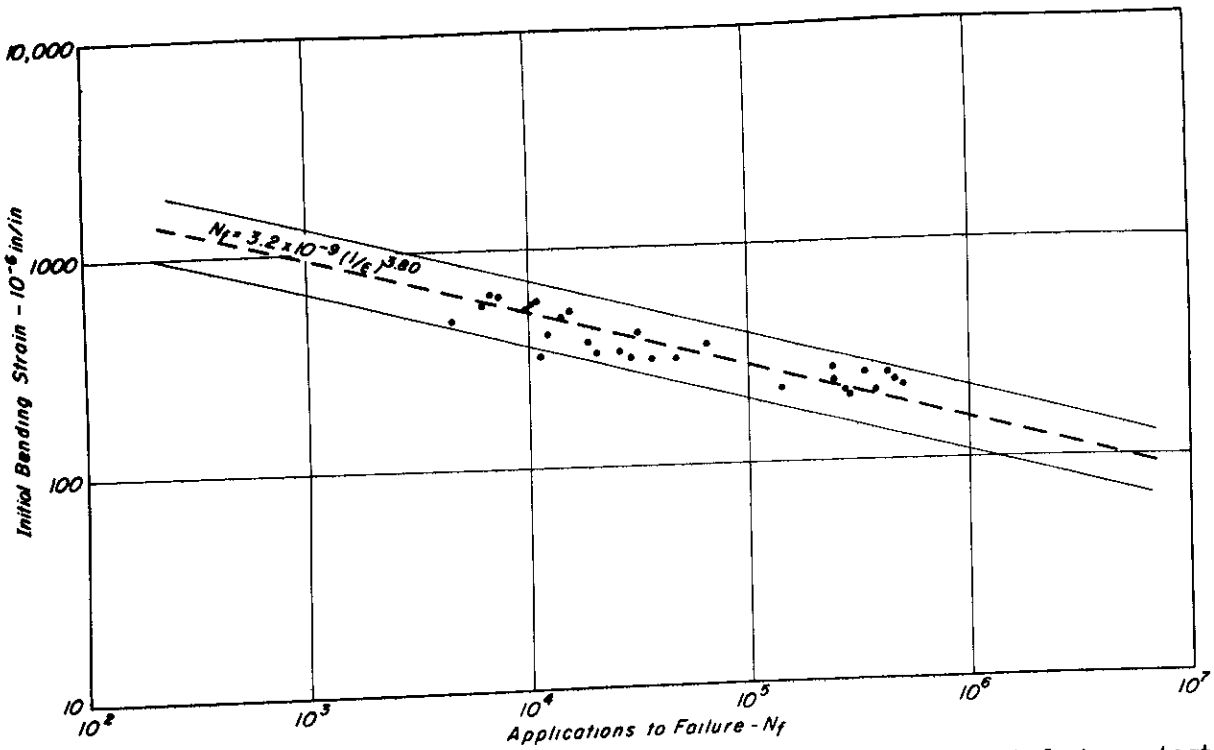

Fig. 10 – Initial mixture bending strain vs applications to failure, controlled stress tests, laboratory prepared specimens, specimen width - 1.5 in., temperature of test - 68°F.

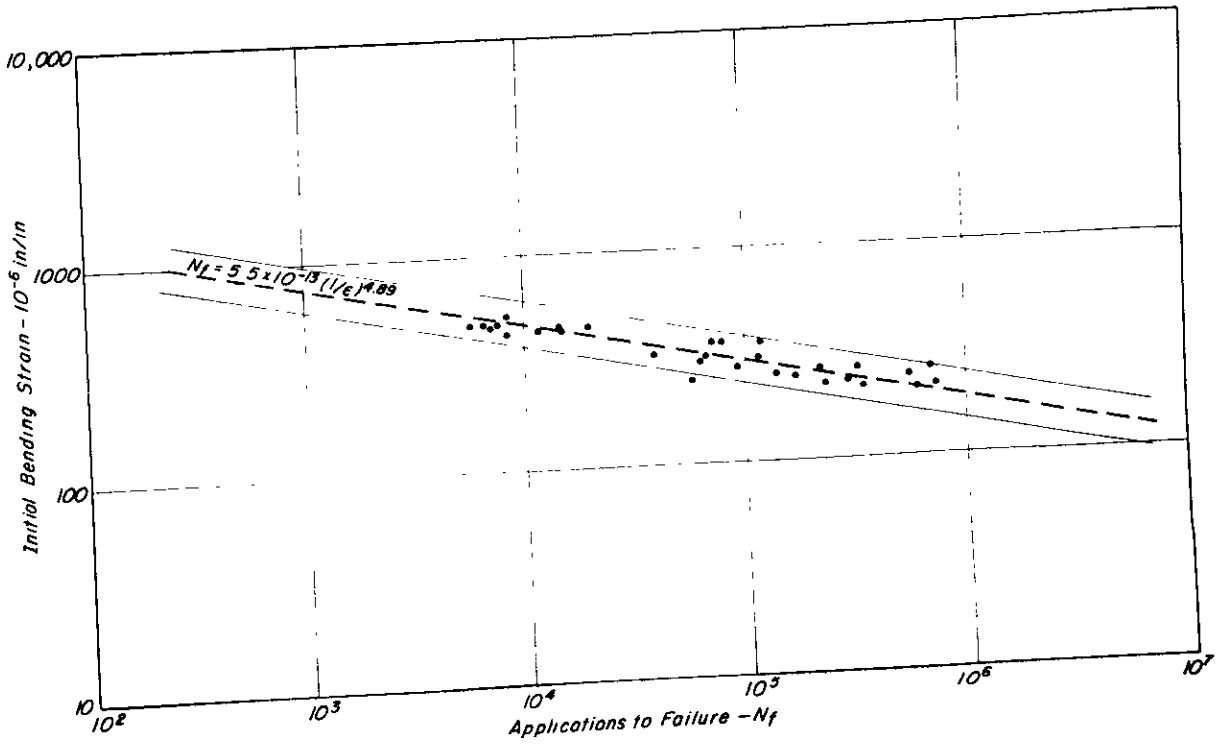

Fig. 11 – Initial mixture bending strain vs applications to failure, controlled stress tests, laboratory prepared specimens, specimen width - 2.0 in., temperature of test - 68°F.

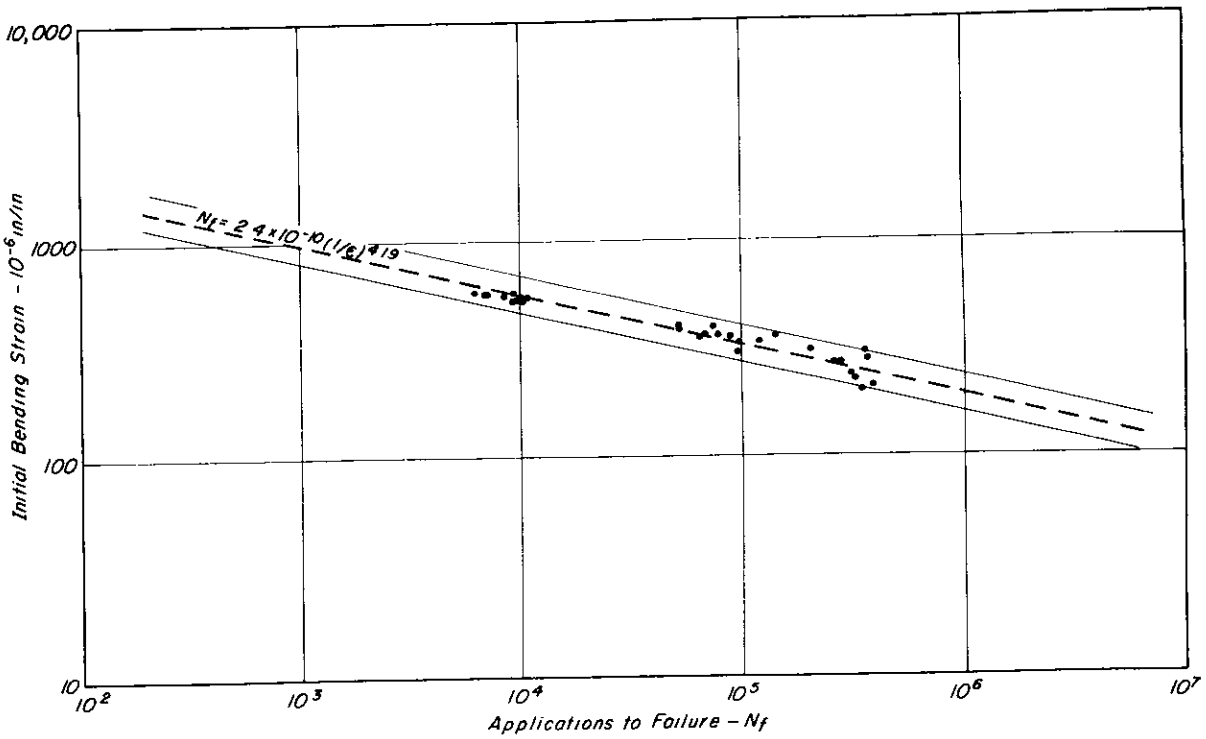

Fig. 12 – Initial mixture bending strain vs applications to failure, controlled stress tests, laboratory prepared specimens, specimen width- 2.5 in., temperature of test - 68°F.

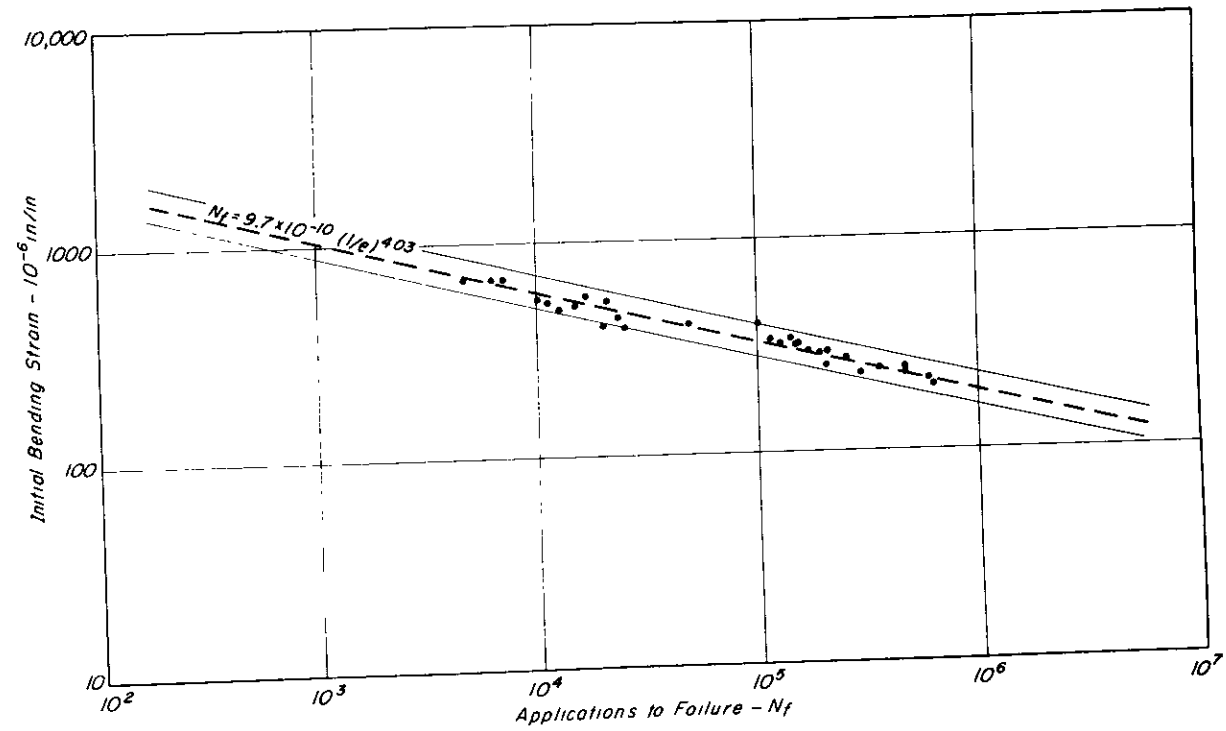

Fig. 13 — Initial mixture bending strain vs applications to failure, controlled stress tests, laboratory prepared specimens, specimen width - 3.0 in., temperature of test - 68°F.

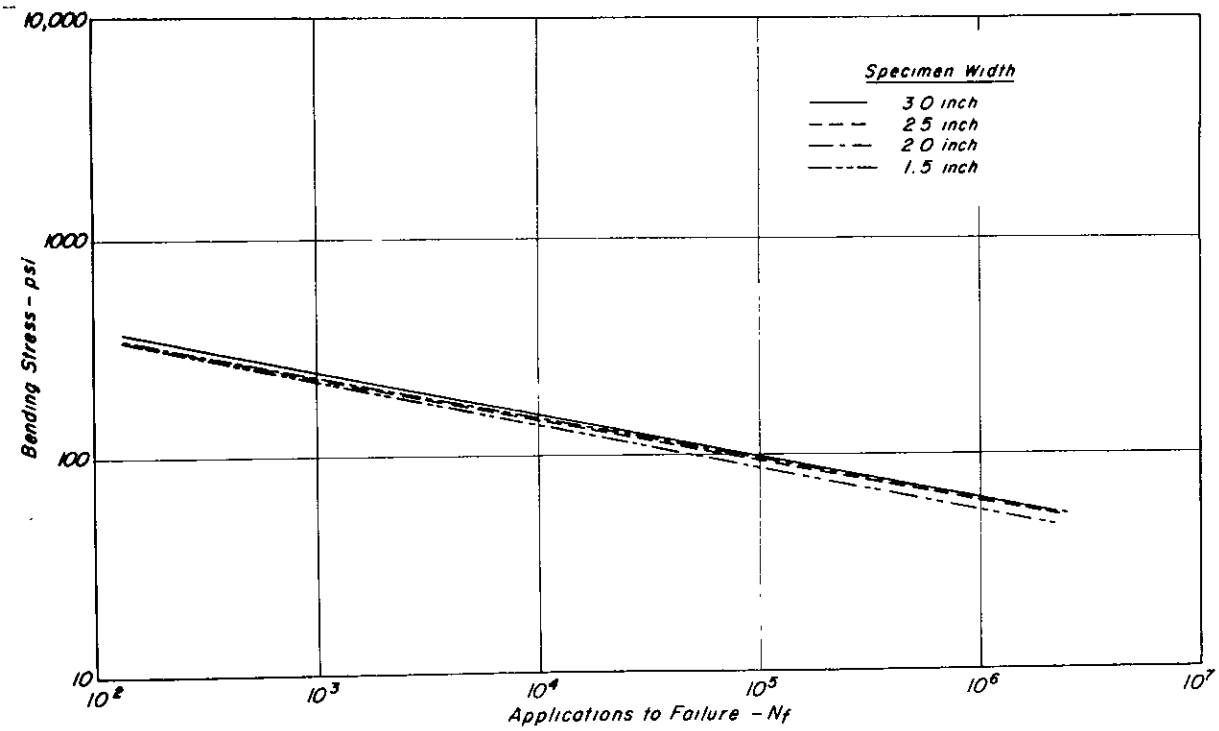

Fig. 14 — Comparison of fatigue test results - stress vs N_f - for specimens with different widths.

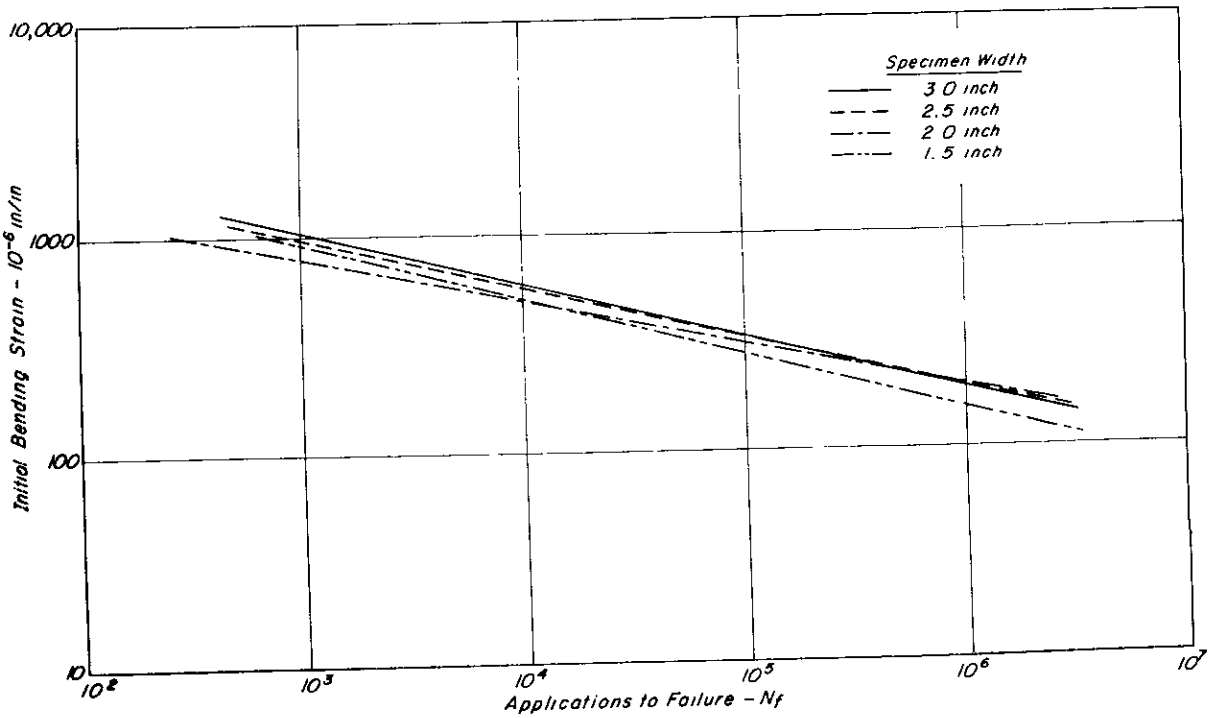

Fig. 15 — Comparison of fatigue test results - strain vs N_f for specimens with different widths.

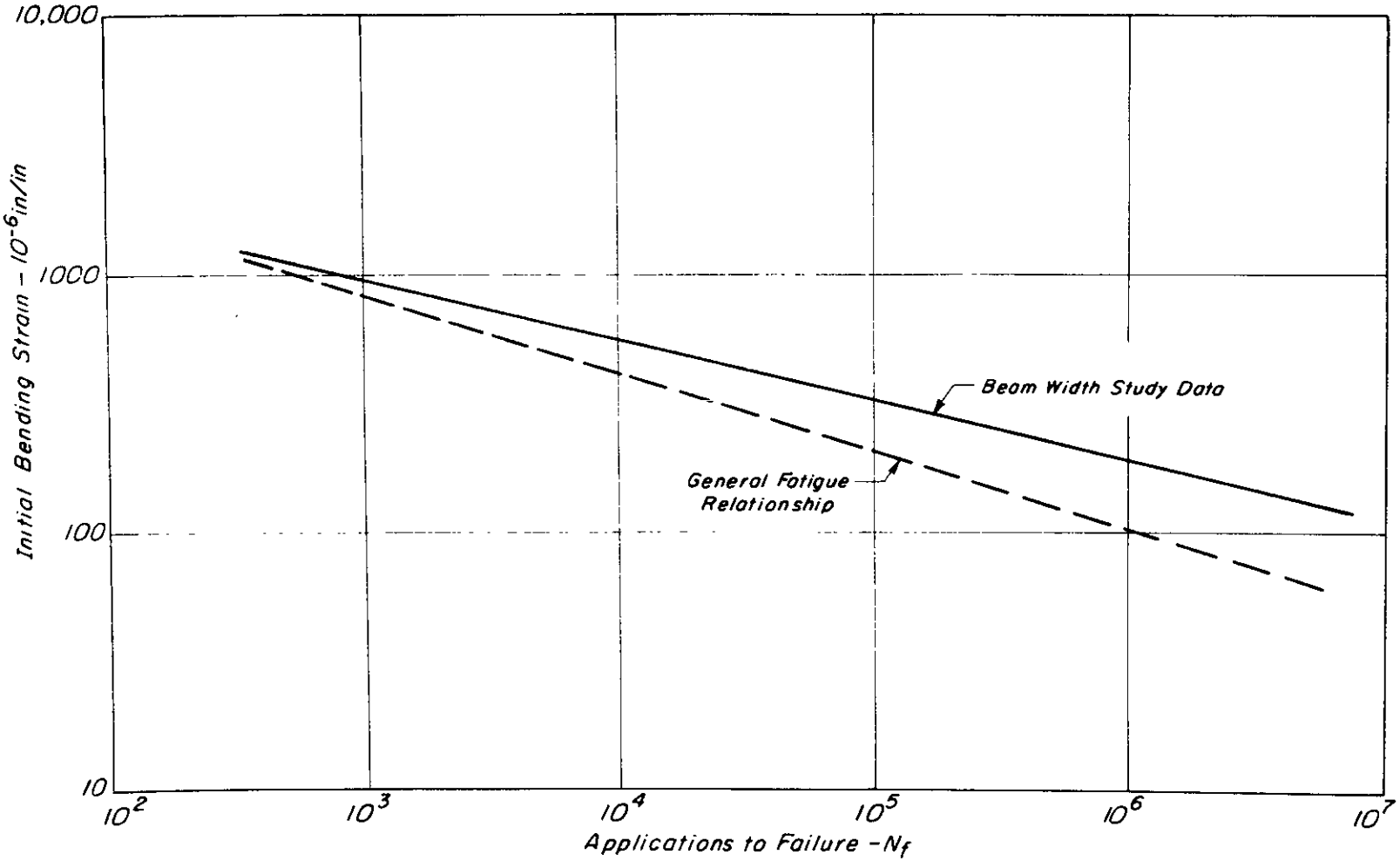

Fig. 16 — Comparison of fatigue curve from beam width study with that from generalized diagram presented in TE 70-5.

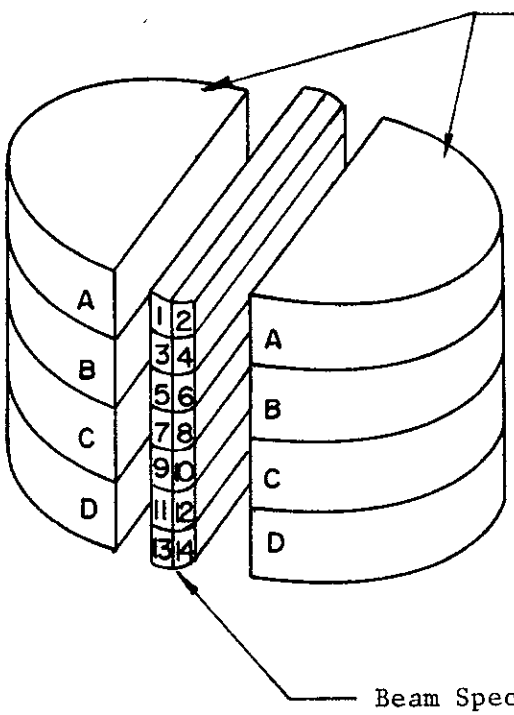

Core Dimensions

Height ≈ 13 inches
Diameter - 12 inches

Specimen Identification Code

YV	-	1	-	12
Ygnacio Valley	-	Site No.	-	Beam No.

YV	-	1	-	A
				Recovery Spec. Code

Site No.	Location
1	Sta 121+06 - RT #1 Lane
2	Sta 127+10 - LT #3 Lane
3	Sta 143+85 - LT #3 Lane

Recovery Specimen	Corresponding Beam Specimens
YV-1-B	1, 2
YV-1-C	3, 4, 5, 6
YV-1-D	7, 8, 9, 10
YV-1-E	11, 12, 13, 14
YV-2-A	1, 2
YV-2-B	3, 4, 5, 6
YV-2-C	7, 8
YV-2-D	9, 10
YV-2-E	11, 12, 13, 14
YV-3-B	1, 2
YV-3-C	3, 4, 5, 6
YV-3-D	7, 8, 9, 10
YV-3-E	11, 12, 13, 14

Fig. 17 — Cutting procedure, sampling location and coding of asphalt concrete cores from Ygnacio Valley Road.

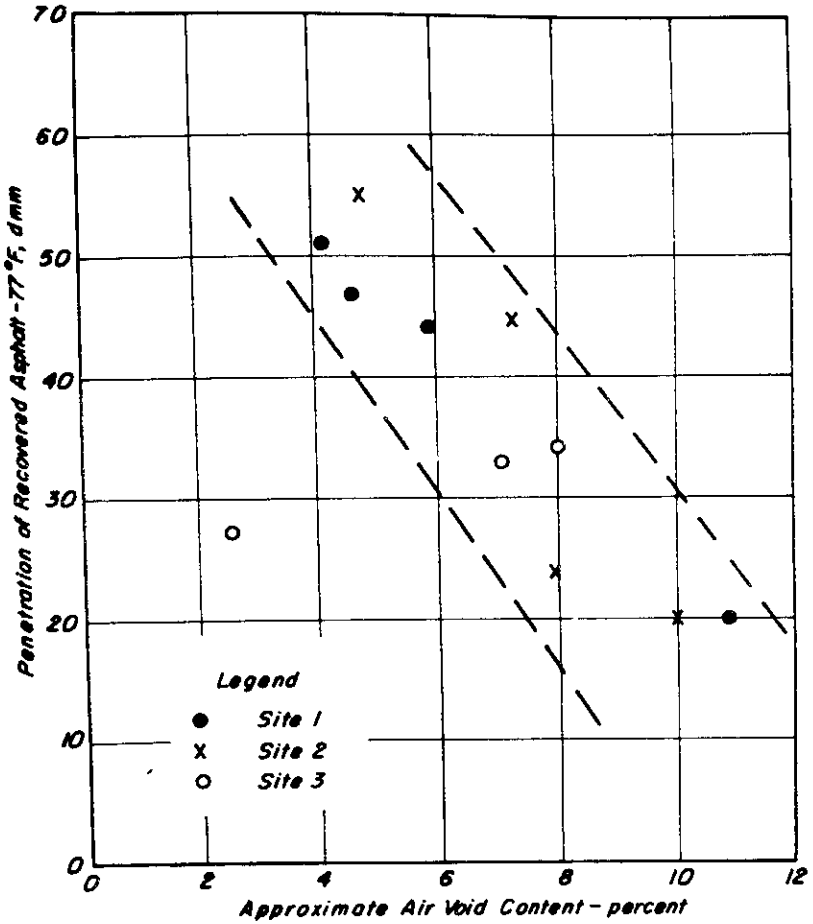

Fig. 18 – Penetration of recovered asphalt vs approximate air void content, Ygnacio Valley Road, 1970.

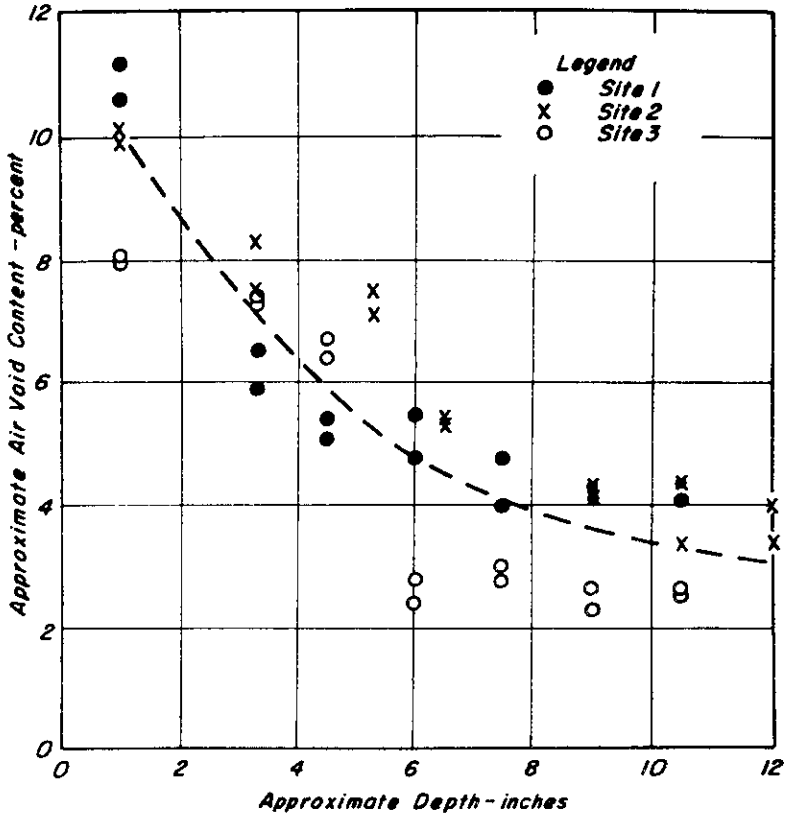

Fig. 19 – Approximate air void content vs pavement depth, Ygnacio Valley Road, 1970.

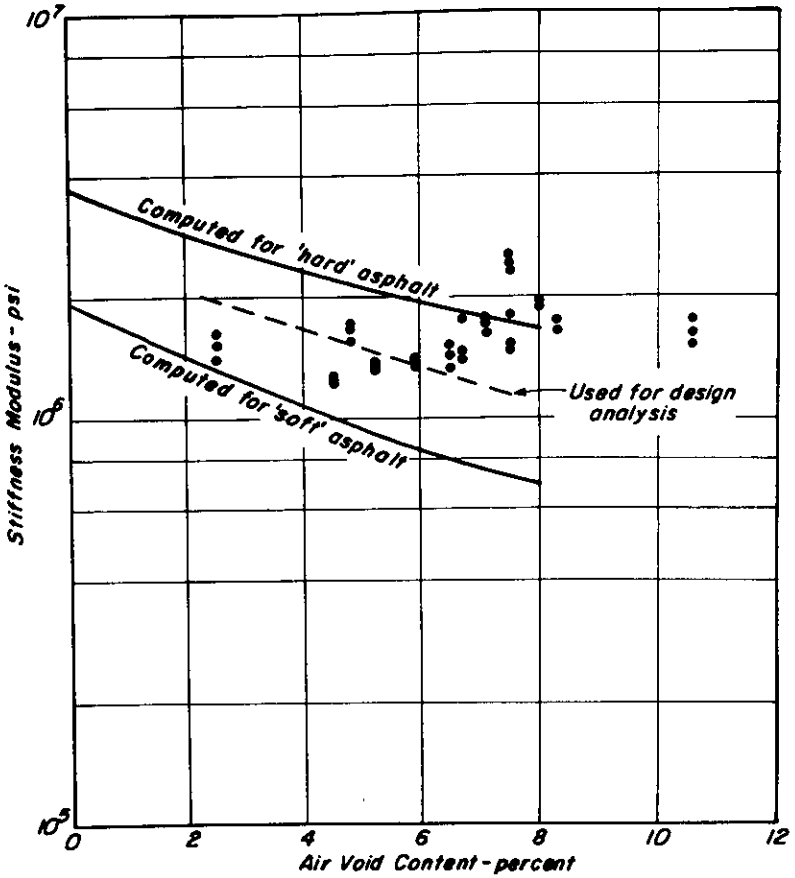

Fig. 20 — Comparison of measured and computed stiffness vs air void content, Ygnacio Valley Road beam specimens; time of loading 0.1 sec.; temperature of test - 38°F.

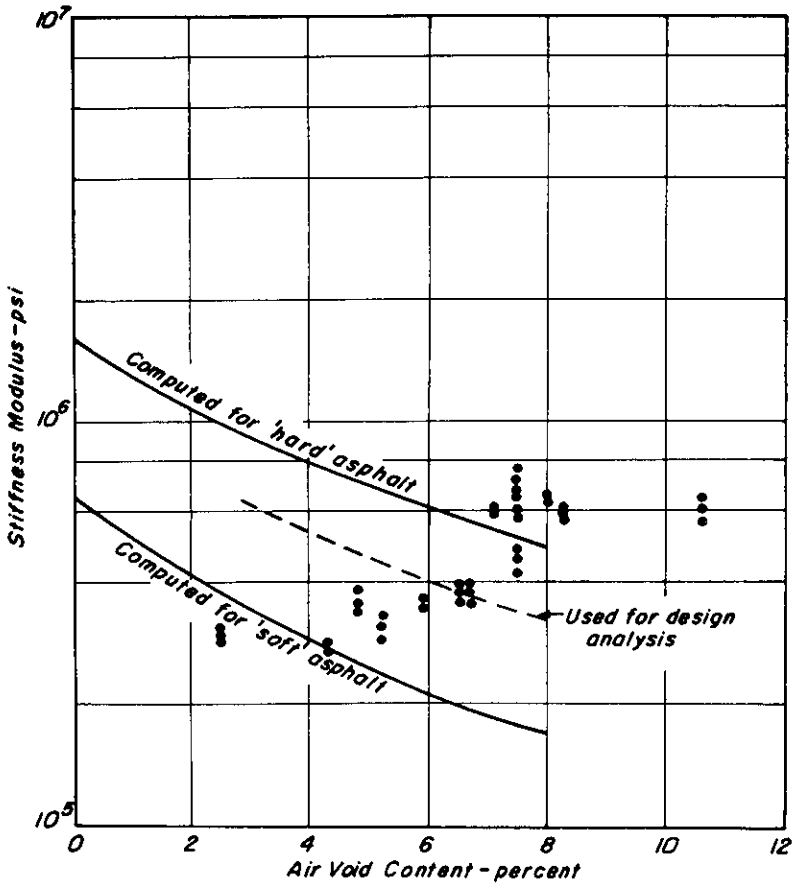

Fig. 21 — Comparison of measured and computed stiffness vs air void content, Ygnacio Valley Road beam specimens; time of loading 0.1 sec.; temperature of test - 66°F.

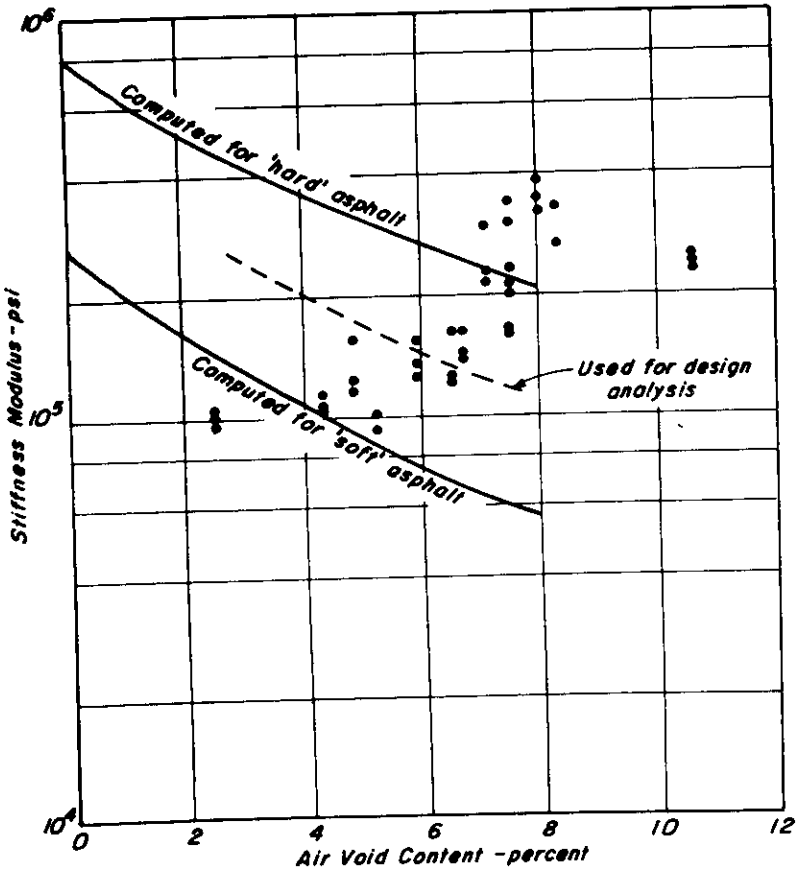

Fig. 22 — Comparison of measured and computed stiffness vs air void content, Ygnacio Valley Road beam specimens; time of loading 0.1 sec.; temperature of test - 82°F.

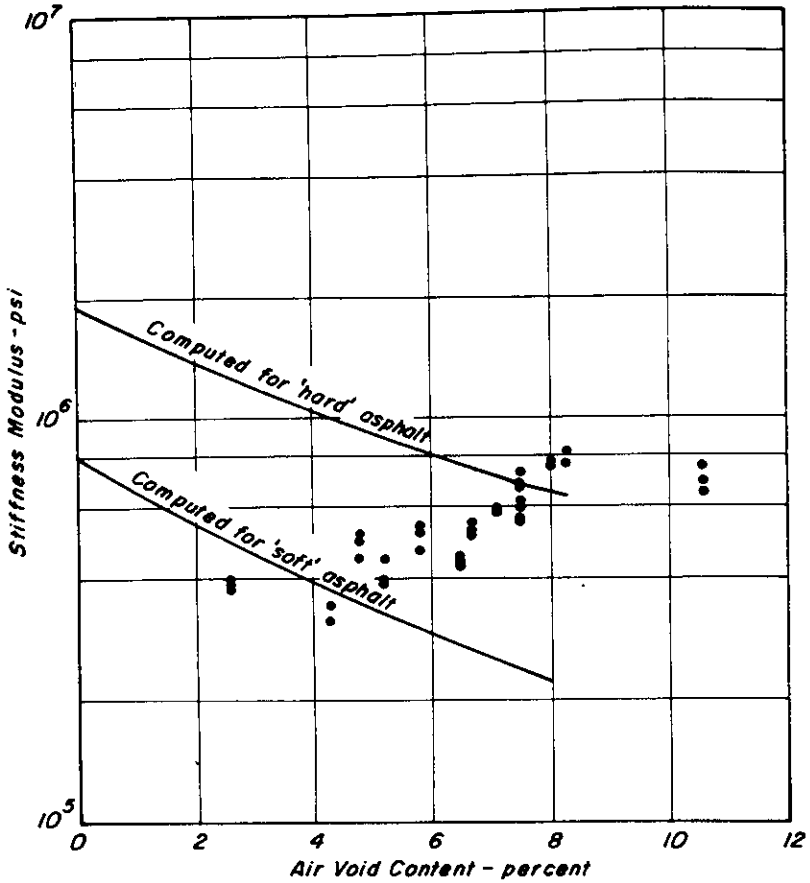

Fig. 23 — Comparison of measured and computed stiffness vs aid void content, Ygnacio Valley Road beam specimens; time of loading 0.05 sec.; temperature of test - 66°F

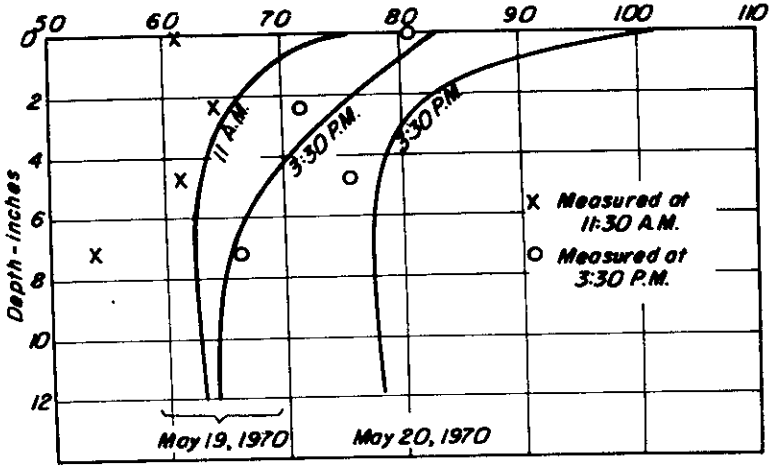

a. Simulated and measured temperature profile.

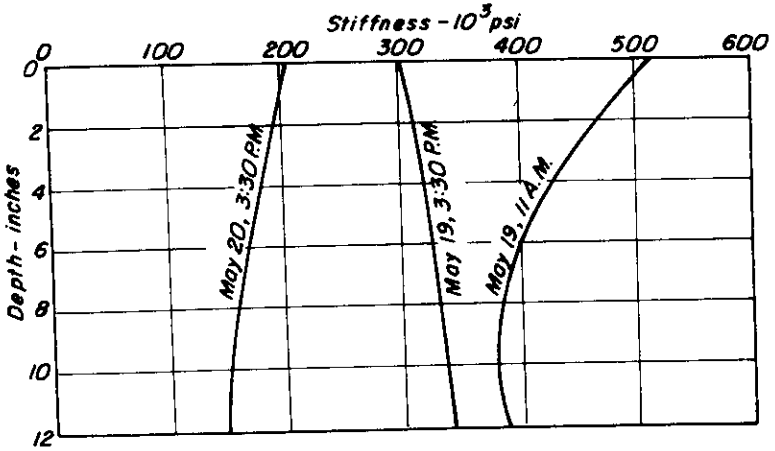

b. Estimated stiffness profile.

Fig. 24 – Temperature and stiffness profiles, Ygnacio Valley Road, May 1970.

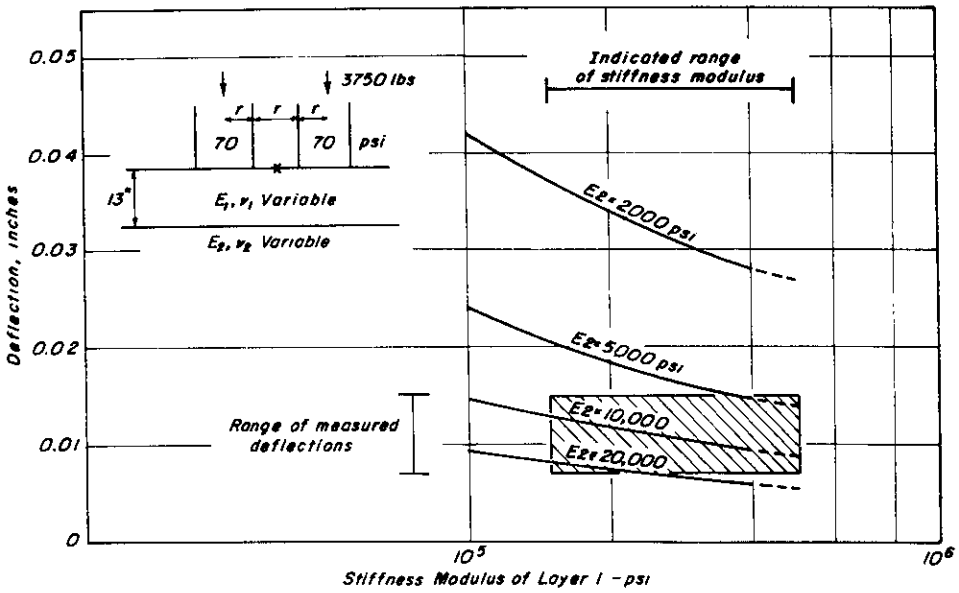

Fig. 25 – Comparison of measured and computed deflections, Ygnacio Valley Road, 1970.

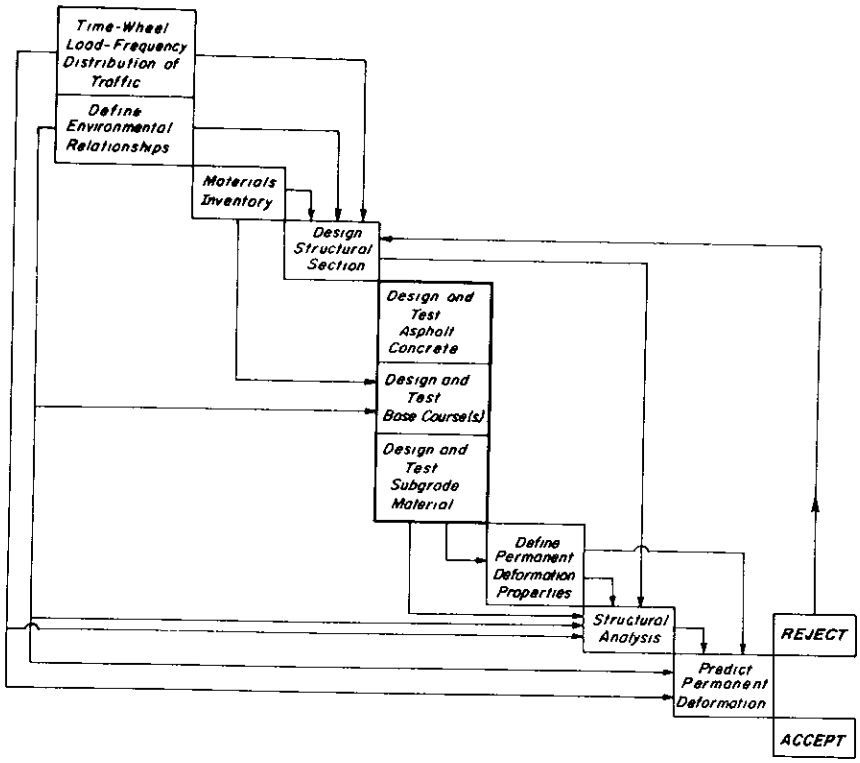

Fig. 26 — Alternative form for distortion subsystem.

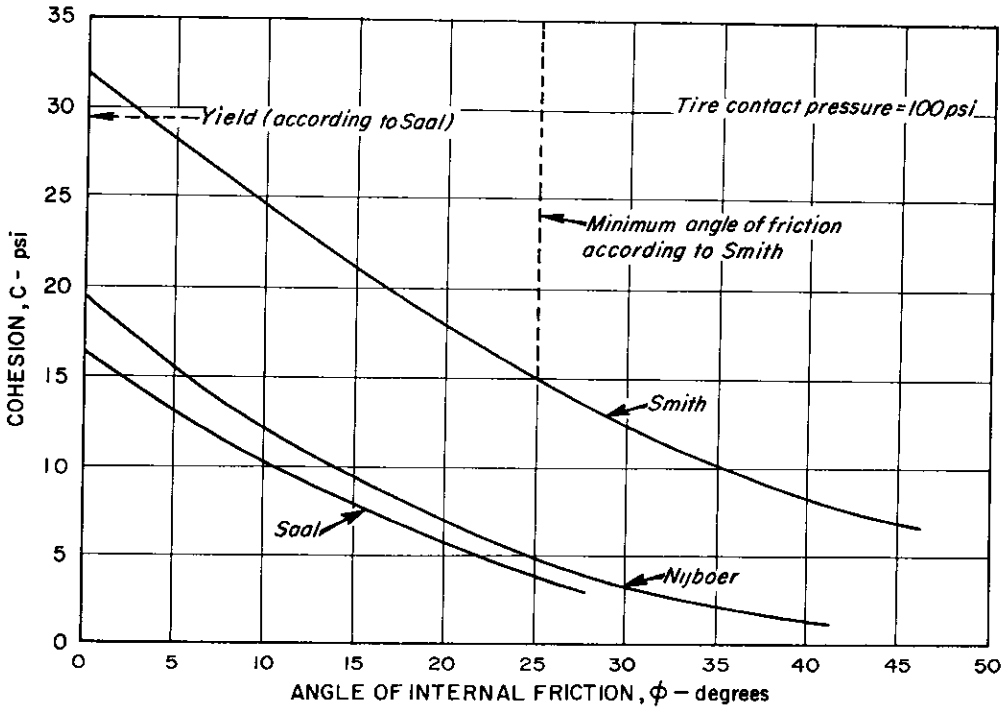

Fig. 27 — Relationship between cohesion and angle of internal friction to prevent plastic flow or overstress at a particular point in an asphalt mixture.

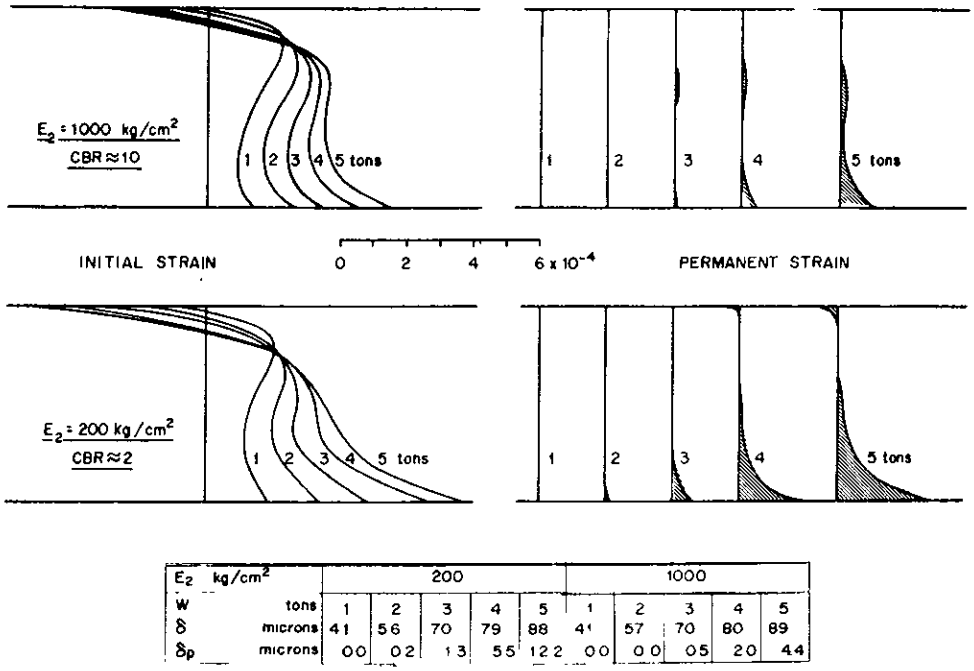

E_2 kg/cm²		200					1000				
W	tons	1	2	3	4	5	1	2	3	4	5
δ	microns	41	56	70	79	88	41	57	70	80	89
δ_p	microns	00	02	13	55	122	00	00	05	20	44

Fig. 28 – Effect of wheel load on initial and permanent deformation (μ = 0.50; h = 30 cm; E_1 = 10,000 kg/cm^2). (After Heukelom and Klomp.)

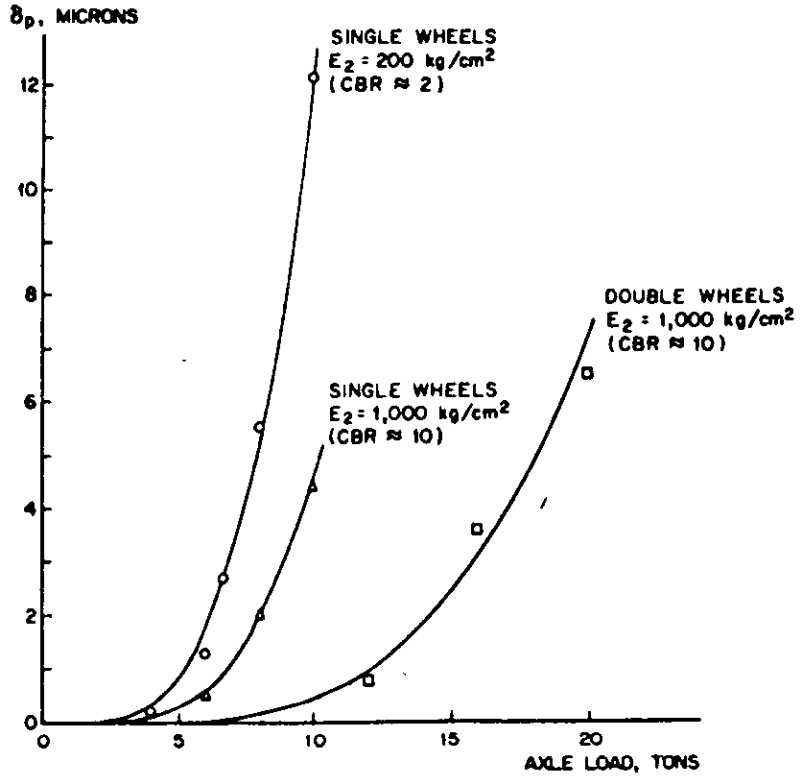

Fig. 29 – Permanent change in thickness as a function of axle load. (Calculated points for μ = 0.50; E_1 = 10,000 kg/cm^2; curves drawn in accordance with (axle load)$^{3.8}$). (After Heukelom and Klomp.)

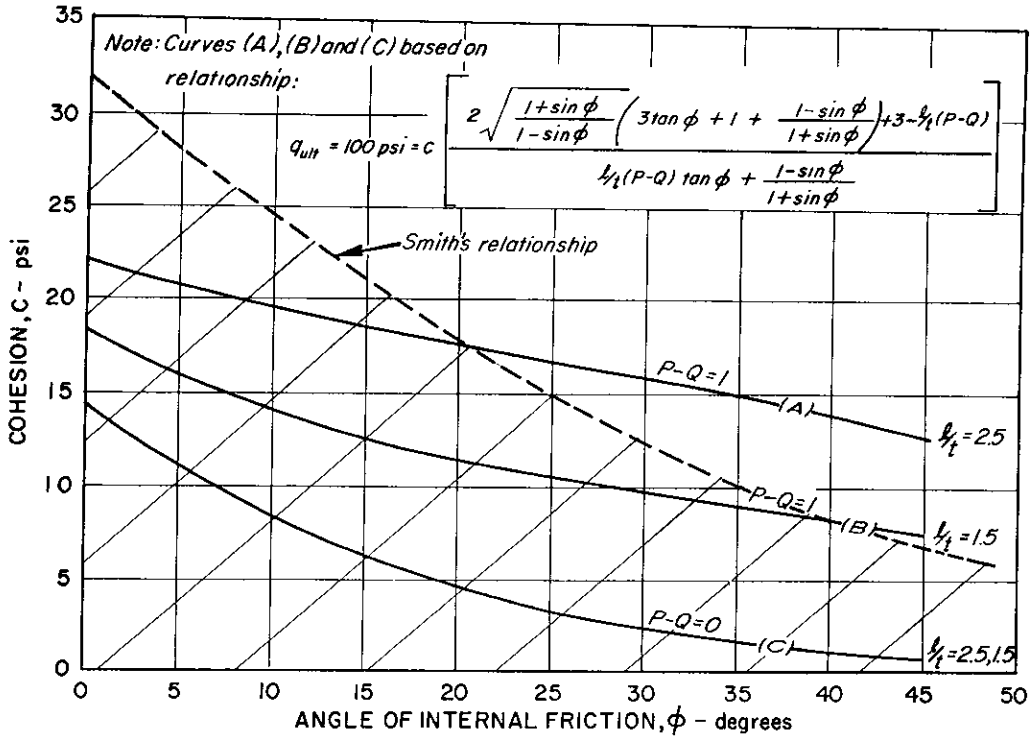

Fig. 30 — Stability curves for asphalt mixtures subjected to braking stresses. (After McLeod)

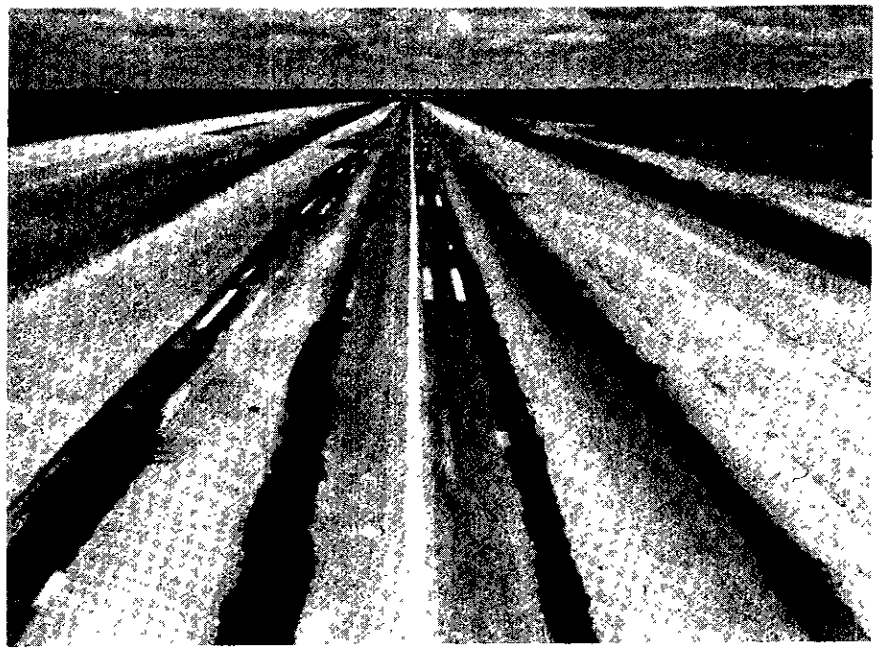

Fig. 31 — Water standing in ruts — asphalt concrete pavement; AASHO Road Test (Ref. (27)).

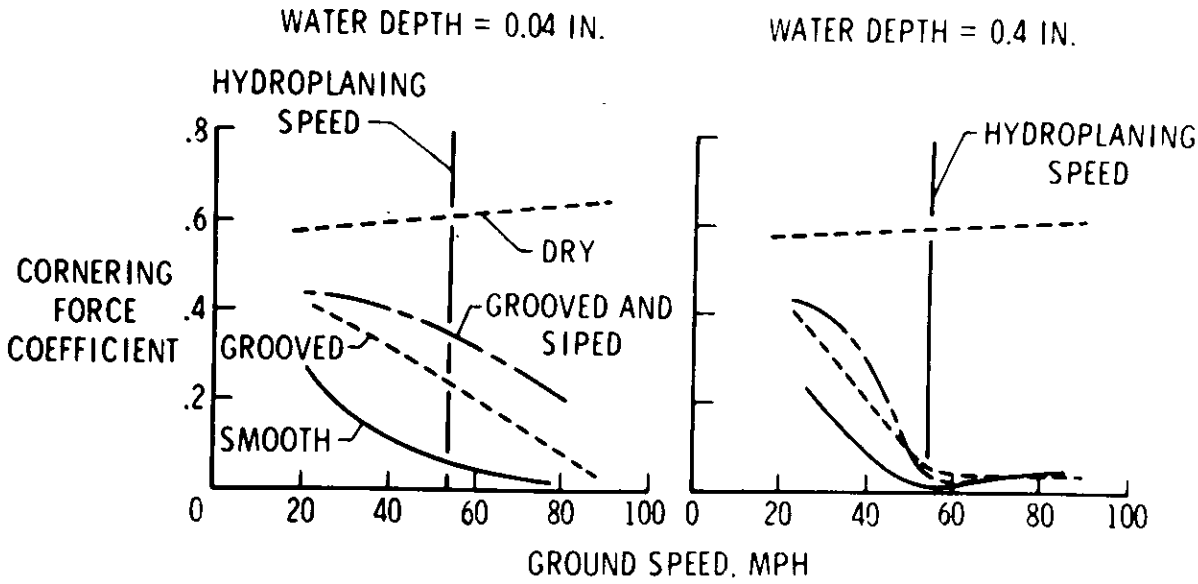

Fig. 32 — Viscous and dynamic pressures predominating (smooth concrete; yaw angle = 6^{o}). (After Ref. (28)).

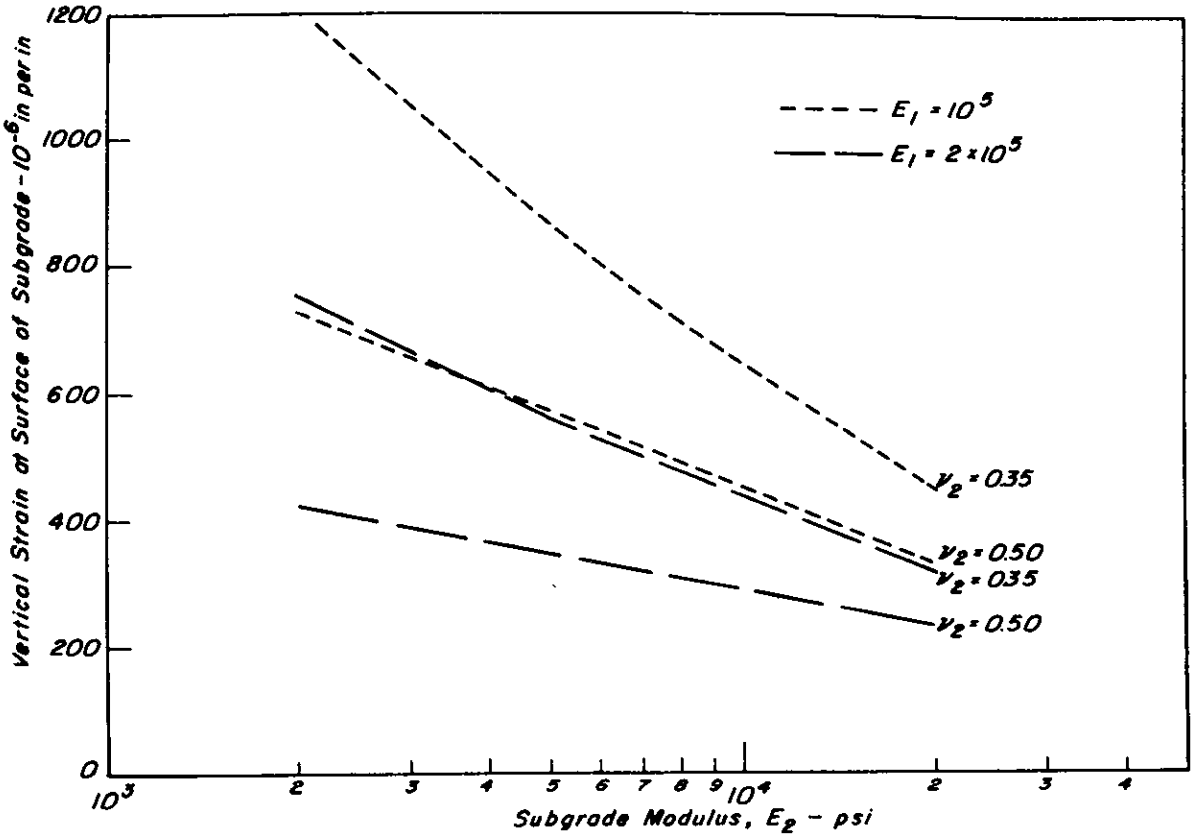

Fig. 33 — Influence of subgrade modulus and Poissons' ratio on subgrade strain.

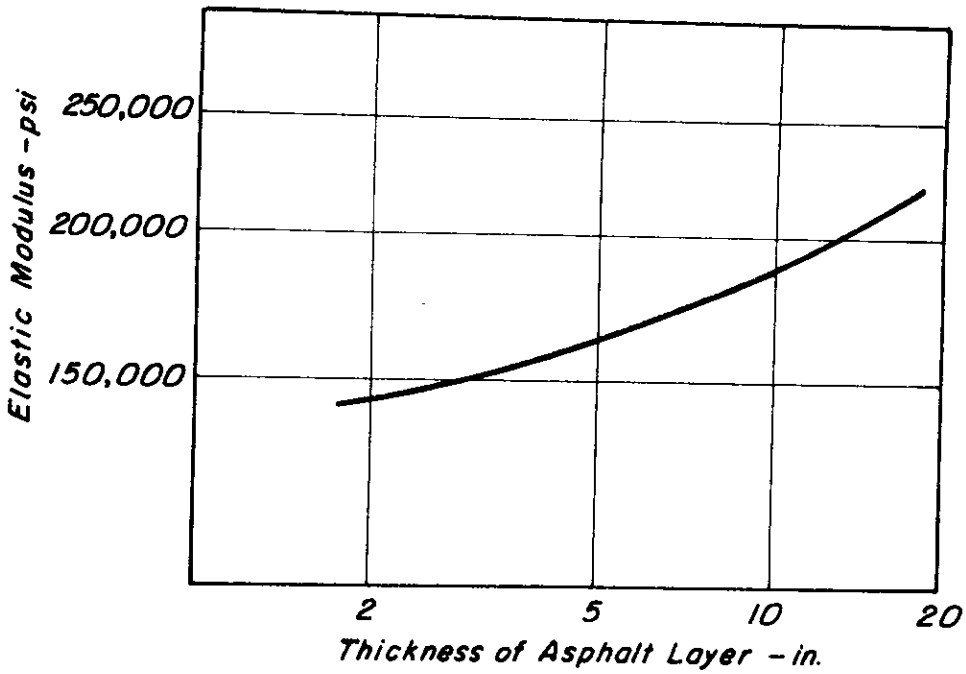

Fig. 34 — Relation of asphalt concrete stiffness (modulus) to thickness of layer, air temperature — 95°F. (After Shell.)

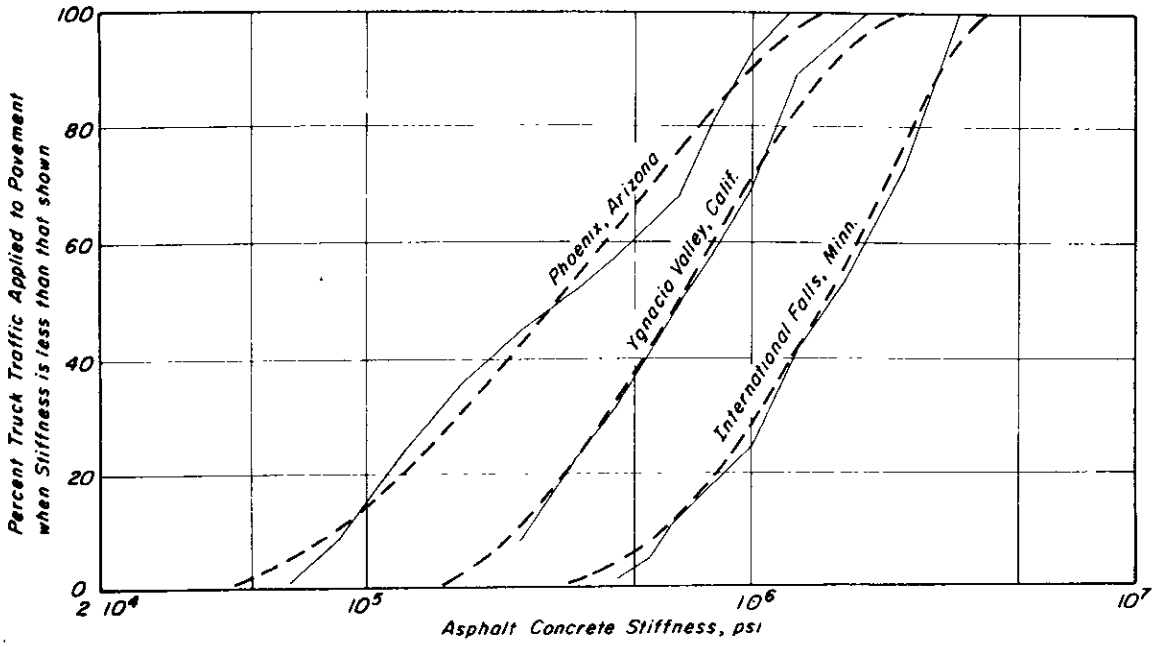

Fig. 35 — Stiffness variations with traffic applications — 12 in. thick asphalt concrete layer.

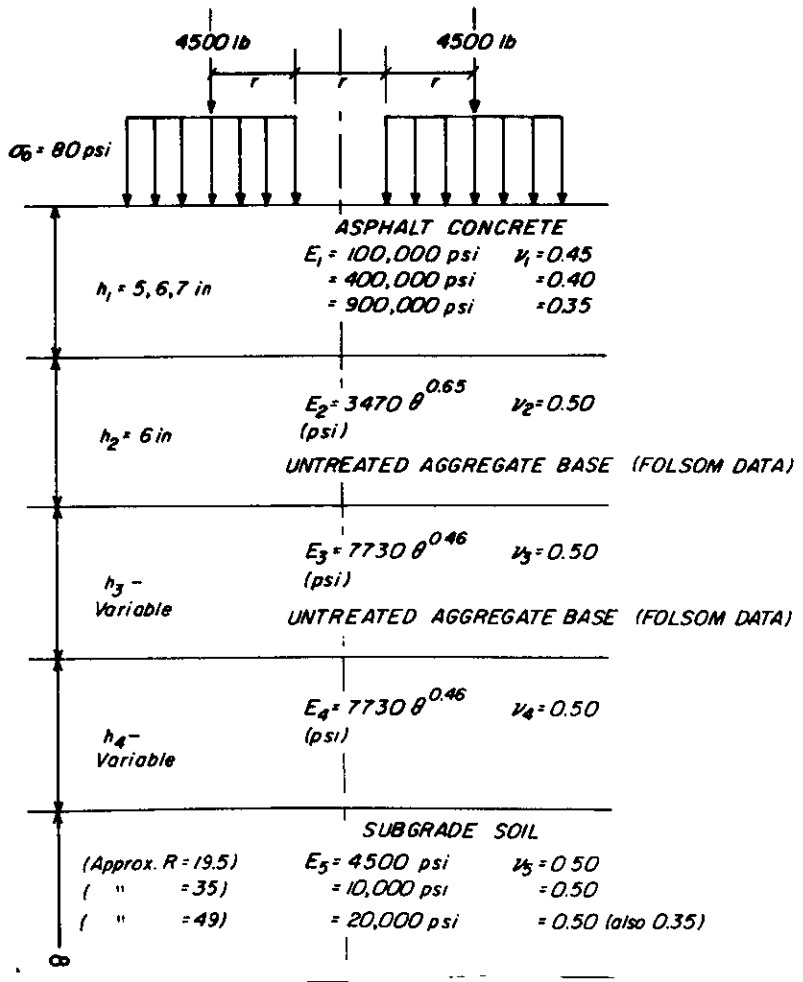

Fig. 36 – Structural pavement sections designed according to State of California procedure and analyzed for compressive strain at subgrade surface.

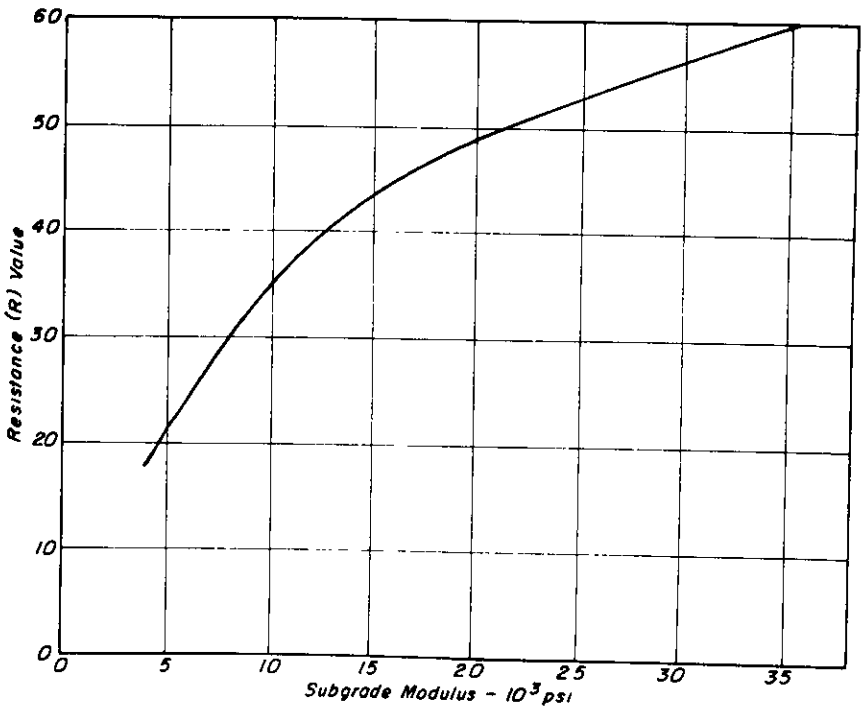

Fig. 37 – Approximate relationship between "R" value and subgrade modulus.

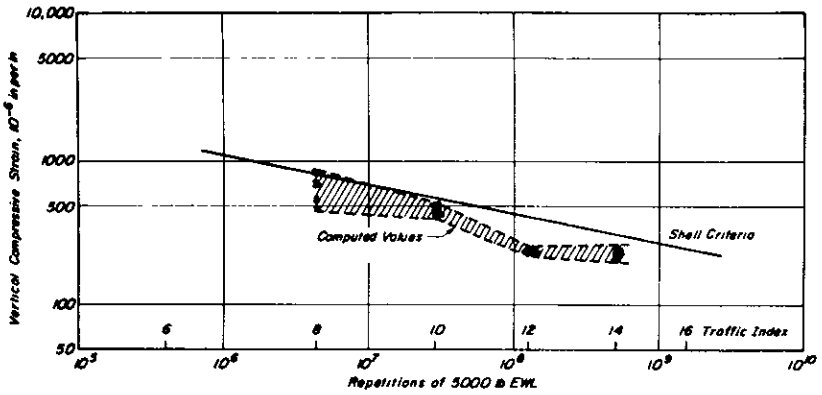

Fig. 38 – Relationships between subgrade strain and repetitions of 5000 lb EWL (and Traffic Index); surface stiffness = 100,000 psi.

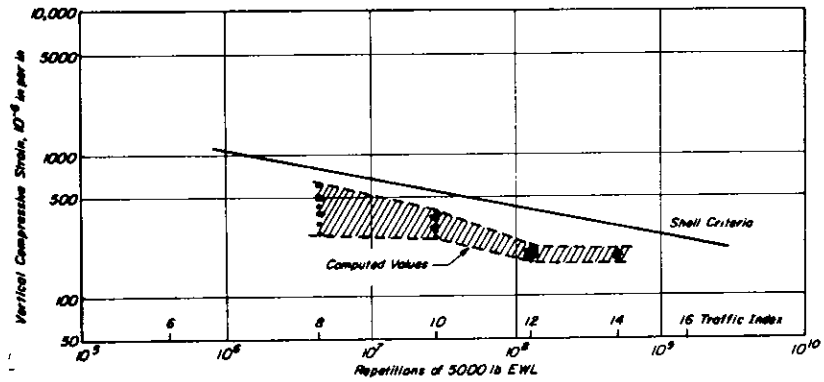

Fig. 39 – Relationships between subgrade strain and repetitions of 5000 lb EWL (and Traffic Index); surface stiffness = 400,000 psi.

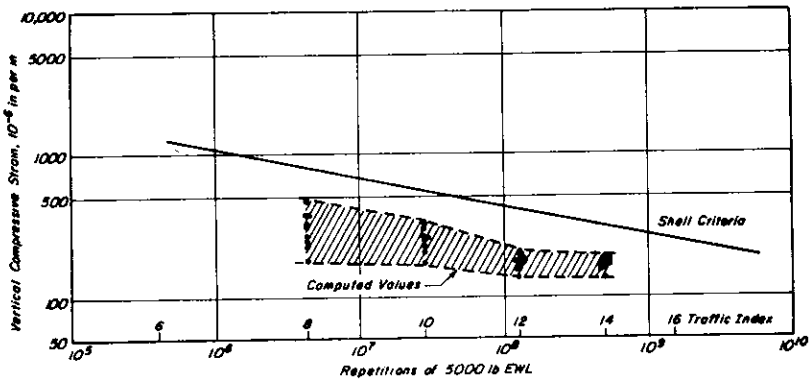

Fig. 40 – Relationships between subgrade strain and repetitions of 5000 lb EWL (and Traffic Index); surface stiffness = 900,000 psi.

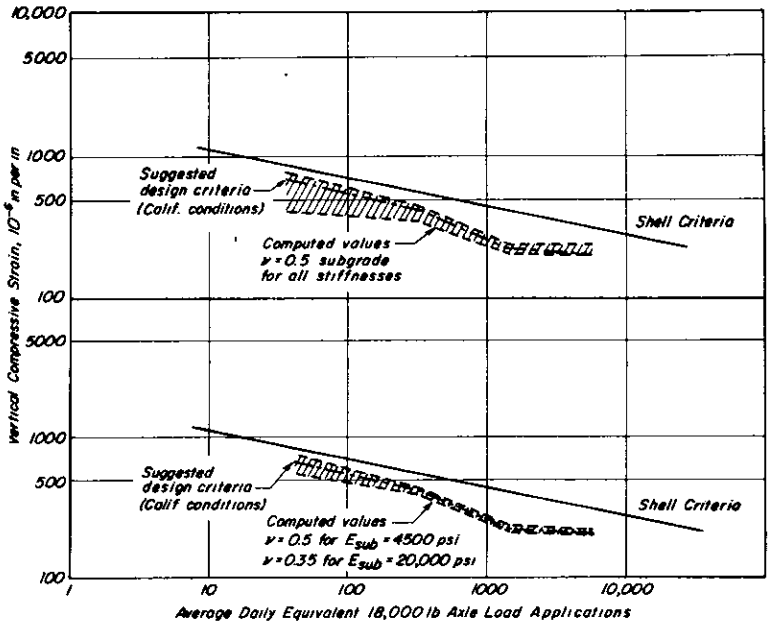

Fig. 41 — Relationships between subgrade strain and DTN.

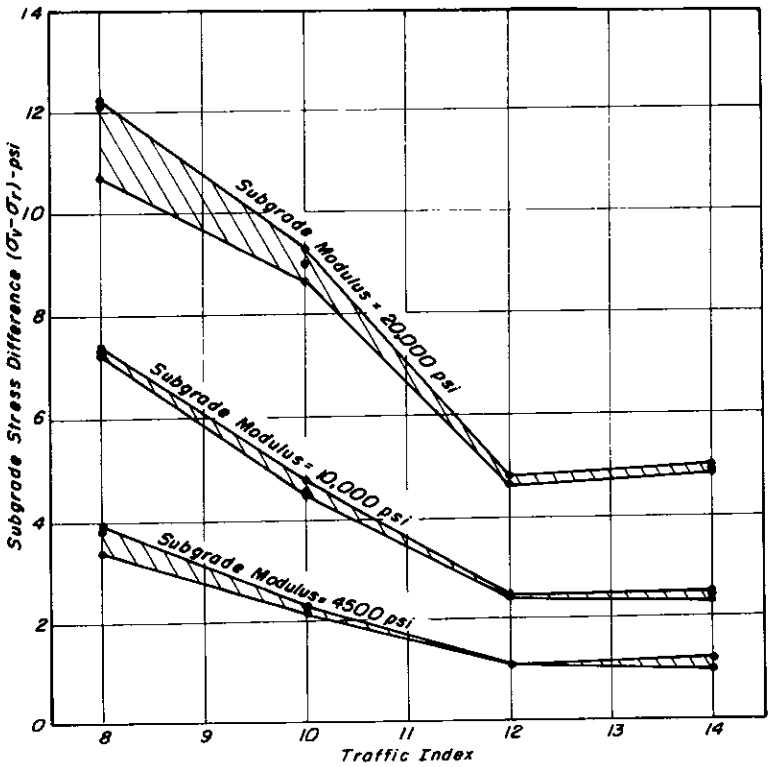

Fig. 42 — Relationship between stress difference $(\sigma_v - \sigma_r)$ at subgrade surface and 'Traffic Index'.

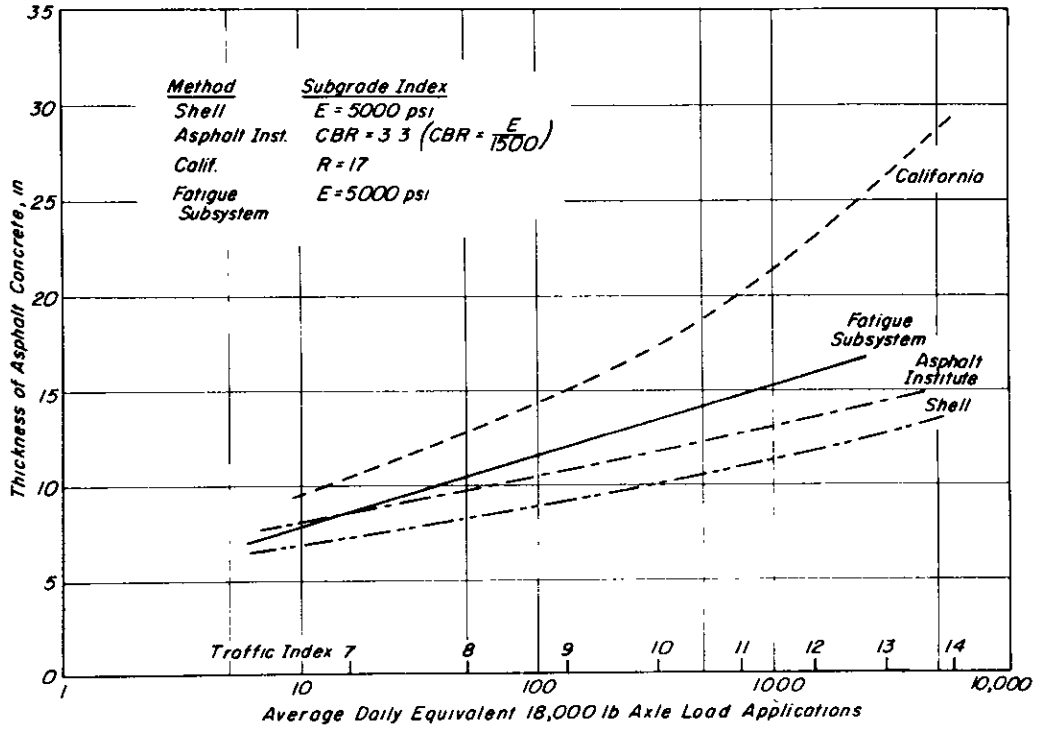

Fig. 43 — Comparison of thickness of asphalt concrete using one form of the fatigue subsystem (Fig. 1) with thicknesses determined by existing procedures.

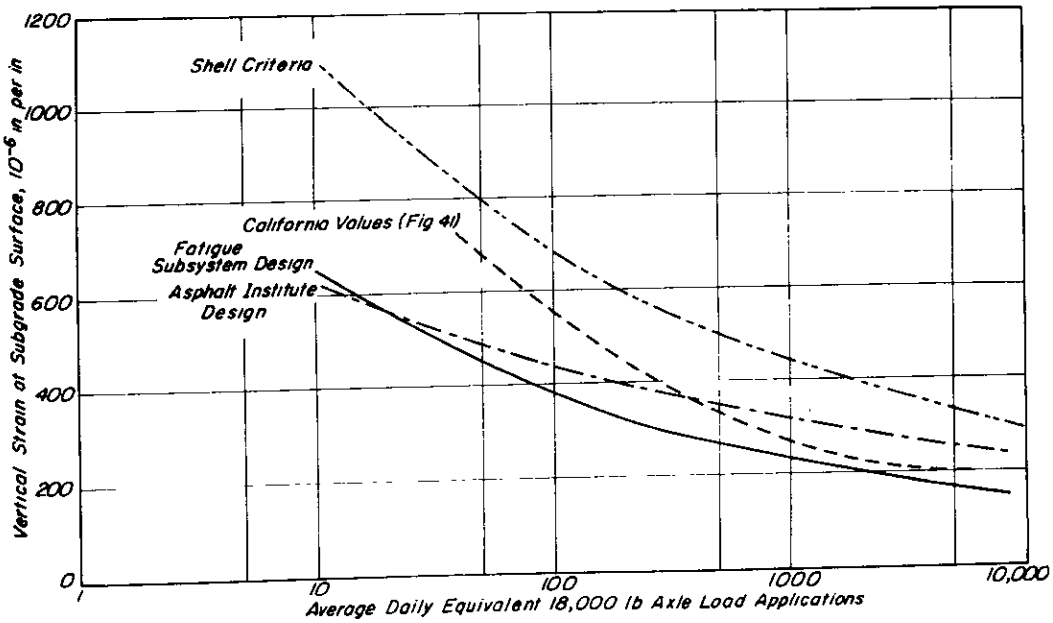

Fig. 44 — Comparison of vertical compressive strains at subgrade surface in pavements whose thicknesses are shown in Fig. 36 with both Shell criteria and those for pavements designed according to California procedure (Fig. 41).

APPENDIX A

PROCEDURE FOR TESTING SOILS TO DETERMINE THEIR RESILIENT MODULI

RESILIENCE TESTING OF UNTREATED SOILS

General

The objective of the method is to define the resilient character of untreated soils for conditions which represent a reasonable simulation of the insitu state of stress in pavements subjected to moving wheel loads. Procedures described define the resilient character in a triaxial state of stress, where the pressure in the triaxial chamber acts as a static all-around stress and where a repeated axial deviator stress, of fixed magnitude, frequency and load duration, is applied to the soil from a force generator located external to the triaxial chamber.

Description of the procedures are divided into three sections as follows:

Section I - Contains a glossary of terms used.

Section II - Describes the triaxial test equipment and measuring devices.

Section III - Describes the compaction and resilience testing, compacted clays and compacted granular materials being considered separately.

I - Definitions

1. σ_1 is the total axial stress.
2. σ_3 is the total radial stress, that is the confining pressure in the triaxial test.
3. $\sigma_d = \sigma_1 - \sigma_3$ is the stress deviator, that is the repeated axial stress in this procedure.
4. ε_1 is the total axial strain due to σ_d.
5. ε_3 is the total radial strain due to σ_d.
6. ε_{R1} is the recovered axial strain.
7. ε_{R3} is the recovered radial strain.

8. $M_R = \frac{\sigma_d}{\varepsilon_{R1}}$ is the resilient modulus.

9. $\nu_R = \frac{\varepsilon_{R3}}{\varepsilon_{R1}}$ is the resilient Poisson's ratio

10. $\Theta = \sigma_1 + 2\sigma_3 = \sigma_d + 3\sigma_3$ - is the sum of the principal stresses in the triaxial state of stress.

11. σ_1/σ_3 - the principal stress ratio.

12. Load duration is the time interval the sample is subjected to a stress deviator.

13. Cycle duration is the time interval between successive applications of a stress deviator.

14. $\gamma_d = \frac{G \cdot \gamma_w}{1 + (wG/S)}$

where

γ_d = unit weight of dry soil

γ_w = unit weight of water

G = specific gravity of soil

W = water content of soil

S = degree of saturation

15. $e = \frac{G}{\gamma_d} \gamma_w - 1$

where e = void ratio

II. Test Equipment

A Triaxial Test Cell

A triaxial cell suitable for use in resilience testing of soils is shown in Fig. 1. This equipment is similar to most standard cells with the exception of being somewhat larger to facilitate the internally mounted

load and deformation measuring equipment and having additional outlets for the electrical leads from the measuring devices. For the type of equipment shown, air would be used as the cell fluid.

The external loading source may be any device capable of providing a variable load of fixed cycle and load duration, ranging from simple cam and switch control of static weights or air pistons to closed loop electro-hydraulic systems. A load duration of 0.1 seconds and cycle duration of 3 seconds has been found to be satisfactory for most applications.

B. Deformation Measurement

The deformation measuring equipment consists of Linear Variable Differential Transformers (LVDT's) attached to the soil specimen by a pair of clamps. Four LVDT's are shown in position on a soil specimen in Figure 1. Details of the clamps are shown in Fig. 2.

Load is measured by placing a load cell between the sample cap and the loading piston as shown in Fig. 1.

Use of the type of measuring equipment described above offers several advantages:

a. It is not necessary to reference deformations to the equipment which deforms during loading.

b. The effect of end cap restraint on soil response is virtually eliminated.

c. The horizontally mounted LVDT's permit the measurement of the resilient Poisson effect.

d. Any effect of piston friction is eliminated by measuring loads at the caps of the sample.

In addition to the measuring devices, it is also necessary to maintain suitable recording equipment. It is desirable to have simultaneous recording of load and deformations. The number of recording channels can be reduced by wiring the leads from the LVDT's such that only the average signal from each pair is recorded. By introducing switching and balancing units, a single channel recorder can be used. However, this will not permit simultaneous records.

C. Additional Equipment

1. Compaction apparatus.
2. Loading machine, 10 to 30-ton capacity.
3. Calipers, micrometer gage, steel rule (calibrated to 0.01 inch).
4. Rubber membranes of 0.01 to 0.025-inch thickness.
5. Rubber O-rings.
6. Vacuum source with bubble chamber and regulator.
7. Membrane stretcher.
8. Scales.
9. Weighing pans.
10. Porous stones.

III. Compacting and Testing

Compacted Clay Soils

The resilient character of compacted clays is dependent upon the structure imparted to the soil particles by a compaction process. Laboratory compaction processes must be selected in accordance with the expected field compaction conditions. Any compaction process which causes shearing deformation in a clay soil of degree of saturation greater than 80 percent results in a dispersed (or parallel) clay structure. Clays with a dispersed

structure exhibit greater deformation than would the same soil with a flocculated (random) structure, when both are tested under identical conditions. Some general criteria which can be used to guide selection of the appropriate compaction conditions for clay soils are as follows:

(i) If the field compaction conditions will be at a water content corresponding to less than 80 percent of the saturation water content and the in-service water content is expected to remain less than the 80 percent saturation value, then any of the standard impact, gyratory, kneading or static procedures may be used to simulate the in-service condition.

(ii) If the field compaction will be at a water content corresponding to greater than 80 percent of the saturation water content and the in-service water content is expected to remain greater than the 80 percent saturation value, then the compaction process must be of the shearing type, that is, one of impact, gyratory or kneading, to simulate the dispersed structure in service.

(iii) If the field compaction conditions will be at a water content corresponding to less than 80 percent of the saturation water water content and the in-service conditions are expected to be a degree of saturation greater than 80 percent, then static compaction must be used to simulate the flocculated structure in service.

In Figure 5(a), resilient modulus is shown as isolines or a graph of dry density versus water content. The form shown in Figure 5(a) has general application to compacted clay soils and may be used to guide the selection of a test program as follows:

(a) If the range of compaction conditions and the range of in-service conditions is known, select an appropriate laboratory compaction method. Prepare and test samples at dry densities and water contents within the in-service range such as that shown in Figure 5(a).

(b) Prepare and test specimen over a substantial range of dry densities and water contents. Display the results as in Figure 5(a) and use the resilient modulus in conjunction with other properties (e.g., swelling) to select the range of field placement conditions.

A. Specimen Size

The diameter of the specimen to be tested is determined by a lower bound of approximately 2.5 inches or by four to five times the maximum size of particle in the material. This lower bound represents a minimum of size which can be expected to provide a reasonable representation of the larger mass of material in a pavement. Specimen length should not be less than two times the diameter.

B. Moisture-Density Relationship

1. Establish the moisture-density relationship for the soil according to one of the following procedures:

   a. ASTM D1557 - AASHO T 180.

   b. ASTM D698 - AASHO T 99.

   c. Calif. 216F.

   d. Other standard method.

Prepare a graph showing dry density and water content as described in the above standard procedures.

2. Determine the specific gravity of the soil according to the appropriate procedure:
   a. ASTM D854
   b. Calif. 209A.
3. Use the data obtained in 1 and 2 to determine 100 percent and 80 percent of saturation at various densities. Place this information on the graph drawn in 1, that is, draw a 100 percent and 80 percent saturation line. (Equations for these computations are given in Section 1.)
4. Select the densities, water contents and compaction method to be used to prepare specimen.

C. Preparation of Soil for Compaction

1. Determine the water content ($W_1\%$) of the soil (if other than oven-dry material is to be used).
2. Determine the volume (V_s) of the compacted specimen to be prepared. For other than static compaction methods the height of the compacted specimen must be greater than that required for resilience testing to allow for trimming of the specimen ends. One-half inch will generally be adequate.
3. Determine the sample weight of oven-dry soils (W_s) and of water (W_w) required to obtain the desired dry density (γ_d) and water content (W%).

$$W_s \text{ (lbs)} = \gamma_d \text{ (pcf)} \times V_s \text{ (cu.ft.)}$$

$$W_s \text{ (gms)} = W_s \text{ (lbs)} \times 453.$$

$$W_w \text{ (lbs)} = \gamma_d \text{ (psf)} \times \frac{W\%}{100}$$

$$W_w \text{ (gms)} = W_w \text{ (lbs)} \times 453.$$

However, molds of the correct dimensions can be obtained and the methods adapted to the new mold sizes. This will generally require adjustments in the number of compacted layers and/or the number of tamps per layer. Large compacted specimen can be prepared and the correct size trimmed from these.

1. Establish the number of layers (N) to be used to compact the soil. Determine the weight of wet soil required per layer (W_L).

$$W_L(\text{grams}) = \frac{W_{wet}}{N}.$$

2. Place W_L grams of the soil in the mold. Compact according to the standard procedure. Scarify the surface of the layer.
3. Repeat as in 2.
4. At completeion of compaction, use approximately 200 grams of the remaining wet soil for determination of the water content.
5. Carefully remove the specimen from the mold. Trim the ends to provide plane surfaces.
6. Weigh the specimen to the nearest gram. Determine the average height and diameter to the nearest 0.01 inches. Record these values in Table 1.
7. The specimen is now ready for resilience testing. If there will be a delay of more than a few minutes before beginning the resilience testing, the specimen should be carefully wrapped in saran to prevent evaporation.

E. Compaction by Static Loading

In the absence of standard methods for static compaction, the following procedure may be used. The process is one of compacting a known weight of wet soil to a volume which is fixed by the configuration of the mold

4. Determine the sample weight of other than oven-dry soil (W_{ss}) required to obtain W_s. An additional amount of approximately 500 gms should be allowed, the excess being used to determine the water content at the time of compaction.

$$W_{ss}(\text{grams}) = (W_s \text{ (grams)} + 500)\ (1 + \frac{W_1}{100}).$$

5. Determine the weight of water (W_{aw}) required to increase the weight from the existing (W_{1w}) to the desired (W_w).

$$W_{1w}(\text{grams}) = (W_s + 500)\ (\frac{W_1}{100})$$

$$W_{aw}(\text{grams}) = W_w - W_{1w}.$$

6. Determine the wet weight of soil (W_{wet}) to be compacted.

$$W_{wet}(\text{grams}) = W_s \times (1 + \frac{W\%}{100})$$

7. Place the weight of soil determined in 3 into a mixing pan.
8. Add the water to the soil in small amounts, mixing thoroughly after each addition.
9. Place the mixture in a plastic bag. Seal the bag and knead the soil with the fingers to obtain uniform dispersion of water throughout the soil. The mixture should be stored in the plastic bag in an atmosphere of relative humidity of 75 percent for a period of 12 to 24 hours. Ensure a complete seal by using two or more bags.
10. After completion of the mixing and storage, weight the wet soil and bag(s) to the nearest gram, recording this value on Table 1.

D. Compaction by Impact or Kneading Methods
(ASTM D1557, ASTM D698, Calif. 216F, Harvard Miniature Compaction, California or Triaxial Institute Kneading Compaction)

Specimen prepared in standard molds associated with the above methods may not be of the correct dimensions for direct use in resilience testing.

assembly. A typical mold assembly for the preparation of 2.8 inch diameter by 6-inch height specimen using three layers is shown in Fig. 3. To meet specific needs, equipment of differing size and number of layers can be developed.

1. Establish the number of layers (N) to be used to compact the soil. Determine the weight of wet soil per layer.

$$W_L(\text{grams}) = \frac{W_{wet}}{N}$$

2. Place one of the loading rams into the sample mold.
3. Place W_L(grams) of soil into the sample mold. Use a spatula to draw the soil away from the edge of the mold, forming a slight mound in the center.
4. Insert the second loading ram and place the assembly in the loading machine. Apply a small load. Adjust the mold such that it rests equally spaced between the clamps of the loading rams. Soil pressures developed by the initial loading will serve to hold the mold in place. By having both loading rams reach the zero volume change positions simultaneously, more uniform layer densities are obtained.
5. Slowly increase the load until the loading ramp caps rest firmly against the mold. Hold the load at or near the maximum load for a period of time. The rate of loading and duration the load must be held depend on the amount the soil rebounds. The slower rate of loading and the longer the load is held, the less the rebound.
6. Decrease the load to zero, and remove the assembly from the loading machine.

7. Remove a loading ram. Scarify the surface of the compacted layer and place the correct weight of soil for a second layer in place, adjusting the soil as in 3. Add a spacer ring and insert the loading ram.
8. Invert the assembly and repeat as in 7.
9. Place the assembly in the loading machine. Load slowly, holding the load at or near maximum when the spacer disc firmly contacts the mold.
10. Repeat 6, 7, 8, and 9 as required.
11. Use approximately 200 grams of the soil remaining for a measurement of water content.
12. Place the extruder ram into the sample mold and force the specimen out of the sample mold into the extruder mold.
13. Use the extruder mold to carefully slide the compacted specimen onto a glass plate.
14. Determine the weight of the compacted specimen to the nearest gram. Measure the height and diameter to the nearest 0.1 inch. Record these values in Table 1.
15. The specimen is now ready for resilience testing. If there will be a delay of more than a few minutes before beginning the resilience testing, the specimen should be carefully wrapped in saran to prevent evaporation.

F. Resilience Testing

1. Place the triaxial cell base assembly on the platform of the loading machine. Tighten the sample base firmly to obtain an airtight seal.

2. Close the valve on the vacuum lead to the sample cap. (This line is not required for testing of clays and closing of the valve will prevent loss of air from the chamber during testing.)
3. Carefully place the specimen on the sample base (Porous stones are not necessary for the testing of clay soils.)
4. Place the sample cap on the specimen.
5. Stretch a membrane tightly over the interior surface of the membrane stretcher. Slip the stretched membrane carefully over the specimen. Roll the membrane off the stretcher onto the sample base and cap. Remove the stretcher. Place O-ring seals around the base and cap.
6. Connect the vacuum/saturation line to the vacuum source through the medium of a bubble chamber (a vacuum of 5 to 10 psi is generally adequate). If bubbles are absent, an airtight seal has been obtained. If bubbles are present, check for leakage caused by poor connections, holes in the membrane, or imperfect seals at the cap and base. The existence of an airtight seal ensures that the membrane will remain firmly in contact with the specimen. This is essential for use of the clamp mounted LVDT's. Leakage through holes in the membrane can frequently be eliminated by coating the surface of the membrane with a rubber latex or by use of a second membrane.
7. When leakage has been eliminated, disconnect the vacuum supply.
8. Extend the lower LVDT clamp and slide it carefully down over the specimen to approximately the lower quarter point of the specimen.
9. Repeat for the upper clamp, placing it at the upper quarter point. Ensure that both clamps lie in horizontal planes.

10. Connect the LVDT's to the recording unit and balance the recording bridges. This will require recorder adjustments and adjustment of the LVDT stems. When a recording bridge balance has been obtained determine, to the nearest 0.01 inch, the vertical spacing between the LVDT clamps and record this value in Table 1.
11. Place the triaxial chamber into position. Set the load cell in place on the sample cap.
12. Place the cover plate on the chamber. Inset the loading piston, obtaining a firm connection with the load cell.
13. Tighten the tie rods firmly.
14. Slide the assembled apparatus into position under the axial loading device. Bring the loading device to a position where it nearly contacts the loading position.

The resilient properties of compacted clays are only slightly affected by the magnitude of the confining pressure, and for most applications the effect of confining pressure can be disregarded. The confining pressure used should approximate the expected in-situ horizontal stresses. These will generally be in the order of 1 to 5 psi. A chamber pressure of 3 psi would be a reasonable value for most testing.

Resilient properties are greatly dependent upon the magnitude of the deviator stress (repeated axial stess). It is, therefore, necessary to conduct the test for a range in deviator stress values. For example, test at 0.5, 1.0, 2.0, 3.0, 4.0, 5.0, 7.6, 10 and 15 psi.

15. Connect the chamber pressure supply line and apply the confining pressure (equal to the chamber pressure).
16. Rebalance the recording bridges for the LVDT's and balance the load cell recording bridge.

17. Begin the test by applying 200 repetitions of a deviator stress of approximately 1 psi followed successively by 200 repetitions at each of 3, 5, 7.5 and 10 psi. The foregoing stress sequence constitutes sample conditioning, that is, elimination of the effects of the interval between compaction and loading and also the effects of initial loading versus reloading.
18. Decrease the deviator load to the lowest value to be used. Apply 200 repetitions of load, recording the recovered deformation both horizontal and vertical at or near the 200th repetition. (Note: The deformation measured by the horizontal LVDT's is approximately twice the actual deformation on the diameter due to the respective locations of the hinge and the LVDT. (Refer to Figure 2).
19. Increase the deviator load, recording deformations as in 18. Repeat over the range of deviator stresses to be used.
20. At the completion of the loading, reduce the chamber pressure to zero. Remove the chamber LVDT's and load cell. Use the entire specimen for purpose of determining the water content.

Calculations and Presentation of Results

The results of resilience tests can be presented in the form of a summary table such as Table 1 and graphically as is shown in Figure 5 for resilient modulus. A form similar to Figure 5(b) may be used to display the resilient Poisson's ratio.

Compacted Granular Soils

Of particular concern in the prepatation of granular soil specimens is the extent that these materials can be handled, that is, in removing them from a mold and transporting and placing in the triaxial cell. Granular

soils which do exhibit sufficient cohesion to permit handling can be prepared by the methods described for compacted clay soils; however, it is generally not necessary to consider soil structure effects. The exception is some silts which may also exhibit strength properties which are dependent upon compaction conditions.

The following description contains some items which are of general application to compacted granular soils, but is mainly directed to compaction of materials which cannot be handled between the compaction and testing stages.

A. Specimen Size

The diameter of the specimen to be tested is determined by a lower bound of approximately 2.5 inches, or by four to five times the maximum size of particle in the material. This lower bound represents a minimum of size which can be expected to provide a reasonable representation of the larger mass of material in a pavement.

Specimen length should not be less than two times the diameter.

B. Moisture-Density Relationship

1. Establish the moisture-density relationship for the soil according to one of the following procedures:

   a. ASTM D1557 - AASHO T180
   b. ASTM D698 - AASHO T99
   c. Calif. 216F
   d. Other standard method

   Prepare a graph of dry density and water content.

2. Determine the specific gravity of the soil using one of the following procedures:

   a. ASTM D854
   b. ASTM C127
   c. Calif. 206D
   d. Calif. 207D
   e. Other standard

3. Use the data of 1 and 2 to detetmine 100 percent of saturation at various densities. Draw the curve of 100 percent saturation on the graph of 1.
4. Select the densities and water contents at which specimens are to be prepared. This will usually consist of several values covering the expected in-service range. Note: Material which has a moderately high permeability and which is to be tested at 100 percent saturation are generally prepared in an oven-dry or air dry state and saturated by back-pressure techniques, described later.

C. Compaction

Cohesionless granular materials are most readily compacted by use of a split mold mounted on the base of the triaxial cell as is shown in Fig. 4. Compaction forces are generated by a vibrator, such as a small hand operated air hammer.*

Porous stones are essential when testing saturated granular materials and may be advantageous when testing wet or dry specimens. The stones facilitate saturation procedures and prevent blocking of the vacuum/saturation inlet of the triaxial cell with soil particles.

1. Determine the water content (W_1%) of the soil (If other than oven-dried material is to be used).
2. Tighten the sample base into place on the triaxial cell base. It is essential that an airtight seal be developed.
3. Place the porous stone(s)** plus the sample cap on the sample base.

---

* For example, Scaling Hammer, Size 0, manufactured by William H. Keller, Inc., Grand Haven, Michigan.

** Two are required for saturated specimens, but generally only the lower stone would be used for tests at lower water contents.

Determine the height of base, cap and stone(s) to the nearest 0.01 inch and record this value in Table 2.

4. Remove the sample cap and upper porous stone. Measure the thickness of the rubber membrane, using a micrometer gage. Record this value in Table 2.
5. Place the rubber membrane over the sample base and lower porous stone. Fix the membrane in place, using an O-ring seal.
6. Place the split mold sample former around the sample base, drawing the rubber membrane up through the mold. Tighten the split mold firmly into place. Exercise care to avoid pinching the membrane.
7. Stretch the membrane tightly over the rim of the mold. Apply a vacuum to the mold to remove all membrane wrinkles. The membrane should now fit smoothly around the inside perimeter of the mold. The vacuum is maintained throughout the compaction procedure.
8. Use calipers to determine, to the nearest 0.01 inch, the inside diameter of the membrane lined mold. Determine, to the nearest 0.01 inch, the distance from the top of the porous stone to the rim of the mold.
9. Determine the volume of specimen to be prepared. The diameter of the specimen is the diameter determined in 8 and the height is a value less than that determined in 8 but at least two times the diameter.
10. Determine the weight of material which must be compacted into the volume determined in 9 to obtain the desired density and water content.*

---

* Refer to Part C of compacted clays for further details.

11. Determine the number of layers to be used for compaction. Normally, layer depths will be 1 to 1.5 inches. Determine the weight of soil required for each layer and the thickness of each layer.
12. Place the required weight of soil into a mixing pan. (Allow approximately 300 gms more than required for compaction, the excess to be used for determining the water content.) Add the required amount of water, mixing thoroughly.
13. Determine the weight of wet soil plus water and record in Table 2.
14. Place the amount of wet soil required for one layer into the mold. Exercise care to avoid spillage. Use a spatula to draw the material away from the edge of the mold, forming a small mound at the center of the mold.
15. Insert the vibrator head and vibrate the soil until the distance from the surface of the compacted layer to the rim of the mold is equal to the distance measured in 8 minus the thickness of the lift determined in 11. This may require removal and re-inserting the vibrator head several times until experience is obtained in gaging the required vibration time.
16. Repeat 14 and 15 for each new lift. The measured distance from surface of the compacted layer to the rim of the mold being successively reduced by the thickness of each new lift from 11. The final surface should be a smooth, horizontal plane.
17. When compaction is completed, observe the weight of mixing pan plus excess soil and record in Table 2. The weight determined in 13 less the weight observed now is the weight of wet soil incorporated in the specimens. Use approximately 200 grams of the excess material for a water content determination.

18. Place the porous stone and sample cap on the surface of the specimen. Roll the rubber membrane off the rim of the mold and over the sample cap. If the sample cap projects above the rim of the mold, the membrane should be sealed tightly against the cap with an O-ring seal. If not, the seal can be applied later.
19. Disconnect the vacuum supply from the mold. Place the entire assembly on the loading machine in preparation for resilience testing.

D. Resilience Testing

1. Connect the vacuum/saturation inlet to a vacuum source, applying 5 to 10 psi of vacuum through the medium of a bubble chamber. The vacuum serves a dual purpose in testing granular materials -- for detection of leakage and to impart a stress-induced rigidity to the material to prevent collapse when the sample mold is removed. This vacuum supply is maintained until Step 9.
2. Carefully remove the sample mold. Seal the membrane to the sample cap if this has not been done previously. Determine to the nearest 0.1 inch the height of specimen plus cap and base and the diameter of the specimen plus membrane. Record these values in Table 2.
3. Observe the presence or absence of air bubble in the bubble chamber. Eliminate system leakage, using methods described previously for compacted clays.
4. When leakage has been eliminated, place the LVDT clamps on the specimen and balance the recorder bridges as described previously for clay soils.

5. Connect the vacuum inlet line to the sample cap, if the specimen is to be tested in a saturated state; otherwise, this line is not connected and is sealed to prevent loss of air from the chamber.
6. Determine, to the nearest 0.01 inch, the spacing between the LVDT clamps and record this value.
7. Place the load cell on the sample cap and assemble the remainder of the cell, tightening the tie rods firmly. Slide the assembly under the axial loading assembly.
8. Connect the chamber pressure supply line and apply a pressure of 5 psi.
9. Remove the vacuum supply from the vacuum/saturation inlet and open this line to the atmosphere.

If the specimen is to be saturated before testing, the following steps are required. Otherwise, the test is continued as described in Step 14.

10. Connect the vacuum supply to the vacuum inlet (to the top of the specimen) and connect the vacuum saturation/inlet to a source of de-aired, distilled water.
11. Apply a vacuum of 2-3 psi and open the water supply valve, allowing water to be drawn slowly upward through the sample.
12. Continue to flush water through the system to remove all entrapped air. To evaluate the presence of or absence of air from the sample requires that pore pressures be observed. When all air has been eliminated, an increase in chamber pressure (with valves to the water supply and vacuum supply closed) will result in an equal increase in pore pressure. In view of the wide variety of pore pressure measuring devices, no attempt will be made here to describe a procedure.

13. Increase the chamber pressure to 10 psi; apply a 5 psi back pressure to the water supply while closing the vacuum inlet valve. The effective confining pressure (5 psi) on the specimen is now equal to the chamber pressure (10 psi) less the back pressure (5 psi).

14. Rebalance the recorder bridges to the load cell and LVDT's.

15. Select the range of stresses at which the test is to be performed.

The resilient modulus of granular soils is dependent upon the magnitude of the confining pressure and nearly independent of the magnitude of the repeated axial stress. The resilient Poisson's ratio is largely dependent upon the principal stress ratio. Therefore, it is necessary to test granular materials over a range of confining and axial stresses. (The confining pressure is equal to the chamber pressure for dry and wet specimens and is equal to the chamber pressure less the back pressure for saturated specimen.) A suggested stress range is:

Confining pressures: 1, 3, 5, 7.5, 10, 15 and 20 psi.

At each confining pressure, test at five values of stress difference corresponding to multiples (1, 2, 3, 4, 5) of the cell pressure.

16. Before beginning to record deformations, a series of conditioning stresses are applied to the material to eliminate initial loading effects. The greatest amount of volume change occurs during the application of the conditioning stresses. Simulation of field conditions suggests that drainage of saturated samples be permitted during the application of these loads, but that the test loading (beginning in step 20) be conducted in an undrained state.

17. Set the axial load generator to apply a deviator stress of 10 psi (that is, a stress ratio equal to 3). Activate the load generator and apply 200 repetitions of this load. Stop the loading.
18. Set the axial load generator to apply a deviator stress of 25 psi (that is, a stress ratio equal to 6). Activate the load generator and apply 200 repetitions of this load. Stop the loading.
19. Repeat as in 18, maintaining a stress ratio equal to 6, using the following order and magnitude of confining pressures: 10 psi, 20 psi, 10 psi, 5 psi, 3 psi, 1 psi.
20. Begin the recorded test using a confining pressure of 1 psi and an equal value of deviator stress. Record the resilient deformations after 200 repetitions. Increase the deviator stress to twice the confining pressure and record the resilient deformations after 200 repetitions. Increase the deviator stress to twice the confining pressure and record the resilient deformations after 200 repetitions. Repeat until a deviator stress of 5 times the confining pressure is reached (stress ratio of 6).
21. Repeat as in 20 for each value of confining pressure.
22. When the test is completed, decrease the back pressure to zero, reduce the chamber pressure to zero, and dismantle the cell. Remove the LVDT clamps, etc. Remove the soil specimen and use the entire amount of soil to determine the water content.

Calculations and Presentations of Results

Calculations can be performed using the tabular arrangement of Table 2. Individual test results and series results are most readily presented in graphical form, such as shown in Figure 6. Plotting the regression constants of Figure 6 versus void ratio as is shown in Figure 8 provides

a convenient means of interpolating for particular field conditions.

Materials such as fine sands, silts and those with only small amounts of clay may display properties somewhat different than those shown in Figure 6, demonstrating a dependence upon both the cell pressure and the deviator stress. Graphical displays such as Figure 7 would then be more appropriate.

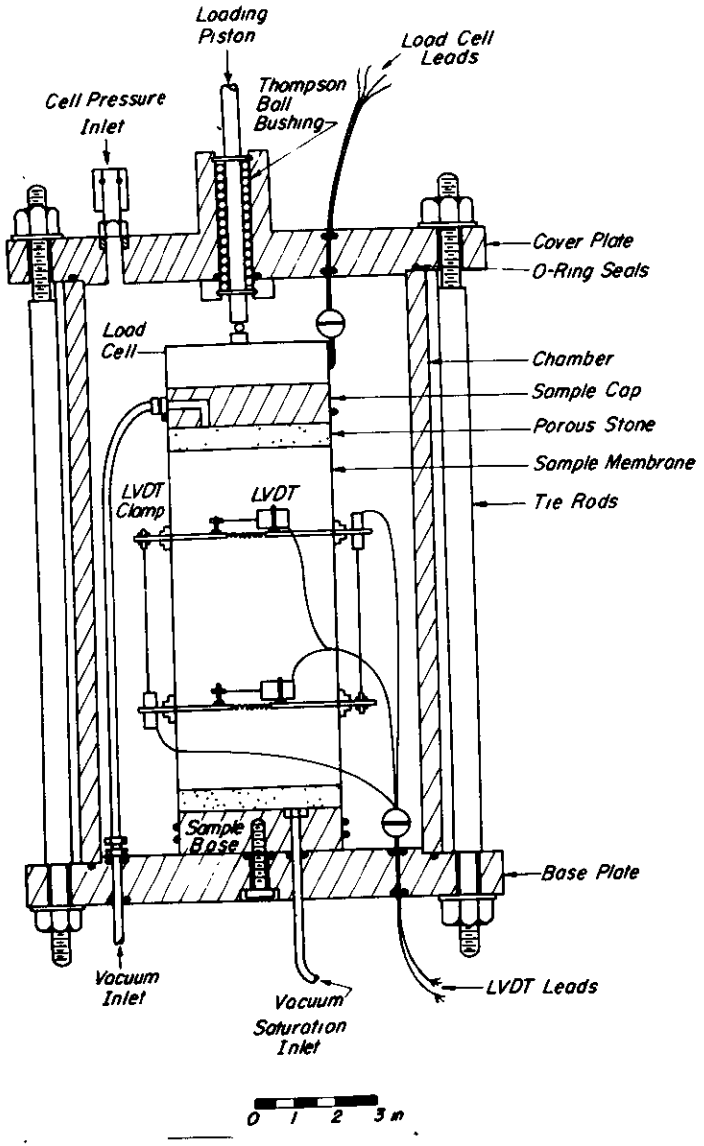

Fig. A-1 — Apparatus for resilience testing of soils.

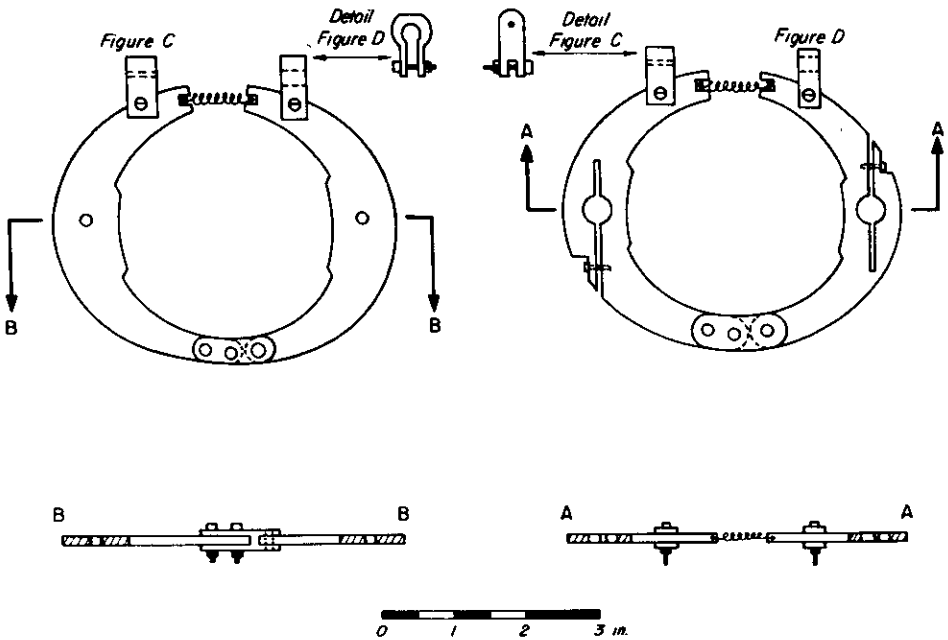

Fig. A-2 — LVDT holders.

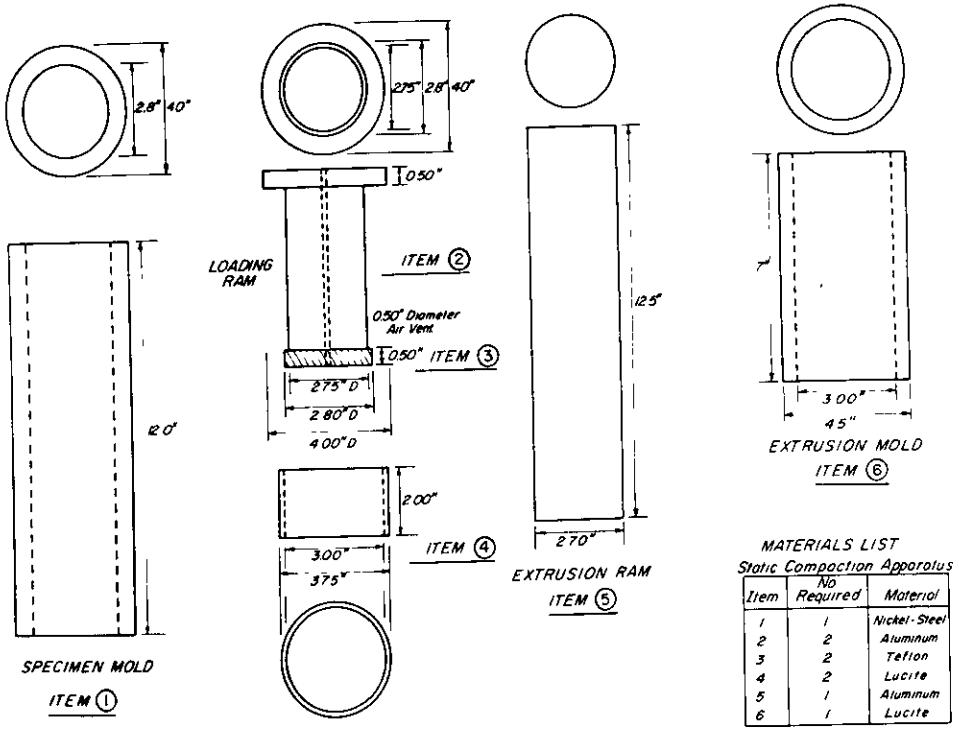

MATERIALS LIST
Static Compaction Apparatus

Item	No. Required	Material
1	1	Nickel-Steel
2	2	Aluminum
3	2	Teflon
4	2	Lucite
5	1	Aluminum
6	1	Lucite

Fig. A-3 — Apparatus for compaction by static loading.

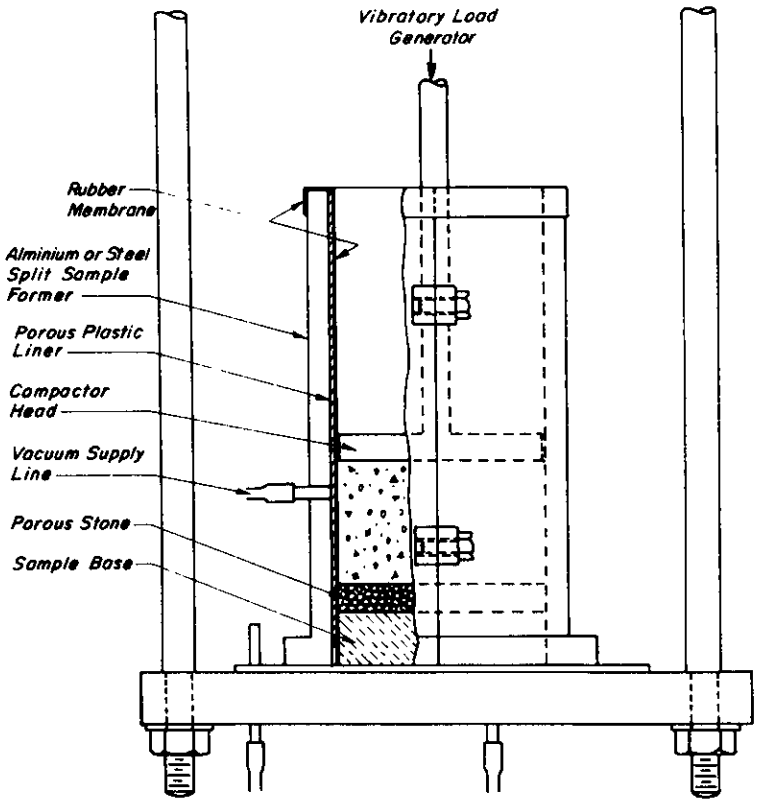

Fig. A-4 — Apparatus for vibratory compaction.

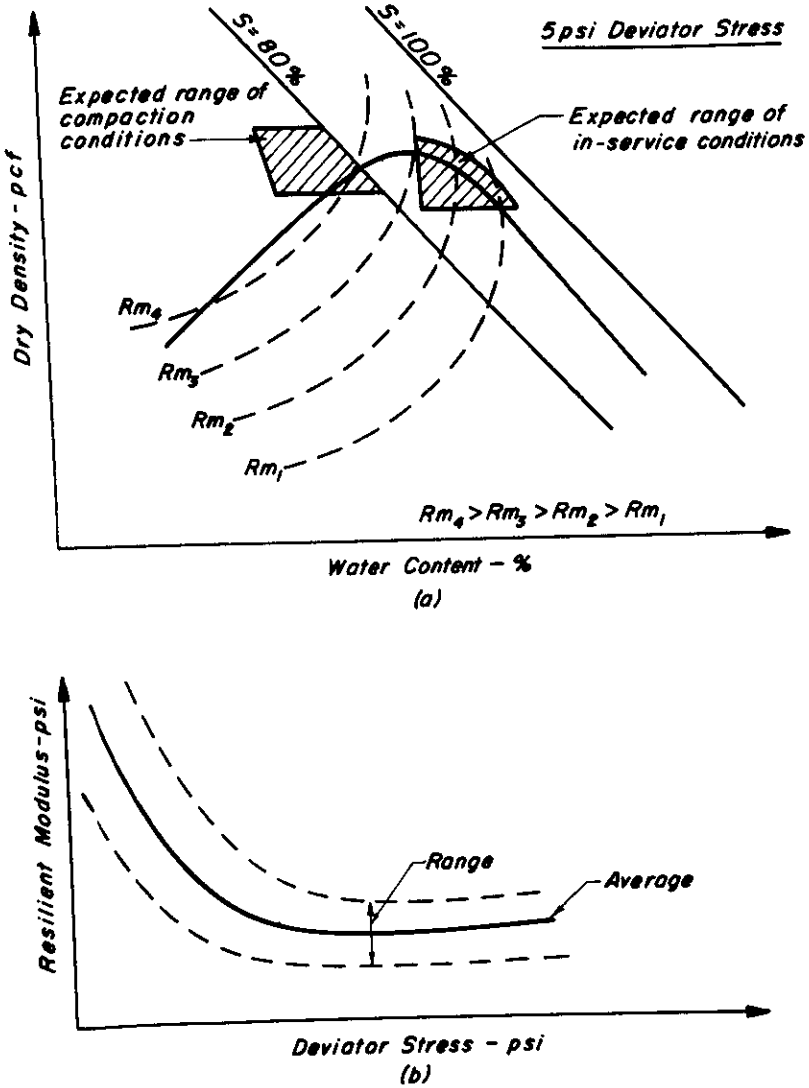

Fig. A-5 — Presentation of results of resilience tests on compacted clays.

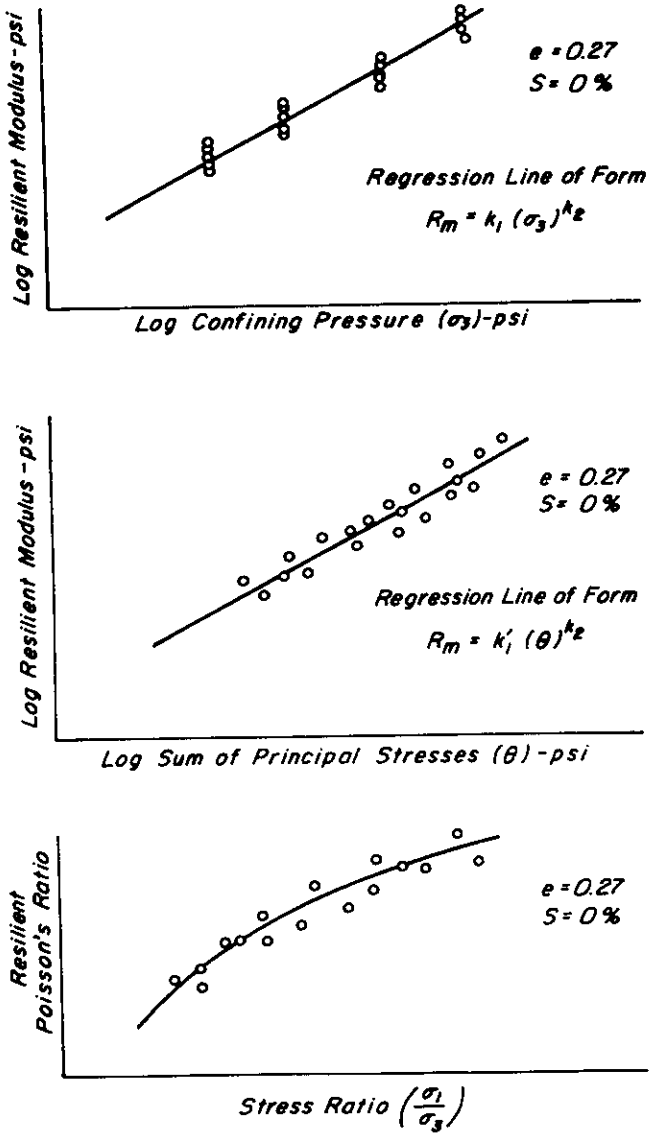

Fig. A-6 — Results of resilience tests on granular soils.

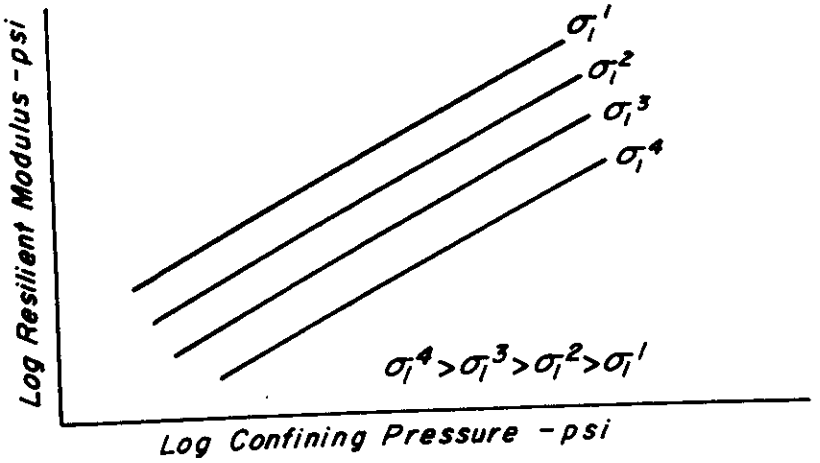

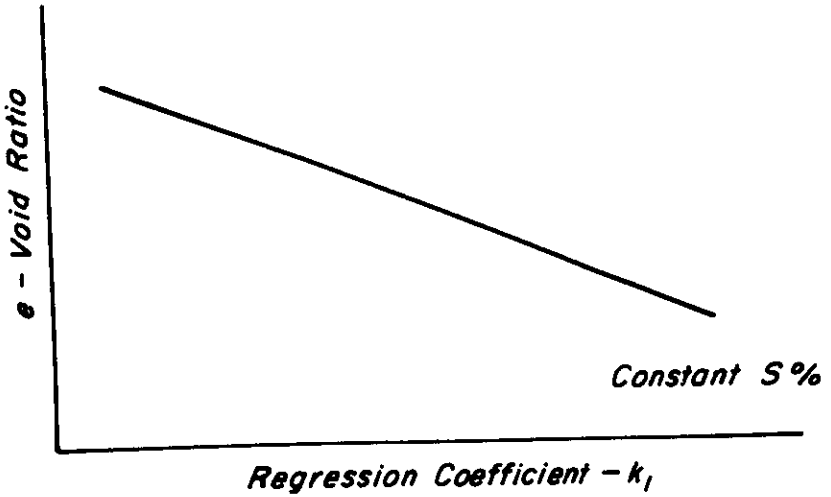

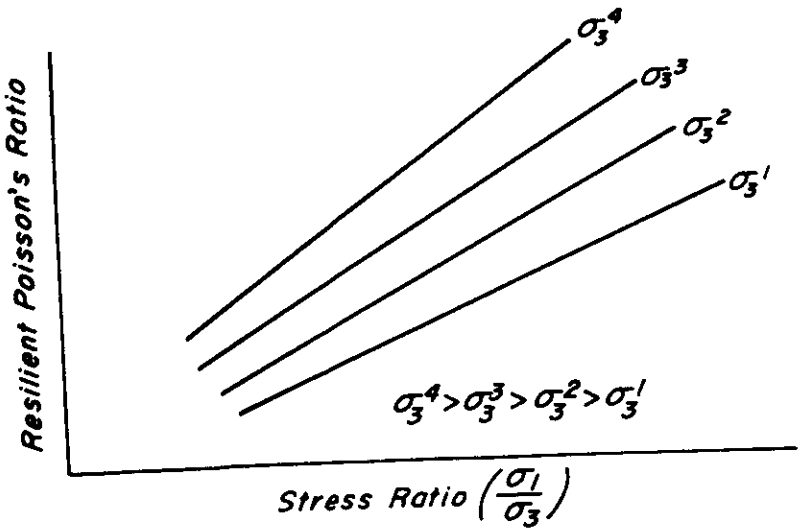

Fig. A-7 — Results of resilience tests on granular soils.

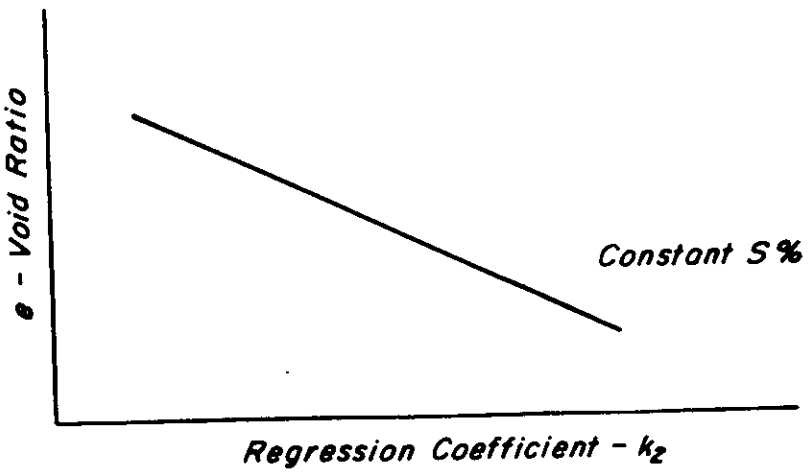

Fig. A-8 – Results of resilience tests on granular soils.

APPENDIX B

SUMMARY OF FATIGUE TEST DATA, BEAM WIDTH STUDY

TABLE B1 - INDIVIDUAL FATIGUE TEST RESULTS FOR 1.5 IN. WIDE SPECIMENS - CALIFORNIA 1/2" MAXIMUM SIZE MEDIUM GRADING, GRANITE AGGREGATE, 85 - 100 PENETRATION ASPHALT, 6.0 PERCENT ASPHALT 68°F (20°C)

Stiffness psi	Initial Strain in. per in.	Fatigue Life	Applied Stress psi	Specific Gravity	Air Void Content Percent
319,992	.000234	460164	75	2.49	4.0
356,379	.000210	280400	75	2.48	4.2
321,711	.000233	245317	75	2.49	4.1
299,636	.000260	425339	75	2.46	5.0
281,470	.000266	240269	75	2.48	4.2
339,895	.000220	507487	75	2.46	5.0
359,280	.000208	378366	75	2.47	4.5
297,400	.000252	331784	75	2.47	4.5
235,280	.000305	36188	100	2.45	5.4
282,477	.000354	64321	100	2.48	4.2
241,951	.000413	31144	100	2.47	4.7
297,095	.000336	20181	100	2.47	4.7
451,773	.000221	142222	100	2.48	3.9
263,741	.000379	18408	100	2.47	4.6
327,073	.000305	46224	100	2.49	4.0
293,847	.000340	26744	100	2.46	4.9
313,503	.000319	11261	100	2.47	4.6
313,449	.000319	29256	100	2.46	5.2
278,896	.000537	9740	150	2.48	4.1
266,181	.000563	6079	150	2.57	4.7
258,472	.000580	10941	150	2.46	4.8
242,448	.000618	7037	150	2.48	4.2
313,283	.000478	4446	150	2.47	4.7
288,574	.000519	15148	150	2.49	4.0
303,885	.000493	14253	150	2.48	4.1
241,735	.000620	6823	150	2.47	4.6
267,757	.000560	10243	150	2.48	4.4
281,871	.000532	9888	150	2.49	4.0

TABLE B2 - INDIVIDUAL FATIGUE TEST RESULTS FOR 2.0 IN. WIDE SPECIMENS - CALIFORNIA 1/2" MAXIMUM SIZE MEDIUM GRADING, GRANITE AGGREGATE, 85 - 100 PENETRATION ASPHALT, 6.0 PERCENT ASPHALT, 68°F (20°C)

Stiffness psi	Initial Strain in. per in.	Fatigue Life	Applied Stress psi	Specific Gravity	Air Void Content Percent
329,066	.0002279	292015	75	2.48	4.4
284,608	.0002635	326222	75	2.48	4.2
353,377	.0002122	345391	75	2.48	4.1
336,040	.0002231	233598	75	2.45	5.3
352,811	.0002126	728374	75	2.49	4.0
357,548	.0002997	599249	75	2.49	4.0
294,436	.0002547	687928	75	2.48	4.3
314,844	.0002307	551448	75	2.48	4.2
280,378	.0002675	218251	75	2.48	4.4
304,771	.0002460	173808	75	2.47	4.8
413,770	.0002416	57598	100	2.48	4.2
281,542	.0003551	117692	100	2.48	4.2
266,356	.0003754	38521	100	2.48	4.4
331,815	.0003014	112921	100	2.49	4.0
276,961	.0003611	77390	100	2.48	4.0
321,028	.0003115	66008	100	2.46	5.0
272,197	.0003674	70361	100	2.44	5.9
342,054	.0002924	63054	100	2.48	4.2
358,772	.0002787	92279	100	2.47	4.7
393,106	.0002544	139501	100	2.48	4.4
344,803	.0004350	11373	150	2.48	4.2
290,196	.0005169	8330	150	2.48	4.4
342,542	.0004379	14936	150	2.47	4.6
322,819	.0004646	7133	150	2.48	4.2
333,114	.0004502	19182	150	2.48	4.2
332,235	.0004514	14559	150	2.48	4.4
316,951	.0004732	6570	150	2.47	4.2
315,879	.0004748	5718	150	2.46	5.1
314,670	.0004766	7577	150	2.49	4.0
352,933	.0004250	8352	150	2.47	4.5

TABLE B3 - INDIVIDUAL FATIGUE TEST RESULTS FOR 2.5 IN. WIDE SPECIMENS - CALIFORNIA 1/2" MAXIMUM SIZE MEDIUM GRADING, GRANITE AGGREGATE, 85 - 100 PENETRATION ASPHALT, 6.0 PERCENT ASPHALT, 68°F (20°C)

Stiffness psi	Initial Strain in. per in.	Fatigue Life	Applied Stress psi	Specific Gravity	Air Void Content Percent
319,659	.0002346	310960	75	2.48	4.4
295,625	.0003647	141384	75	2.45	5.3
251,512	.0002981	358860	75	2.46	5.0
379,477	.0001976	341480	75	2.45	5.2
244,811	.0003063	201480	75	2.45	5.6
269,975	.0002778	366363	75	2.47	4.5
285,730	.0002624	267394	75	2.45	5.4
281,685	.0002662	279191	75	2.47	4.7
335,368	.0002236	322483	75	2.46	5.1
360,919	.0002078	382361	75	2.48	4.3
251,229	.0003980	75754	100	2.46	5.0
258,109	.0003874	53527	100	2.45	5.3
282,284	.0003542	65115	100	2.45	5.3
253,121	.0003950	52752	100	2.44	5.8
300,901	.0003323	97787	100	2.48	4.4
276,001	.0003623	77332	100	2.47	4.6
280,467	.0003565	88743	100	2.48	4.1
294,001	.0003401	120144	100	2.48	4.4
278,980	.0003584	58284	100	2.46	5.1
328,582	.0003043	97101	100	2.47	4.5
260,291	.0005762	6948	150	2.44	5.6
281,685	.0005325	10179	150	2.47	4.5
270,606	.0005543	10049	150	2.48	4.1
272,053	.0005513	10842	150	2.48	4.3
261,507	.0005736	7124	150	2.46	4.9
269,530	.0005565	9328	150	2.48	4.4
254,313	.0005898	6253	150	2.45	5.2
269,888	.0005558	8592	150	2.45	5.6
279,268	.0005371	9920	150	2.47	4.6
259,086	.0005700	9287	150	2.45	5.3

TABLE B4 - INDIVIDUAL FATIGUE TEST RESULTS FOR 3.0 IN. WIDE SPECIMENS - CALIFORNIA 1/2" MAXIMUM SIZE MEDIUM GRADING, GRANITE AGGREGATE, 85 - 100 PENETRATION ASPHALT, 6.0 PERCENT ASPHALT, 68°F (20°C)

Stiffness psi	Initial Strain In. per in.	Fatigue Life	Applied Stress psi	Specific Gravity	Air Void Content Percent
305,988	.0002461	473111	75	2.48	4.2
347,479	.0002158	609579	75	2.49	3.8
369,462	.0002030	624704	75	2.48	4.2
318,388	.0002355	470092	75	2.49	3.9
369,472	.0002030	603735	75	2.48	4.1
270,151	.0002776	250118	75	2.46	4.9
320,298	.0002341	297219	75	2.46	4.8
301,970	.0002434	365699	75	2.49	4.0
245,783	.0003051	171531	75	2.42	6.4
291,708	.0002571	200875	75	2.44	5.9
292,162	.0003422	118793	100	2.48	4.1
245,464	.0004073	20532	100	2.44	5.8
309,949	.0003226	129104	100	2.49	4.0
292,829	.0003414	143256	100	2.48	4.3
342,728	.0002918	194014	100	2.49	3.9
311,579	.0003200	154483	100	2.49	4.0
239,975	.0004167	49670	100	2.46	5.1
246,472	.0004057	102524	100	2.48	4.5
255,043	.0003921	25639	100	2.43	6.1
332,912	.0003004	210075	100	2.49	3.9
279,084	.0005375	21083	150	2.48	4.2
333,592	.0004497	23613	150	2.49	3.9
278,166	.0005397	11508	150	2.49	3.9
302,964	.0004951	12854	150	2.49	4.0
219,248	.0006842	6955	150	2.45	5.4
269,709	.0005567	10337	150	2.49	4.0
219,685	.0006830	6372	150	2.46	5.1
291,241	.0005150	15485	150	2.49	4.0
263,337	.0005696	16701	150	2.48	4.4
218,523	.0006864	4740	150	2.44	5.9

				2.51	3.0
		162838	100	2.51	3.0
	0002980	152943	100	2.49	3.7

TABLE B5 - INDIVIDUAL FATIGUE TEST RESULTS FOR 1.5 IN. WIDE SPECIMENS (REPEAT SET TESTED TO INVESTIGATE MACHINE EFFECT), CALIFORNIA 1/2" MAXIMUM SIZE MEDIUM GRADING, GRANITE AGGREGATE, 85 - 100 PENETRATION ASPHALT, 6.0 PERCENT ASPHALT, 68°F (20°C)

Stiffness psi	Initial Strain in. per in.	Fatigue LIfe	Applied Stress psi	Specific Gravity	Air Void Content Percent
396,847	.0001890	661757	75	2.50	3.6
497,153	.0001508	845984	75	2.50	3.3
444,716	.0001686	485701	75	2.50	3.8
460,894	.0001627	578398	75	2.50	3.6
466,724	.0001607	868142	75	2.48	4.1
513,315	.0001461	904314	75	2.50	3.6
386,653	.0001940	633517	75	2.49	3.7
470,873	.0001593	790654	75	2.51	3.2
296,416	.0002530	302238	75	2.49	3.9
421,737	.0001778	701654	75	2.50	3.6
368,386	.0002715	184697	100	2.50	3.3
247,954	.0004033	53723	100	2.49	3.9
285,488	.0003503	139302	100	2.51	3.2
248,134	.0004030	119458	100	2.46	5.0
278,783	.0003597	72723	100	2.48	4.7
372,869	.0002682	174765	100	2.49	3.8
411,609	.0002420	257817	100	2.50	3.3
313,449	.0003190	110003	100	2.51	3.0
406,259	.0002461	162838	100	2.51	3.0
335,597	.0002980	152943	100	2.49	3.7
264,383	.0005674	5282	150	2.50	3.3
261,507	.0005736	11622	150	2.50	3.3
458,092	.0003274	20372	150	2.49	3.8
406,628	.0003680	20111	150	2.50	3.4
417,024	.0003597	20233	150	2.50	3.3
493,688	.0003038	26357	150	2.47	4.5
268,996	.0005576	8610	150	2.49	3.9
396,583	.0003782	22701	150	2.51	3.0
418,139	.0003587	26293	150	2.50	3.5
293,598	.0005110	19107	150	2.51	3.0

APPENDIX C

STIFFNESS AND FATIGUE MEASUREMENTS; BEAMS OBTAINED FROM CORE SPECIMENS, YGNACIO VALLEY ROAD

SUMMARY OF TEST RESULTS ON BEAM SPECIMENS OBTAINED FROM CORES FROM YGNACIO VALLEY ROAD

Sample	Stiffness	Initial Strain - in. per in.	Applied Stress	Specific Gravity	Air Void Content Percent
		Time of loading - 0.1 sec; temperature 38°F			
YV1-2	1530000	0.000163	250	2.28	10.6
YV1-3	1330000	0.000188	250	2.39	6.5
YV1-4	1340000	0.000187	250	2.40	5.9
YV1-6	1310000	0.000191	250	2.42	5.2
YV1-8	1580000	0.000158	250	2.43	4.8
YV2-3	1530000	0.000163	250	2.36	7.5
YV2-4	1670000	0.000150	250	2.34	8.3
YV2-5	1620000	0.000154	250	2.37	7.1
YV2-6	2340000	0.000107	250	2.36	7.5
YV2-9	1240000	0.000202	250	2.44	4.3
YV3-1	1900000	0.000132	250	2.35	8.0
YV3-3	1450000	0.000172	250	2.36	7.6
YV3-6	1410000	0.000177	250	2.38	6.7
YV3-14	1430000	0.000175	250	2.49	2.6
YV1-2	1640000	0.000122	200	2.28	10.6
YV1-2	1440000	0.000139	200	2.39	6.5
YV1-4	1400000	0.000143	200	2.40	5.9
YV1-6	1330000	0.000150	200	2.42	5.2
YV1-8	1650000	0.000121	200	2.43	4.8
YV2-3	1540000	0.000130	200	2.36	7.5
YV2-4	1670000	0.000100	200	2.34	8.3
YV2-5	1710000	0.000117	200	2.37	7.1
YV2-6	2400000	0.000083	200	2.36	7.5
YV2-9	1270000	0.000158	200	2.44	4.3
YV3-1	1990000	0.000100	200	2.35	8.0
YV3-3	1710000	0.000117	200	2.36	7.6
YV3-6	1490000	0.000134	200	2.38	6.7
YV3-14	1510000	0.000132	200	2.49	2.6
YV1-2	1770000	0.000085	150	2.28	10.6
YV1-3	1520000	0.000099	150	2.39	6.5
YV1-4	1390000	0.000108	150	2.40	5.9
YV1-6	1390000	0.000108	150	2.42	5.2
YV1-8	1730000	0.000087	150	2.43	4.8
YV2-3	1550000	0.000097	150	2.36	7.5
YV2-4	1770000	0.000085	150	2.34	8.3
YV2-5	1790000	0.000084	150	2.37	7.1
YV2-6	2580000	0.000058	150	2.36	7.5
YV2-9	1270000	0.000118	150	2.44	4.3
YV3-1	1930000	0.000078	150	2.35	8.0
YV3-3	1800000	0.000083	150	2.36	7.6
YV3-6	1800000	0.000083	150	2.38	6.7
YV3-14	1670000	0.000090	150	2.49	2.6

SUMMARY OF TEST RESULTS ON BEAM SPECIMENS OBTAINED FROM CORES FROM YGNACIO VALLEY ROAD

Sample	Stiffness	Initial Strain - in. per in.	Applied Stress	Specific Gravity	Air Void Content Percent
		Time of Loading - 0.1 sec; temperature 66°F			
YV1-2	560000	0.000134	75	2.28	10.6
YV1-3	360000	0.000208	75	2.39	6.5
YV1-4	338000	0.000222	75	2.40	5.9
YV1-6	289000	0.000259	75	2.42	5.2
YV1-8	344000	0.000218	75	2.43	4.8
YV2-3	578000	0.000130	75	2.36	7.5
YV2-4			75	2.34	8.3
YV2-5	585000	0.000128	75	2.37	7.1
YV2-6	676000	0.000111	75	2.36	7.5
YV2-9	266000	0.000282	75	2.44	4.3
YV3-1	629000	0.000119	75	2.35	8.0
YV3-3	419000	0.000179	75	2.36	7.6
YV3-6	350000	0.000214	75	2.38	6.7
YV3-14	282000	0.000266	75	2.49	2.6
YV1-2	612000	0.000098	60	2.28	10.6
YV1-3	376000	0.000160	60	2.39	6.5
YV1-4	343000	0.000175	60	2.40	5.9
YV1-6	309000	0.000194	60	2.42	5.2
YV1-8	351000	0.000171	60	2.43	4.8
YV2-3	602000	0.000100	60	2.36	7.5
YV2-4			60	2.34	8.3
YV2-5	597000	0.000100	60	2.37	7.1
YV2-6	709000	0.000085	60	2.36	7.5
YV2-9	266000	0.000226	60	2.44	4.3
YV3-1	659000	0.000091	60	2.35	8.0
YV3-3	459000	0.000131	60	2.36	7.6
YV3-6	375000	0.000160	60	2.38	6.7
YV3-14	294000	0.000204	60	2.49	2.6
YV1-2	654000	0.000076	50	2.28	10.6
YV1-3	395000	0.000127	50	2.39	6.5
YV1-4	366000	0.000136	50	2.40	5.9
YV1-6	337000	0.000148	50	2.42	5.2
YV1-8	386000	0.000130	50	2.43	4.8
YV2-3	645000	0.000078	50	2.36	7.5
YV2-4			50	2.34	8.3
YV2-5	618000	0.000081	50	2.37	7.1
YV2-6	767000	0.000065	50	2.36	7.5
YV2-9	283000	0.000177	50	2.44	4.3
YV3-1	705000	0.000071	50	2.35	8.0
YV3-3	476000	0.000105	50	2.36	7.6
YV3-6	391000	0.000128	50	2.38	6.7
YV3-14	313000	0.000160	50	2.49	2.6

SUMMARY OF TEST RESULTS ON BEAM SPECIMENS OBTAINED FROM CORES FROM YGNACIO VALLEY ROAD

Sample	Stiffness	Initial Strain - in. per in.	Applied Stress	Specific Gravity	Air Void Content Percent
	Time of loading - 0.1 sec; temperature 82°F				
YV1-2	230000	0.000218	50	2.28	10.6
YV1-3	120000	0.000416	50	2.39	6.5
YV1-4	135000	0.000370	50	2.40	5.9
YV1-6	92000	0.000543	50	2.42	5.2
YV1-8	117000	0.000427	50	2.43	4.8
YV2-3	212000	0.000236	50	2.36	7.5
YV2-4			50	2.34	8.3
YV2-5	215000	0.000232	50	2.37	7.1
YV2-6	305000	0.000164	50	2.36	7.5
YV2-9	103000	0.000485	50	2.44	4.3
YV3-1	322000	0.000155	50	2.35	8.0
YV3-3	159000	0.000315	50	2.36	7.6
YV3-6	142000	0.000352	50	2.38	6.7
YV3-14	95000	0.000526	50	2.49	2.6
YV1-2	243000	0.000185	45	2.28	10.6
YV1-3	125000	0.000360	45	2.39	6.5
YV1-4	126000	0.000357	45	2.40	5.9
YV1-6	93000	0.000485	45	2.42	5.2
YV1-8	127000	0.000354	45	2.43	4.8
YV2-3	214000	0.000210	45	2.36	7.5
YV2-4	258000	0.000123	45	2.34	8.3
YV2-5	230000	0.000196	45	2.37	7.1
YV2-6	345000	0.000130	45	2.36	7.5
YV2-9	106000	0.000425	45	2.44	4.3
YV3-1	350000	0.000129	45	2.35	8.0
YV3-3	165000	0.000272	45	2.36	7.6
YV3-6	140000	0.000322	45	2.38	6.7
YV3-14	100000	0.000450	45	2.49	2.6
YV1-2	251000	0.000119	30	2.28	10.6
YV1-3	164000	0.000183	30	2.39	6.5
YV1-4	154000	0.000195	30	2.40	5.9
YV1-6	107000	0.000280	30	2.42	5.2
YV1-8	159000	0.000189	30	2.43	4.8
YV2-3	238000	0.000126	30	2.36	7.5
YV2-4	282000		30	2.34	8.3
YV2-5	300000	0.000100	30	2.37	7.1
YV2-6	432000	0.000069	30	2.36	7.5
YV2-9	116000	0.000258	30	2.44	4.3
YV3-1	386000	0.000078	30	2.35	8.0
YV3-3	201000	0.000149	30	2.36	7.6
YV3-6	167000	0.000180	30	2.38	6.7
YV3-14	107000	0.000280	30	2.49	2.6

SUMMARY OF TEST RESULTS ON BEAM SPECIMENS OBTAINED FROM CORES FROM YGNACIO VALLEY ROAD

Sample	Stiffness	Initial Strain - in. per in.	Applied Stress	Specific Gravity	Air Void Content Percent
Time of loading - 0.05 sec; temperature 66°F					
YV1-2	650000	0.000115	75	2.28	10.6
YV1-3	422000	0.000178	75	2.39	6.5
YV1-4	465000	0.000162	75	2.40	5.9
YV1-6	381000	0.000197	75	2.42	5.2
YV1-8	458000	0.000164	75	2.43	4.8
YV2-3	615000	0.000122	75	2.36	7.5
YV2-4	772000	0.000097	75	2.34	8.3
YV2-5	591000	0.000127	75	2.37	7.1
YV2-6	684000	0.000110	75	2.36	7.5
YV2-9	319000	0.000235	75	2.44	4.3
YV3-1	848000	0.000089	75	2.35	8.0
YV3-3	546000	0.000137	75	2.36	7.6
YV3-6	507000	0.000148	75	2.38	6.7
YV3-14	371000	0.000202	75	2.49	2.6
YV1-2	68000	0.000087	60	2.28	10.6
YV1-3	432000	0.000139	60	2.39	6.5
YV1-4	522000	0.000115	60	2.40	5.9
YV1-6	393000	0.000153	60	2.42	5.2
YV1-8	495000	0.000121	60	2.43	4.8
YV2-3	610000	0.000098	60	2.36	7.5
YV2-4	760000	0.000079	60	2.34	8.3
YV2-5	578000	0.000104	60	2.37	7.1
YV2-6	665000	0.000090	60	2.36	7.5
YV2-9	316000	0.000190	60	2.44	4.3
YV3-1	860000	0.000070	60	2.35	8.0
YV3-3	550000	0.000109	60	2.36	7.6
YV3-6	518000	0.000116	60	2.38	6.7
YV3-14	382000	0.000157	60	2.49	2.6
YV1-2	745000	0.000067	50	2.28	10.6
YV1-3	456000	0.000110	50	2.39	6.5
YV1-4	537000	0.000093	50	2.40	5.9
YV1-6	445000	0.000112	50	2.42	5.2
YV1-8	516000	0.000097	50	2.43	4.8
YV2-3	688000	0.000073	50	2.36	7.5
YV2-4	820000	0.000061	50	2.34	8.3
YV2-5	574000	0.000087	50	2.37	7.1
YV2-6	720000	0.000069	50	2.36	7.5
YV2-9	341000	0.000147	50	2.44	4.3
YV3-1	889000	0.000056	50	2.35	8.0
YV3-3	600000	0.000083	50	2.36	7.6
YV3-6	546000	0.000092	50	2.38	6.7
YV3-14	392000	0.000128	50	2.49	2.6